

POLITECNICO DI MILANO

**School of Industrial and Information Engineering Department of Electronics, Information and
Bioengineering**



**DEVELOPMENT AND EVALUATION OF AND
ANDROID APP TO EXPLOIT SMARTPHONE-
EMBEDDED CAMERA AND INERTIAL SENSORS
FOR MONITORING OF PHYSIOLOGICAL
PARAMETERS**

Supervisor: Prof. Enrico Gianluca CAIANI

Co-Supervisor: Dott.ssa Ing. Sarah SOLBIATI

M.Sc. Thesis by:
Claudio Pighini, 899701

Academic Year: 2018-2019

Desidero esprimere un ringraziamento speciale al Professore Enrico Gianluca Caiani per aver condiviso le sue conoscenze, per avermi seguito con grande professionalità e per le opportunità che mi ha concesso durante questo percorso di laurea.

Un sentito grazie alla Dott.ssa Ing. Sarah Solbiati per il supporto fornito durante il compimento di questo lavoro, aiutandomi nella pratica e con grande disponibilità.

Vorrei ringraziare tutti i miei amici, poiché mi hanno permesso di crescere in un ambiente unico, che ha fatto di me ciò che sono, ma soprattutto, ciò che volevo essere.

Vorrei ringraziare quelle persone che nella mia vita sono state fondamentali, con cui sono cresciuto, e quelle che ho avuto la fortuna di conoscere negli anni, e che allo stesso modo sono diventate parte integrante della mia vita.

Ringrazio infinitamente un ingegnere che ha fatto sì che questo giorno arrivasse.

Un grazie particolare va alla mia famiglia, per avermi dato modo di arrivare fino qui, ed ai miei importantissimi zii, che mi hanno cresciuto e continuano da sempre a starmi vicino.

Vorrei ringraziare infinitamente quella persona che mi ha formato, lavorativamente e non, che ha creduto in me e per la quale nutrirò sempre una profonda stima.

Infine vorrei ringraziare un'ultima persona che, in ogni fase della mia vita, resterà sempre uno dei miei punti di riferimento.

GENERAL INDEX

General index	3
List Of Figures	5
List of Tables.....	15
Abstract	18
Sommario	25
1 Introduction.....	32
1.1 Smartphone as a digital healthcare technology	32
1.2 Smartphone for sensing signals	33
1.2.1 Smartphone embedded MEMS: accelerometer and gyroscope sensors.....	34
1.2.2 The smartphone camera sensor	39
1.3 Smartphone as device for investigating cardiovascular system	43
1.3.1 Smartphone for HR and HRV detection.....	46
1.3.2 Smartphone PPG for HR and HRV detection	46
1.3.3 Smartphone SCG for HR and HRV detection.....	51
1.4 Apps for acquisition of SCG and PPG	54
1.5 Aim of the thesis.....	56
2 Materials and methods	57
2.1 Materials: smartphone hardware and the integrated development environment (IDE)	
57	
2.1.1 The smartphone hardware	57
2.1.2 The integrated development environment.....	63
2.2 Methods: the application design	64
2.2.1 The design of an Android smartphone 3 module-based app for retrieving	
biological markers by using PPG and SCG signals	65
3 The experimental protocols and outcome analysis	104
3.1 First protocol: hr estimation and app usability evaluation	104

3.1.1	The experimental setup	104
3.1.2	Protocol	105
3.2	Second protocol: hr measurement validation and ptt estimation.....	109
3.2.1	The experimental setup	110
3.2.2	Protocol	111
3.3	First protocol: data analysis.....	115
3.3.1	Smartphone data processing and HR extraction.....	115
3.3.2	Questionnaire score <i>analysis</i>	120
3.4	Second protocol: data analysis.....	124
3.4.1	HR extraction from smartphone and Nexfin signals	124
4	Results.....	130
4.1	first protocol	130
4.1.1	HR results from smartphone PPG and SCG signals	130
4.1.2	Questionnaires results	132
4.2	Second protocol	138
5	Discussions and conclusions.....	143
5.1	App modules for the separate SCG and PPG acquisitions	143
5.2	App module for Simultaneous PPG and SCG acquisition	148
5.3	Limitations.....	150
5.4	Conclusions	151
	Appendix A- SUS questionnaire data	158
	Appendix B- Ad-hoc questionnaire data.....	159
	Appendix C- TWEETS questionnaire data	160

LIST OF FIGURES

Figure 1.1.1 It shows the top funded health IT technologies worldwide since 2010. About 3.5 billion U.S. dollars of funding has been provided for mHealth apps which makes it the top most funded HIT technology in 2010-17	33
Figure 1.2.1 The Kardia Mobile App by AliveCor company transforms the smartphone in a standalone medical device for ECG and atrial fibrillation detection approved by the Food And Drug Administration (FDA). The results can be read by the user and also e-mailed to a physician. Image available on: https://www.alivecor.com/kardiamobile	34
Figure 1.2.2 Mechanical model of a mono-axial accelerometer, schematized as a spring, a damping and a mass within a moving box (Li et al., 2018)	35
Figure 1.2.3 A micro mechanical capacitive sensor (Minhang Bao, 2005)	36
Figure 1.2.4 The signal detection circuit (Minhang Bao, 2005)	36
Figure 1.2.5 (a) Coriolis acceleration (a_c) acting on a moving particle; and (b) mass-spring model of a MEMS gyroscope (Passaro et al., 2017)	38
Figure 1.2.6 Example of capacitance variation of a MEMS gyroscope due to the Coriolis force F_c along the z axis, that is read by an electronic interface (https://www.eetimes.com/document.asp?doc_id=1313226#)	38
Figure 1.2.7 Simultaneous single channel electrocardiogram (ECG) and seismocardiographic (SCG) recordings (sampling rate, 250 Hz) with following points identified: MC = Mitral (Valve) Closure, A0 = Aortic (Valve) Opening, RE = Rapid (Ventricular) Ejection, PE = Peak (Ventricular) Ejection, MO = Mitral (Valve) Opening, RF = Rapid (Ventricular) Filling, AS = Atrial Systole, AC = Aortic (Valve), Closure (Carson A. Wick, 2008).....	39
Figure 1.2.8 Digital image acquisition pipeline. Ray-lights reflected from the scene are focused by the lens on a Color Filter Array (CFA) superimposed to a CCD/CMOS sensor. The sensor output is processed and an RGB image is produced as output (Amerini et al., 2016).....	40
Figure 1.2.9 Example of photo detector and LED for transmission mode configuration (a) and photo detector and LED combination in reflection mode (b) (Moraes et al., 2018).....	41
Figure 1.2.10 The photodetector captures the variations (Light out) of the light emitted by the LED (Light in) due to the blood volume changes (Moraes et al., 2018).....	41
Figure 1.2.11 An HTC hero used reflection mode for PPG acquisition (Abinaya, Prabhakaran and Jaisankar, 2014).....	42

Figure 1.2.12 In the figure, the pulsatile (AC) component of PPG and the corresponding ECG are shown (Allen, 2007)	42
Figure 1.3.1 Statistic showing the most attractive healthcare sectors for mHealth app companies as of 2017	43
Figure 1.3.2 Commercial FirbriCheck app: example of PPG, tachogram and poicarré signals analyzed to detect atrial fibrillation.....	44
Figure 1.3.3 “Instant heart rate” app: heart rate detection using PPG signal through smartphone camera.....	45
Figure 1.3.4 PPG ac signal processing results. (a.i) Typical single frame measuring 320x240 pixels showing selected 3 ROI’s (grey squares) along a left diagonal. (a.ii) RGB profiling along observation line (in red) marked AB where A is towards the WLED position confirming green channel signal can be detected throughout the imaging area while red and blue channels detected in marked zones. (b) Raw PPG signal traces, (c) FFT spectra and (d) PSD spectra for (i) ROI 1 Red, (ii) ROI 2 Green and (iii) ROI 3 Blue channels (Jonathan and Leahy, 2011) .	47
Figure 1.3.5 Schematic drawing of the experimental setup. The directions of the horizontal and vertical added motions are also shown. NIR = near-infrared, PPG = photoplethysmogram, and ECG = electrocardiogram (Matsumura et al., 2014)	48
Figure 1.3.6 Schematization of the two positions and orientation of the mobile devices used during acquisition: in supine, two smartphones were simultaneously placed in POS1 and POS2; in standing, the smartphone was kept by the subject in POS1 (Landreani et al., 2015)	52
Figure 1.3.7 Example of the ECG, simultaneous filtered SCG signals, obtained from POS1 (A-P) and POS2 (H-F), and BCG (H-F), with the relevant adopted nomenclature (Landreani et al., 2015).....	53
Figure 1.3.8 PTT measurement from SCG and PPG using Seismo app on Google Pixel smartphone. The temporal result of PAT differs from PTT due to the inclusion of PEP time (Wang et al., 2018).....	54
Figure 1.4.1 Hamm Seismograph app: the app allows the real-time visualization of 3-axis of smartphone accelerometer. The app ratings amounts to 4.4 out of 5 total, with 128 reviews on the Google Play Store (https://play.google.com/store/apps/details?id=de.inovation)	54
Figure 1.4.2 The Sensor Kinetics app screenshots. This app has a rating of 4.2 out of 5 total with 13 reviews https://apps.apple.com/us/app/sensor-kinetics/id579040333)	55
Figure 2.1.1 Smartphone: Android Xiaomi Redmi Note 7. Image available on: https://www.androidpit.com/redmi-note-7-review	58

Figure 2.1.2 Xiaomi Redmi Note 7 dual camera: this module is composed of the principal 48 MP back camera, the 5 MP camera depth sensor and the flashlight. Image available on: https://www.awaqa.com/xiaomi-redmi-note-7-review-test-low-price-buy/	61
Figure 2.1.3 Standard image coordinate system: the coordinate of a pixel can be described with the typical cartesian notation (x, y) (on the left) or using the corresponding raw and column position of the same pixel (r, c) (on the right).....	62
Figure 2.1.4 Android smartphone 3 axial accelerometer orientations (on the left), whose rotations around their axes are sensed as angular velocities by the gyroscope (on the right)..	63
Figure 2.1.5 Android official IDE screenshot for Google's Android operating system.....	64
Figure 2.2.1 The InitialActivity is the first page which the user can interact with when the application is run. On the left, the possible actions that can be made by using the objects indicated by the arrows (on the right)	66
Figure 2.2.2 Android Studio IDE: the list of the different java classes created for this project	67
Figure 2.2.3 The .txt file with the acquisition information and the personal user parameters is shown on the left. The file is extracted by using the Device File Explorer of Android Studio from the smartphone internal storage (on the right).....	68
Figure 2.2.4 Google Firebase Cloud storage (arrow 1). The arrow 2 indicates the folder created at the moment of the information saving. The root folder that contains the .txt file shown in fig. 2.2.3 has the same univocal name. The arrow 3 indicates the folder content....	68
Figure 2.2.5 Flowchart of the first app activity, from the “InitialActivity” to the “ChooseOptionActivity”	69
Figure 2.2.6 ChooseOptionActivity allows the user to choose among 3 different modules using the indicated buttons. The first one (indicated by arrow 1) will open the activity to capture the PPG signal; the arrow 2 indicates the button to pass to the activity for sensing the SCG signal, and the third one (indicated by arrow 3) will open the activity to simultaneously record the SCG and PPG signals.....	70
Figure 2.2.7 The RecordHfrPpgActivity first visualization. Before starting the acquisition, the user chooses if the PPG will be computed on-board or not (arrow 1), in the meanwhile the activity run on the background (arrow 2). After this choice, the images acquired by the smartphone camera are shown on the page center (indicated by arrow 3), while the user positions the finger on the camera objective. The arrow 4 indicates the button to start the acquisition	71

Figure 2.2.8 Before starting the acquisition, the user positions the fingertip of the index finger in vertical position on the camera objective (indicated by arrow 2), covering the flashlight (arrow 3), but leaving uncovered the depth sensor (arrow 1) 72

Figure 2.2.9 RecordHfrPpgActivity after the user has pushed the button to run the acquisition: a 5 seconds-countdown will start, and the button will be visualized as orange (arrow 2)..... 72

Figure 2.2.10 RecordHfrPpgActivity: a message “Frame acquisition is run!” will be pop-up over the button after the 5 seconds-countdown (arrow 2). During this phase, a video at the set frame rate is acquired for the extraction of PPG. The video is shown where the arrow 1 indicates..... 73

Figure 2.2.11 RecordHfrPpgActivity after the video acquisition: a message “Frame acquisition is done and video saved!” is shown, followed by two beeps. In this moment, the PPG computation (if set) starts using the frames of the acquired video 74

Figure 2.2.12 RecordHfrPpgActivity: when the PPG computation is complete, a message “Computation is done!” is shown. In the meantime, a sequence of beeps warns the user and the button becomes clickable again with the text “GET PPG DATA” (arrow 2) on it. If the on-board PPG computation was not activated, the button would be clickable without the message “Computation is done!”..... 74

Figure 2.2.13 GraphActivity shows the plot of the obtained signal. The arrow 1 indicates the message when activity is opened, which refers to the internal storage path of the .txt file, while the arrow 2 indicates the graph of the computed PPG, after the user having zoomed the graph..... 76

Figure 2.2.14 When the “GET PPG DATA” is pressed, the .txt file relevant to the PPG data is saved on the smartphone internal storage and on Google Cloud (fig. 2.2.4, indicated by arrow 3). The .txt file name begins with the words “PPG_DATA_ ...” followed by the info inserted initially and the date and time of the moment of the button pressing to save the file..... 76

Figure 2.2.15 Flowchart of the possible operations that the user can perform, from the choice of the “RecordHfrPpgActivity” to the graph of the PPG signal on “GraphActivity” 77

Figure 2.2.16 The algorithm for on-board PPG computation placed the 50x50 ROI on the frame center, which presupposes the ROI left-upper corner positioned at $(\text{frameWidth}/2 - 25, \text{frameHeight}/2 - 25)$ coordinate. 79

Figure 2.2.17 On the top, the instantaneous sampling frequency of the camera sensor, calculated as the inverse of time interval between 2 consecutive frames. The decreased value represented by the peaks corresponds to the skip in frame acquisitions shown in the picture on

the bottom, which results in an increase of the time interval between those 2 consecutive frames..... 81

Figure 2.2.18 The plot represents the instantaneous sampling frequencies in a single trial, calculated as the inverse of the time interval between two consecutive frames. The peaks below 110 Hz are due to the missing of frame acquisition, which implies a decrease of sampling frequency. The dotted lines represent the 1st and 3rd quartiles of the distribution. This trial was done setting the app at 120 fps with an acquisition duration of 30 seconds..... 82

Figure 2.2.19 Right hand finger position: without cover the depth sensor and covering the flashlight..... 83

Figure 2.2.20 Left hand finger position: without cover the depth sensor and covering the flashlight..... 83

Figure 2.2.21 Right hand finger position: covering the depth sensor and covering the flashlight..... 83

Figure 2.2.22 Right hand finger position: covering the depth sensor and covering the flashlight..... 84

Figure 2.2.23 Right hand finger position: covering the depth sensor, without using the flashlight..... 84

Figure 2.2.24 Left hand finger position: covering the depth sensor, without using the flashlight..... 84

Figure 2.2.25 Right hand finger position: without covering the depth sensor and without using the flashlight..... 85

Figure 2.2.26 Left hand finger position: without covering the depth sensor and without using the flashlight..... 85

Figure 2.2.27 RecordScgActivity contains a real-time graph (arrow 1) to visualize the data from the accelerometer axis direction indicated by arrow 4. The button to change the visualized axis is indicated by arrow 3, while the arrow 2 indicates the button to run the acquisition. 86

Figure 2.2.28“RecordScgActivity” after the user has pressed the button indicated by arrow 2. The button becomes orange (arrow 2) and not clickable for all the acquisition duration, while the graph is frozen (arrow 1) during the 5-seconds countdown together to 5 synchronized beeps..... 87

Figure 2.2.29 RecordScgActivity during the acquisition. When the detection of SCG signal starts, a message “Seismocardiography acquisition is run!” is shown over the button (arrow 2). The real-time graph shows the acquired data along the direction indicated by arrow 4..... 87

Figure 2.2.30 “RecordScgActivity” at the end of acquisition: the real-time is once again frozen (arrow 1), while the button is now clickable with the hint “GET SEISMOCARDIOGRAPHY” (arrow 2). A pop-up “Acquisition is done!”, which warns the user about the acquisition end, is also shown, followed by 2 beeps. 88

Figure 2.2.31 “GraphActivity” shows the SCG signal along the direction visualized previously on the “RecordScgActivity”. When the “GraphActivity” is opened, a message which indicates the internal storage path of the .txt containing the SCG data is shown (arrow 1). By scrolling and zooming the graph with the touch screen, the user can appreciate the acquired signal (arrow 2)..... 89

Figure 2.2.32 The .txt file containing the accelerometer and gyroscope data, with the corresponding timestamp vectors, the mean sampling rates during the acquisition, the vector of the sampling rate calculated at each second, the acquisition beginning system time and the effective acquisition end time. The .txt file name saved by the “RecordScgActivity” begins with the words “ACC_DATA_” followed by the parameters inserted initially by the user and the date and time at the moment of the storage..... 90

Figure 2.2.33 Flowchart of the possible operations that the user can act, from the choice of the “RecordScgActivity” to the graph of the SCG signal on “GraphActivity” 91

Figure 2.2.34 The inverse of time intervals calculated for each couple of consecutive samples, along the entire acquisition of 30 seconds, are shown on the top for the samples acquired by the accelerometer sensor, while on the bottom the for gyroscope samples. The dotted lines represent the 1s and 3rd quartiles around the median value..... 93

Figure 2.2.35 “RecordHfrPpgAndScgActivity”: when this activity is launched, a window dialog is pop-up (arrow 1) to choose if the PPG on-board computation will be run or not. After this operation, a second pop-up will be shown (arrow 3), which allows the user to set different acquisition time for PPG and SCG, respectively on the left and on the right of the window columns. The maximum time was set at the beginning through the “InitialActivity”. In the meanwhile, the activity is working in background (arrow 2) 94

Figure 2.2.36 “RecordHfrPpgAndScgActivity”: after the chosen of the acquisition times for the PPG and SCG, the main activity appears in the foreground. Here, the visualization of the data given by the accelerometer (arrow 1) and the frames captured by the smartphone camera (arrow 2) are shown. The button indicated by arrow 3 is used to run the simultaneous acquisition of the two signals. The button 4 allows to change the visualized accelerometer axis, which is indicated by arrow 5 95

Figure 2.2.37 “RecordHfrPpgAndScgActivity” : when the button is pressed to run the acquisition, this latter becomes orange (arrow 3) and not clickable for all the acquisition and PPG computation (if set). The real-time graph (arrow 1) and the video visualization (arrow 2) are frozen and a 5-seconds countdown will start, synchronized with 5 beeps..... 96

Figure 2.2.38 “RecordHfrPpgAndScgActivity” : after the 5 beeps and the 5-seconds countdown, a message “Frame and scg acquisition is run!” is shown, which indicates the beginning of the accelerometer and gyroscope data collection and of the video recording 97

Figure 2.2.39 “RecordHfrPpgAndScgActivity” : when both IMU and camera sensor acquisitions are completed, a message “All acquisition are done and video saved”! (arrow 3) is shown, followed by 2 beeps, which indicates the beginning of PPG computation in background (if selected). In the meantime, the real-time graph (arrow 1) and video (arrow 2) visualizations are stopped and the acquired video is saved in the internal storage 98

Figure 2.2.40 “RecordHfrPpgAndScgActivity” : when the PPG computation in background is concluded, a message “Computation is done!” is shown simultaneously to a sequence of beeps to warn the user. The button (arrow 3) will be newly clickable..... 98

Figure 2.2.41 “Graph3Activity” shows the resulted signals from the PPG acquisition (arrow 1) and from the acquired SCG, along the axis visualized during the acquisition (arrow 2). A pop-up indicates the internal storage path of the .txt file with the sensor data (arrow 3) 99

Figure 2.2.42 Flowchart of the possible operations that the user can act, from the choice of the “RecordHfrPpgAndScgActivity” to the graphs of the PPG and SCG signals on “Graph3Activity” 100

Figure 3.1.1 Before signal acquisition, the subjects chose autonomously the best smartphone position on the chest for capturing the SCG signal, by looking at the real time SCG graph offered by the app..... 105

Figure 3.1.2 The picture shows a house living room artificially illuminated. The subject assumed a supine position lying down on a sofa during the PPG acquisition. 105

Figure 3.1.3 The flowchart of the first experimental protocol. The subject initially inserted his/her info on the app and the acquisition setting (camera fps and duration), recording them on a txt file on the cloud and in the smartphone internal storage. After, the subject assumed a supine or a standing position, during that the SCG and PPG signals were acquired in a basal condition. At the end, the subject filled in 3 types of questionnaire about app usability and e-health patient engagement. 107

Figure 3.1.4 Flowchart of PPG acquisition session. The subject chose the PPG app module and set the option of saving the recorded video without on-board PPG computation. The

subject run the acquisition with the button and positioned the fingertip on the camera. After the acquisition time (30 seconds), the subject saved the recorded data and video on the cloud by pressing the designated button 107

Figure 3.1.5 Flowchart of SCG acquisition session: the subject chose the SCG app module and run the acquisition with the button. The smartphone was placed at the position chosen by the subject looking at the real-time plot. At the end of acquisition time (30 seconds), the subject saved the recorded SCG data on the cloud by pressing the designated button 108

Figure 3.2.1 Nexfin monitor of Istituito Auxologico San Luca. 109

Figure 3.2.2 A series of three beeps is played through the phone’s speaker to synchronize the camera and accelerometer subsystems (Wang et al., 2018). 110

Figure 3.2.3 Configuration of Nexfin ECG module electrodes and the Nexfin cuff on the index finger of the left hand of the subject. The smartphone was positioned on the upper-middle chest..... 111

Figure 3.2.4 Flowchart of the steps during the simultaneous PPG and SCG acquisition session 114

Figure 3.3.1 The figure shows the red (a), green (b) and blue (c) channel PPGs extracted with a central 50x50 ROI on the frame center. The red channel PPG is the only one that does not saturate. This acquisition was done at 60 Hz for a duration of 30 second 116

Figure 3.3.2 The figure on the bottom shows the red channel PPG signal behavior using 3 different 50x50 ROI positions: the blue line indicates the PPG extracted with a ROI centered in the frame (ROI 2 on the top figure)); the green line represents the PPG with the nearest ROI to the flash (ROI 3, on the top figure) and the yellow line represents the ROI far from the flash (ROI 1, on the top figure). All the signals were extracted from a video captured at 60 fps as camera frame rate..... 117

Figure 3.3.3 Example of raw PPG signal from subject 7 in standing posture..... 118

Figure 3.3.4 Example of the FFT of the raw PPG signal of the subject 7, acquired in standing position. The peak chosen as the heart frequency is underlined by the red circle. 118

Figure 3.3.5 Example of filtered SCG along the z axis of the subject 4 in standing position. 119

Figure 3.3.6 The plot on the top shows the envelope superimposed on the absolute value of the zSCG signal, which allowed to identify the pattern for the frequency domain analysis. The plot on the bottom represents the envelope FFT, with the red circle that identifies the mean heart frequency during entire 30 second acquisition..... 120

Figure 3.3.7 This radar plot represents the ideal pattern that the item scores (variables) of the SUS and ad-hoc questionnaire should follow to have the best result.	123
Figure 3.3.8 This radar plot represents the ideal pattern that the item scores (variables) of the TWEETS questionnaire should follow to have the best result.....	124
Figure 3.4.1 Example of the ECG captured by the Nexfin ECG module during the second session of the experiment (camera frame rate at 60 fps). The red circles superimposed to the signal represent the detected R-peaks.	125
Figure 3.4.2 Example of the PLT signal captured by the Nexfin cuff at the index finger during the second session of the experiment (camera frame rate at 60 fps). The red circles superimposed to the signal represent the foot PLT fiducial points.	125
Figure 3.4.3 The plot shows a correct identified AO point detected by the customized peak detection algorithm. The zSCG was acquired during the second session, when the camera frame rate was set at 60 fps.	126
Figure 3.4.4 The plot shows a series of correct identified foot points detected by the MATLAB built-in peak detection algorithm. The PPG was acquired during the second session, when the camera frame rate was set at 60 fps.....	127
Figure 3.4.5 The graph on the top represents the AO point extracted from the SCG signal, that is used as proximal reference for the PTT calculus, while the bottom plot represents the PPG foot point used as the distal reference. The time difference between them identifies the PTT estimation.	127
Figure 3.4.6 The PPG and SCG signals during the first 5 seconds: the time difference between the time instant in which the flashlight was turned off and the vibration started represented the internal time delay between the camera and IMU sensors.	128
Figure 3.4.7 The graph on the top represents the R-peak extracted from the subject ECG signal, that is used as proximal reference for the PAT calculus, while the bottom plot represents the PLT foot point used as the distal reference. The time difference between them identifies the PAT estimation.	129
Figure 3.4.8 Overview of the analysis steps executed separately for the first and second protocols.	129
Figure 4.1.1 Results of the comparison of HR obtained from PPG in standing and supine, presented as boxplot with median and 25 th and 75 th percentiles. Dashed lines represent the individual values.	131

Figure 4.1.2 Results of the comparison of HR obtained from SCG in standing and supine, presented as boxplot with median and 25 th and 75 th percentiles. Dashed lines represent the individual values.	131
Figure 4.1.3 Item score medians from SUS among all subjects (yellow) over the ideal series (red).....	132
Figure 4.1.4 Item score means from ad-hoc questionnaire among all subjects (yellow) over the ideal series (red)	134
Figure 4.1.5 Item score median values from TWEETS among all subjects (yellow) over the ideal series (red)	136
Figure 4.2.1 PPG signal extracted from the first session at 30 fps, where the high corruption by noise is visible, preventing beats identification.....	139
Figure 4.2.2 Segment of the PPG signal extracted from the third session at 120 fps, where the noise in correspondence to the PPG valleys made impossible the accurate detection of the foot fiducial points.....	139
Figure 4.2.3 On the left, the linear correlation obtained considering all the corresponding beat-to-beat PAT and PTT measurements, with a $r^2 = 0,01$,. On the right, the same plot where the two outliers were removed ($r^2 = 0,13$).	141
Figure 4.2.4 a) Bland-Altman plot comparing beat-to-beat values of smartphone PTT with gold standard PAT. The dotted line represents the mean of the differences as a measure of the bias among the two measurements, whereas the horizontal continuous lines represent the 95% confidence interval [bias – 2*SD; bias + 2*SD]. In b) the same plot is shown, where the two outliers were removed.	142
Figure A1 Item scores obtained by subject 1 to 7 (yellow) from the administered SUS over the ideal series (red).....	158
Figure B1 Item scores obtained by subject 1 to 7 (yellow) from the administered ad-hoc questionnaire over the ideal series (red).....	159
Figure C1 Item scores obtained by subject 1 to 7 (yellow) from the administered TWEETS over the ideal series (red).....	160

LIST OF TABLES

Table 1.3.1 Commonly used HRV parameters	49
Table 1.3.2 An overview of the works in literature to extract PPG signal through the smartphone camera.....	50
Table 2.1.1 Redmi Note 7 (64GB + 4) specification. Data available from: https://en.wikipedia.org/wiki/Redmi_Note_7	59
Table 2.1.2 Redmi note 7 embedded sensors with specifications. Data available from: https://www.devicespecifications.com/en/editor-review/91b096/8	60
Table 2.1.3 Redmi Note 7 video specification: resolution with the corresponding frame rates and the possible video-audio format. Data available from: https://www.mi.com/global/redmi-note-7/specs	61
Table 2.2.1 Camera mean sampling frequencies evaluated at three different possible frame rates (30, 60 and 120 fps) at three different acquisition time (10, 20 and 30 seconds).....	80
Table 2.2.2 Summary of accelerometer and gyroscope sampling frequency stability and jitters evaluation. For every acquisition time period, the values represent the median sampling frequency among the trials with the associated 1 st and 3 rd quartiles	92
Table 2.2.3 An overview of trial results to test the sensor sampling frequency stability during simultaneous acquisitions of the SCG and PPG data. The tests were conducted at three acquisition durations (10, 20, 30 seconds) at three different possible camera frame rates (30, 60 and 120 fps).....	102
Table 2.2.4 Ratio of accelerometer samples over a camera cycle calculated at three different acquisition times (10, 20, 30 seconds) at every possible camera frame rate. The obtained ratio is compared to the reference value, which is equal to the ratio between the accelerometer sampling frequency and the set camera frame rate	103
Table 3.1.1 First experimental protocol used sampling frequencies: the camera frame rate was set for every acquisition at 30 fps, while the accelerometer and gyroscope sampling frequency at 250 Hz, which is the maximum reachable by the inertial sensors.....	106
Table 3.2.1 The number of sessions is based on the used smartphone camera frame rate (30, 60 and 120), with the respective motion sensor sampling frequencies. The subject always assumed a standing posture.	112
Table 4.1.1 Comparison of HR values extracted from the PPG and SCG signals of the subjects, passing from a standing (left column) to a supine posture (right column).....	130

Table 4.1.2 The SUS answer scores exposed subject-by-subject for each item (item 1 to 10, where + and – highlight the positive or negative meaning) and the summation of recalculated scores (last column) between 0 and 100. The last row represents the medians along the rows for each column.....	133
Table 4.1.3 The ad-hoc questionnaire answer scores exposed subject-by-subject for each item (item 1 to 10, where + and – highlight the positive or negative meaning) and the summation of recalculated scores (last column) with a ranking between 0 and 100. The last row represents the median along the rows for each column.....	135
Table 4.1.4 The scores are subdivided in three compartments: the “Compartment 1” that represents the behavioral engagement , identified by the sum of the first three items (item 1-3); the “Compartment 2” that represents the cognitive engagement, identified by the sum of the items from 4 to 6, and the “Compartment 3” that represents the affective engagement equal to the sum of the last three items (items 7-9). The last row contains the median scores for each compartment among all subjects.	137
Table 4.1.5 The TWEETS answer scores exposed subject-by-subject for each item (item 1 to 9) and the summation of overall scores (last column) with a ranking between 0 and 36. The last row represents the median along the rows for each column.....	138
Table 4.2.1 The HR values extracted from the smartphone SCG and PPG FFT analysis are compared to the HRs calculated from the PLT and ECG gold standards \pm their standard deviations.	140
Table 4.2.2 The mean PTT extracted by the difference of the smartphone PPG and SCG fiducial points compared to the mean PAT calculated from the difference of the Nexfin ECG and PLT fiducial points.	140
Table 5.1.1 Summary of the obtained median HR values subdivided by the acquired signal and the assumed posture.....	145
Table 5.1.2 Summary of the administered questionnaire question texts. The orange indicates the questions which were answered by the users with a median neutral agreement (3 for the SUS and the ad-hoc questionnaire, while 2 for the TWEETS), while the green represents the answers that obtained a median score over the neutral value (4 or 5 for the SUS and ad-hoc questionnaire, while 3 or 4 for TWEETS). The (+) indicated the question phrased positively, while (-) symbolized the questions phrased negatively.....	146
Table 5.1.3 Overview of the median scores among the subjects obtained for the SUS and ad-hoc questionnaire, after the rearrangement of the ranking between 0 and 100, that were compared with the respective thresholds.....	147

Table 5.1.4 Overview of the median scores for each TWEETS compartment among the users, accompanied by the median of the overall rankings.	147
Table 5.2.1 Results for the mean HR comparison between the smartphone and gold standard measurements. The PPG was compared with the Nexfin PLT, while the SCG with the ECG.	149
Table A1 Sentences associated to the SUS items. The (+) sign flanked to the item number indicates that the sentences have a positive meaning, while (-) indicates the opposite.....	158
Table B1 Sentences associated to the ad-hoc questionnaire items. The (+) sign flanked to the item number indicates that the sentences have a positive meaning, while the (-) indicates the opposite.....	159
Table C1 Sentences associated to the TWEETS items. The (+) sign flanked to the item number indicates that the sentences have a positive meaning, while the (-) indicates the opposite.....	160

ABSTRACT

Introduction

The recent technological evolution of the micro-electromechanical systems (MEMS), and complementary MOS (CMOS) active pixel sensor (CMOS sensor) development has enabled the creation of smartphone device with embedded sensors that can be used for sensing different signals related to the health status and wellbeing of the users. In the last years, the researchers have consolidated the feasibility of extracting physiological signals by the use of the smartphone camera and motion sensors, such as the photo-plethysmography (PPG) and seismocardiography (SCG) signals, that could be useful to overcome the lack of standard clinical instruments (e.g. the electrocardiogram (ECG)) in remote setting. This fact, added to the continuous increase in the smartphone users over the world (around 30% in 2020), constitutes a huge opportunity for encouraging the use of the smartphone as monitoring device to keep track of important physiological parameter, such as the heart rate (HR), that can be extracted from the smartphone PPG and SCG signals. In this context, different companies belonging to the mobile Health (m-health) field are riding this wave, developing smartphone apps aiming at engaging the user in health self-assessment and monitoring.

Aims

Lacking a specific application that allows acquiring both SCG and PPG and targeted to a usability design approach, the aim of this thesis was to develop such a versatile, user-friendly and multi-purpose smartphone application for the acquisition of SCG and PPG signals, both singularly or simultaneously, exploiting the motion and camera sensors embedded in an Android smartphone, the Redmi Note 7 (Xiaomi, China). The tool resulting from this study will provide the researchers with an incredible opportunity to conduct research in various experimental protocols in order to validate the biomarkers that can be obtained by the analysis of SCG and PPG signals (alone or in combination) and to analyze the potentiality of this technology in the e-health patient engagement.

Two different experimental protocols were designed to explore the app feasibility of recording signals, and accurately obtain the HR and the pulse transit time (PTT), and to analyse the app usability and to study the performance of this solution in the user e-health engagement.

Materials and methods

For the app development, the freely available Android integrated development environment (IDE), together with the tools offered by Java Development Kit (JDK), was used.

The Xiaomi Redmi Note 7 smartphone was chosen, due to its low cost and high performances in terms of computation and sensors, compared to other smartphones of the last generation. Its camera module is composed of a main back camera with 48 MP of resolution and a low-resolution secondary back-camera (5 MP), which works as depth sensor. Its inertial measurement unit (IMU) embeds two MEMS sensors represented by a BOSCH 2062701 3 axial accelerometer and gyroscope. The motion and camera sensors were used to extract the SCG and PPG signals (from recorded movies), respectively.

The app design started from the creation of an initial Android activity that allowed the users to insert his/her personal biometric data parameters and to choose among different camera frame rates (30, 60 or 120 fps). In addition, the duration of the acquisition (from 1 to 30 seconds) can be set, with the possibility of saving the data both on the Google Cloud Firebase service and in the smartphone internal storage. Successively, in a second Android activity, the end-user has to choose among 3 different modules, representing the core of the app: the first one for the PPG acquisition; the second one for the SCG, and the last one for the simultaneous acquisition of the PPG and SCG signals. The acquired data in using each module were collected on the cloud and in the smartphone internal storage. In addition, by an additional Android activity, signals can be visualized in an easy scrollable and zoomable plot for the SCG and for the on-board computed PPG signal, obtained by an ad-hoc algorithm.

To evaluate the sensors stability during data acquisitions, and to evaluate the best choice for the PPG computation from the acquired movie, different trials were performed during the development phases. The motion sensor sampling frequency was found to be quite constant at 250.14 [249.34; 250.94] Hz, whereas the camera sampling frequency followed the initially selected frame rate: 30.02 [30.00; 30.04] Hz when set at 30 fps; 59.74 [59.55; 59.92] Hz when set at 60 fps, and 120 [119.47; 120.53] Hz when set at 120 fps for a 10 sec acquisition duration. However, some periodic jitters were found for 120 fps when duration was lengthened up to 30 sec (120 [113.34; 126.66]). For the on-board PPG computation algorithm, a qualitative offline video frame comparative analysis led to the choice of a 50x50 (pixels) region of interest (ROI), positioned on center of the frame, and to the analysis of the red channel for the extraction of the pixel video intensity values within the ROI.

A last evaluation was done to test the simultaneous PPG and SCG acquisition module. By counting the number of the accelerometer samples over one camera acquisition cycle (between two consecutive frames), a high stability of the two sensors, even when working simultaneously, was proven for 30 e 60 fps.

The experimental protocols and outcome analysis

Two different experimental protocols were designed.

First protocol: seven healthy subjects (4 F and 3 M, age 28 ± 1 years old) were recruited. The aim was to evaluate the capability of the developed app to obtain the user mean HR and, in the meanwhile, while in a home environment, leaving the volunteers as free as possible after an initial informative training. The mean HR was obtained by the frequency spectrum analysis of the PPG and SCG signals, acquired separately during two 30-second sessions, one in standing position and one in supine posture, for each signal, with PPG camera frame rate set at 30 fps for all the sessions. At the end of the experiments, three types of questionnaires (two standard and one created “ad hoc”) were administered to the users in order to evaluate the app usability and the participant e-health engagement.

Second protocol: this experimental protocol was conducted on one female subject (age 22 years old) at the IRCSS Istituto Auxologico of San Luca (MI), with the aim of comparing the accuracy of the smartphone HR parameters with typical gold standard HR (from ECG) and PPG measurements, acquired using a Nexfin clinical instrumentation. For this purpose, 3 sessions of simultaneous PPG and SCG data acquisition in standing position were performed, each with a different camera frame rate (i.e., 30, 60 and 120 fps). While studying the accuracy of the extracted mean HR from the PPG and SCG frequency spectrum analysis, also a first proof-of-concept of estimating the PTT parameter by beat-to-beat (time-domain) signal analysis from the PPG (distal reference) and SCG (proximal reference) signals was performed.

To this aim, an ad-hoc algorithm, exploiting the smartphone vibration actioned simultaneously to the shutdown of the flashlight at the beginning of the acquisition, was implemented, thus obtaining synchronization reference points before the 30 seconds of each data acquisition.

The signal pre-processing: for the explained purposes, the PPG signals did not need any filtering, while the acceleration along the accelerometer z axis was chosen to represent the

SCG signal and filtered by using a 8th order Butterworth bandpass filter with a bandwidth of [5, 25] Hz.

The HR estimation: for the extraction of HR from the SCG, the FFT algorithm was applied to the signal envelope, calculated in order to detect the artefact-free heartbeat sinusoidal pattern, while the FFT was applied directly to the signal for the PPG. The first peak on the spectrum of the signals after the DC component was taken and multiplied by 60 to obtain the heart frequency as beat-per-minute (bpm).

The PTT estimation: the simultaneously acquired smartphone and Nexfin signals were initially synchronized, exploiting the marker points that were inserted inside in the ECG and Nexfin photoplethysmographic (PLT) signals at the beginning and at the end of the acquisitions, in correspondence to the smartphone speaker beeps. For the smartphone SCG and PPG synchronization, the delay computed by the dedicated algorithm was manually extracted and used to align the signals. The beat-to-beat analysis allowed the extraction of the PPG (the foot of the curve) and SCG (the peak corresponding to the aortic opening (AO)) fiducial points. From the Nexfin, the R-peak from the ECG and the foot of the curve of PLT were used to compute the pulse-arrival-time (PAT), and compared to the smartphone PTT in a beat-to-beat basis, by correlation and Bland-Altman analyses.

The questionnaires score extraction: to evaluate the goodness of the implemented app design, two types of surveys were administered to the volunteers. The first type was constituted by 2 questionnaires to evaluate the system usability: the system usability scale (SUS) and an ad-hoc questionnaire, in which the odd questions (1, 3, 5, 7 and 9) were phrased as positive and the even questions (2, 4, 6, 8 and 10) were phrased with a negative meaning. They could be answered on a five-point Likert scale from "Strongly Disagree" to "Strongly Agree." The scores were then transformed to obtain a final score in a range between 0 and 100, which was compared to threshold values equal to 68 and 50, for the SUS and the ad-hoc questionnaire, respectively. The second type of survey was represented by the "Twente engagement with eHealth technologies scale" (TWEETS), which aimed to evaluate the participant e-health engagement and their expectation for a future app use. This questionnaire was composed of 9 items subdivided into 3 compartments to cover behavioral, cognitive and affective engagement, with scores from 0 (strongly disagree) to 4 (strongly agree).

Results

For the first protocol on the seven subjects, for both the PPG ($p < 0.003$) and the SCG ($p < 0.02$) signals, the ability of the app to obtain the HR and capture the change of posture, from standing to supine, was confirmed.

For the app design evaluation, the SUS obtained a median total score of 70 [64;76], which passed the imposed threshold of 68, underlining a general good user evaluation in terms of system usability. The ad-hoc questionnaire resulted in a median total score of 68 [56; 79], thus underlining the good appreciation of the app in terms of usability and maneuverability during the acquisitions. At last, the TWEETS obtained a median total score equal to 23 [19; 27], while a median of 8 [7; 9], 8 [6; 10] and 6 [4; 8] for the behavioral, cognitive and affective engagement, respectively, was obtained, thus confirming the app potentialities in both behavioral and cognitive engagement.

For the second protocol on a single subject, the feasibility of obtaining the HR from SCG was 100%, from PPG was 83%, while for PTT was only of 33%, as only data acquired during the 60-fps session were analyzable, due the high levels of noise that corrupted the PPG signals at both 30 and 120 fps, thus precluding the beat-to-beat analysis.

Compared to the Nexfin gold standard ECG, the mean HR extracted from both SCG and PPG signals showed errors $< 5\%$. These results offered an indirect validation of the HR measurements obtained during the first protocol, where no gold standard signal was purposely acquired.

The comparison of the PTT with Nexfin PAT resulted in low correlation ($r^2 = 0.13$), with a bias (PAT – PTT) in the Bland-Altman (B-A) plot of 83 msec and CI (± 2 SD) of 16 msec, thus resulting in a CV = $100 \cdot \text{SD} / \text{bias}$ of about 10%, suggesting a low uncertainty in PTT measurements spread around the measured value.

Discussions and conclusions

In this study, an Android app was developed in order to acquire separately or simultaneously the PPG and SCG signals with a Xiaomi smartphone Redmi Note 7, creating a Data storage on the smartphone internal memory and in a remote cloud integrated service.

The project exploited the ability of the Xiaomi smartphone sensors of acquiring the PPG at three different frame rates (30, 60 and 120 fps), with an implemented on-board PPG computation, and the SCG with a high and stable sampling frequency at 250 Hz. Moreover,

the camera and inertial sensor stabilities were proved in the development phases to be maintained during the simultaneous acquisition of the PPG and SCG signals as well, opening an opportunity to explore physiological biomarkers related to the combined analysis of them.

The first proposed protocol aimed to capture separately from the PPG and SCG signals the mean subject HR, using the two app dedicated modules, without any gold standard measurements, thus leaving the 7 healthy subjects (28 [27; 29] years old) without any constraints to evaluate also the app usability and engagement. The t-paired test results demonstrated the feasibility of the smartphone PPG ($p < 0.003$) and SCG ($p < 0.02$) to capture the subject postural changing, extracting the mean HR by a simple frequency analysis.

From the questionnaire analysis, the SUS and the ad-hoc questionnaires suggested that the app was generally appreciated in terms of usability, which overcame the respective thresholds (68 and 50, respectively), demonstrating a positive outcome. For the TWEETS, the scores relevant to behavioral and cognitive engagements resulted greater than the affective engagement, due to the stronger appreciation regarding the app capacity in encouraging the user to understand the biomedical purpose behind the app and to be not invasive during the use. In general, the TWEETS median overall score symbolized a good e-health engagement provided by the app. Thus, the proposed tool could be thought as a capable persuasive technology.

The second protocol analysis, executed with only one female volunteer (22 years old), was principally intended for 2 aims: 1) to validate the app as an instrument to retrieve the mean HR from the PPG and SCG signal spectra; 2) to perform a proof-of-concept test to verify the possibility of extracting physiological parameters which presupposed the PPG and SCG simultaneous acquisition, such as the PTT.

The first goal was achieved by comparing the mean smartphone HR, that were acquired simultaneously by the PPG and SCG signals, to that acquired by the respective Nexfin gold standard measurements, the PLT and ECG, respectively. The ability of PPG and SCG signals in measuring the mean HR with an error $<5\%$ with respect to the gold standard, when the signal is not corrupted by noise, using a simple frequency analysis method, allowed a first validation of using the app to acquire the mean HR through its signals, without the use of clinical standard measurements. These results were aligned with the actual literature, that demonstrated the feasibility of extracting the HR from a simple frequency analysis of the PPG and SCG, supporting the idea of using the app signals for this purpose.

For the second goal, a low correlation values between the PTT and PAT ($r^2 = 0,13$) was found, probably due to the narrow range of values recorded in one single subject during 30 seconds, together with a bias showing an underestimation of 83 msec of the smartphone measured PTT versus the gold standard PAT, that included also the PEP time. However, the relatively narrow confidence interval for the PTT measurements around the measured value ($CV \approx 10\%$) proved a potential coherence in time of the two sensors during the 30 seconds of acquisition, without any drift along the duration of the acquisition.

These results has demonstrated the app feasibility in extracting the user mean HR by a simple sampling frequency analysis, which in future could be implementable as additional feature, offering to the end-users a readable outcome, and the app potentiality in terms of e-health engagement. These features suggest different types of usage exploitable in different contexts, such as in research and, perhaps, in new scenarios concerning the user engagement for a remote monitoring and the self-assessment, exploiting the ductile design to improve its persuasive capacity. Further research is needed to evaluate feasibility and accuracy for the PTT measurement obtained from synchronous acquisition of the SCG and PPG signals.

SOMMARIO

Introduzione

Il recente sviluppo tecnologico nella produzione dei “micro-electromechanical systems” (MEMS) e dei “complementary MOS (CMOS) active pixel sensor” (sensori CMOS) ha permesso la creazione di dispositivi smartphone con sensori integrati capaci di acquisire differenti segnali potenzialmente indicativi dello stato di salute e benessere dei loro utilizzatori. Negli ultimi anni, i ricercatori hanno consolidato la fattibilità di estrarre segnali fisiologici dall’utilizzo della fotocamera e dei sensori di movimento degli smartphones, come ad esempio il segnale foto-pletismografico (PPG) a la sismocardiografia (SCG), che potrebbero sopperire alla mancanza di strumentazioni cliniche standard (esempio l’elettrocardiogramma (ECG)) in una configurazione remota. Questo fatto, combinato con il continuo incremento del numero di utilizzatori di smartphone nel mondo (circa il 30% nel 2020), costituisce una grande opportunità per incoraggiare l’utilizzo di sistemi smartphone come strumenti di monitoraggio per tenere traccia di importanti parametri fisiologici, come la frequenza cardiaca o “heart rate” (HR), estraibili dai segnali PPG e SCG dello smartphone. In questo contesto, differenti aziende appartenenti al campo del “mobile Health” (m-health) si stanno già adoperando per sviluppare apps per smartphone capaci di incoraggiare gli utenti all’auto-monitoraggio e all’auto-valutazione della propria salute.

Obiettivi

Mancando un’applicazione specifica che permetta di acquisire entrambi i segnali PPG e SCG e che miri ad un approccio progettuale di usabilità, lo scopo di questa tesi era lo sviluppo di una applicazione smartphone che fosse versatile, “user-friendly” e multiscopo per acquisire i segnali PPG e SCG, singolarmente o simultaneamente, sfruttando i sensori della camera e di movimento integrati in uno smartphone Redmi Note 7 (Xiaomi, Cina). Lo strumento risultante da questo studio fornirà ai ricercatori un’incredibile opportunità per condurre studi attraverso diversi protocolli sperimentali, con lo scopo di validare bio-marcatore che possono essere ottenuti dall’analisi dei segnali PPG e SCG (da soli o in combinazione), e per analizzare le potenzialità di questa tecnologia nel “e-health engagement” dei pazienti.

Due differenti protocolli sperimentali sono stati elaborati per esplorare la fattibilità di registrare segnali con la app, ed accuratamente ottenere la frequenza cardiaca ed il parametro

“pulse transit time” PPT, ed analizzare l’usabilità percepita e studiando la capacità della soluzione proposta nel “e-health engagement” degli utenti.

Materiali e metodi

Per lo sviluppo della app, l’ambiente di sviluppo integrato (IDE) gratuito di Android, insieme agli strumenti offerti dal kit di sviluppo java (JDK), è stato utilizzato.

Lo smartphone Xiaomi Redmi Note 7 è stato scelto per il suo basso costo ed alte prestazioni in termini computazionali e di sensoristica, rispetto agli altri smartphone di ultima generazione. Il suo modulo per la fotocamera è composto da una camera principale da 48 MP di risoluzione e da una camera secondaria a bassa risoluzione (5 MP), la quale funziona come sensore di profondità. La sua unità di misurazione inerziale (IMU) integra 2 sensori MEMS rappresentati da un accelerometro ed un giroscopio tri-assiale BOSCH 2062701. I sensori della camera e di movimento sono stati utilizzati per estrarre i segnali PPG (dai video registrati) ed SCG, rispettivamente.

Lo sviluppo della app è iniziato dalla creazione di un’attività Android che permettesse all’utente di inserire i suoi dati biometrici personali e di scegliere tra le differenti frequenze di campionamento della camera (30, 60 e 120 fps). Inoltre, il tempo di acquisizione (da 1 a 30 secondi) è settabile, con la possibilità di salvare i dati sia sulla piattaforma cloud Firebase di Google che nella memoria interna dello smartphone. Successivamente, tramite una seconda attività Android, l’utente finale deve scegliere tra tre differenti moduli, rappresentanti il cuore dell’applicazione: il primo per l’acquisizione del PPG; il secondo per SCG e l’ultimo per l’acquisizione simultanea dei segnali PPG e SCG. I dati acquisiti usando ogni modulo venivano salvati sul cloud e nella memoria interna dello smartphone. Infine, grazie ad una attività Android addizionale, i segnali potevano essere visualizzati su un grafico semplice ed interattivo per il SCG e per il PPG calcolato tramite app, ottenuto con un algoritmo ad-hoc.

Per valutare la stabilità dei sensori durante l’acquisizione dei dati e scegliere le migliori specifiche per il calcolo del PPG dai video acquisiti, differenti prove sono state fatte durante le fasi di sviluppo. La frequenza di campionamento dei sensori inerziali è risultata essere pressoché costante a 250,14 [249,34; 250,94] Hz, mentre la frequenza di campionamento della camera seguiva la frequenza inizialmente settata: 30,02 [30,00; 32,04] Hz quando settata a 30 fps; 59,74 [59,55; 59,92] Hz quando settata a 60 fps e 120 [119,47; 120,53] HZ quando settata a 120 fps, per una durata di acquisizione di 10 secondi. Comunque sia, alcune fluttuazioni periodiche sono state riscontrate a 120 fps, quando la durata era stata allungata a

30 sec (120 [113,34; 126,66]). Per il calcolo del PPG direttamente sulla app, un'analisi qualitativa e di confronto delle immagini del video per il PPG offline ha portato alla scelta di una regione di interesse (ROI) di 50x50 pixels, posizionata nel centro dell'immagine, e all'analisi del canale rosso per estrarre l'intensità media dei pixel all'interno ROI.

Un'ultima valutazione è stata fatta per testare il modulo di acquisizione simultanea dei segnali PPG e SCG. Contando il numero dei campioni dell'accelerometro in un ciclo di acquisizione della camera (tra 2 immagini del video consecutive), un'alta stabilità dei due sensori, anche quando lavoravano in simultanea, è stata riscontrata a 30 e 60 fps.

Protocolli sperimentali e analisi degli esiti

Due differenti protocolli sperimentali sono stati ideati.

Il primo protocollo: 7 soggetti sani (4 F e 3 M, età 28 ± 1 anni) sono stati reclutati. L'obiettivo era di studiare la capacità della app sviluppata nell'ottenere l'HR medio degli utenti e, allo stesso tempo, lasciare i volontari liberi nell'utilizzo della app, in un ambiente casalingo, dopo un training informativo iniziale. Gli HR medi sono stati ottenuti da un'analisi dello spettro in frequenza dei segnali PPG e SCG, acquisiti separatamente durante due sessioni di 30 secondi, una in posizione eretta ed una in posizione supina, per ogni segnale, con la camera per il PPG sempre impostata a 30 fps. Alla fine degli esperimenti, tre tipi di questionari (due standard ed uno creato "ad-hoc") sono stati somministrati agli utenti per valutare l'usabilità della app e l'e-health engagement dei partecipanti.

Il secondo protocollo: questo protocollo sperimentale è stato condotto su un soggetto femmina (età 22 anni) all'IRCSS Istituto Auxologico di San Luca (MI), con lo scopo di confrontare l'accuratezza dei parametri HR dello smartphone con le tipiche misure "gold standard" del HR (dall'ECG) e del PPG, acquisite con una strumentazione clinica Nexfin. Per questo scopo, 3 sessioni di acquisizione simultanea del PPG e SCG in posizione eretta sono state eseguite, ognuna con una differente frequenza di cattura della camera (cioè, 30, 60 e 120 fps). Oltre a studiare l'accuratezza del HR medio estratto dall'analisi dello spettro in frequenza del PPG e SCG, anche una prima verifica teorica di stima dall'analisi battito-battito (nel dominio del tempo) del PPG (riferimento distale) e del SCG (riferimento prossimale) del parametro PTT è stata eseguita.

Per questo scopo, un algoritmo ad-hoc, che sfruttava la vibrazione del telefono azionata contemporaneamente allo spegnimento del flash all'inizio dell'acquisizione, è stato

implementato, quindi ottenendo dei punti di riferimento di sincronizzazione prima dei 30 secondi di ogni acquisizione.

Il pre-processing dei segnali: per gli scopi definiti, il segnale PPG non necessitava di alcun filtraggio, mentre il segnale accelerometro lungo l'asse z è stato selezionato per rappresentare il segnale SCG e filtrato usando un filtro Butterworth di ordine 8° con una banda passante di [5, 25] Hz.

La stima del HR: per l'estrazione del HR dal segnale SCG, l'algoritmo "fast Fourier's transform" (FFT) è stato applicato all'involuppo del segnale, utilizzato per enfatizzare il pattern sinusoidale del battito cardiaco, mentre il FFT è stato applicato direttamente per il PPG. Il primo picco nello spettro dei segnali dopo la componente continua (DC) è stato selezionato e moltiplicato per 60 per ottenere la frequenza cardiaca in battiti-al-minuto (bpm).

La stima del PTT: i segnali Nexfin e smartphone acquisiti contemporaneamente sono stati inizialmente sincronizzati sfruttando dei marcatori, i quali sono stati inseriti nei segnali ECG e foto-pletismografico del Nexfin (PLT) all'inizio ed alla fine delle acquisizioni, in corrispondenza di segnali acustici emessi dallo stereo dello smartphone. Per la sincronizzazione del PPG e SCG, il ritardo calcolato dall'algoritmo specializzato è stato manualmente estratto ed usato per allineare i segnali. L'analisi battito-battito ha permesso l'estrazione dei punti caratteristici dei segnali PPG (il cosiddetto "foot" della curva) e SCG (il picco corrispondente all'apertura dell'aorta (AO)). Dal Nexfin, il picco-R del ECG ed il "foot" della curva del PLT sono stati usati per calcolare il "pulse-arrival-time" (PAT), comparato con i PTT dello smartphone, battito-battito, tramite analisi di correlazione e Bland-Altman.

L'estrazione dei punteggi dai questionari: per analizzare il design della app, due tipi di questionari sono stati somministrati ai volontari. Il primo tipo era rappresentato da due questionari per valutare l'usabilità del sistema: il "system usability scale" (SUS) ed un questionario ad-hoc, nei quali le domande dispari (1, 3, 5, 7 e 9) sono state concepite con un'accezione positiva, mentre quelle pari (2, 4, 6 e 8) sono state scritte con un'accezione negativa. Le risposte potevano essere valutate con punteggi su una scala Likert a 5 punti, da "fortemente d'accordo" a "fortemente in disaccordo". Questi punteggi sono stati poi trasformati per ottenere un punteggio finale in un intervallo tra 0 e 100, il quale è stato confrontato con valori soglia di 68 e 50, per il SUS e il questionario ad-hoc, rispettivamente. Il secondo tipo di questionario era rappresentato dal "Twente engagement with eHealth

technologies scale” (TWEETS), il quale mirava a valutare l’e-health engagement dei partecipanti e la loro aspettativa per un uso futuro della app. Questo sondaggio è stato realizzato con 9 domande suddivise in 3 compartimenti che coprono l’engagement comportamentale, cognitivo ed emotivo, con punteggi delle risposte che variavano da 0 (fortemente in disaccordo) a 4 (fortemente d’accordo).

Risultati

Per il primo protocollo sui sette soggetti, per entrambi i segnali PPG ($p < 0.003$) ed SCG ($p < 0.02$), l’abilità della app di ottenere l’HR e catturare il cambiamento di postura, da eretta a supina, è stata confermata.

Per la valutazione del design della app, il SUS ha ottenuto un punteggio totale mediano di 70 [64;76], il quale ha superato la soglia imposta di 68, sottolineando una generale buona valutazione in termini di usabilità del sistema. Il questionario ad-hoc ha ottenuto un punteggio totale mediano di 68 [56; 79], sottolineando dunque un buon apprezzamento della app in termini di usabilità e manovrabilità durante le acquisizioni. Infine, il TWEETS ha ottenuto un punteggio totale mediano uguale a 23 [19; 27], mentre ha ottenuto una mediana di 8 [7; 9], 8 [6; 10] and 6 [4; 8] per l’engagement comportamentale, cognitivo ed emotivo, rispettivamente, confermando le potenzialità della app in entrambi gli engagements cognitivo e comportamentale.

Per il secondo protocollo su un singolo soggetto, la fattibilità di ottenere un HR dal SCG è stata del 100%, per il PPG del 83%, mentre per il PTT del 33%, dato che solo i dati acquisiti durante la sessione a 60 fps erano analizzabili, a causa dell’alto livello di rumore che ha corrotto i segnali PPG a 30 e 120 fps, quindi precludendo un’analisi battito-battito.

Comparato con l’ECG “gold standard” del Nexfin, l’HR medio estratto da entrambi i segnali ha mostrato errori $< 5\%$. Questi risultati hanno offerto una validazione indiretta delle misure del HR ottenute dal primo protocollo, dove nessun segnale “gold standard” è stato volutamente acquisito.

Il confronto tra PTT e PAT del Nexfin ha ottenuto una bassa correlazione ($r^2 = 0.13$), con un errore medio (PAT – PTT) nel grafico di Bland-Altman (B-A) di 83 msec ed un CI (± 2 SD) di 16 msec, risultando quindi in un $CV = 100 \cdot SD / \text{bias}$ di circa il 10%, suggerendo una bassa incertezza delle misure del PPT attorno al valore misurato.

Discussioni e conclusioni

Nello studio proposto, una app Android è stata sviluppata in modo da acquisire separatamente o simultaneamente i segnali PPG e SCG utilizzando uno smartphone Xiaomi Redmi Note 7, con un metodo di memorizzazione dati locale, nella memoria interna dello smartphone, e remoto, nel servizio cloud integrato.

Il progetto ha sfruttato l'abilità dei sensori dello smartphone Xiaomi di acquisire il PPG a tre differenti frequenze di cattura della camera (30, 60, 120 fps), con il calcolo del PPG direttamente implementato nella app, ed il segnale SCG con un'alta e stabile frequenza di campionamento a 250 Hz. Inoltre, durante le fasi di sviluppo le stabilità dei sensori inerziali e della fotocamera hanno dimostrato di essere mantenute anche durante l'acquisizione contemporanea dei segnali PPG ed SCG, offrendo l'opportunità di poter esplorare biomarcatori relativi all'analisi combinata dei segnali acquisiti.

Il primo protocollo proposto mirava ad acquisire separatamente dal PPG e SCG gli HR medi dei soggetti, estratti dall'utilizzo dei due moduli dedicati, senza l'uso di misurazioni "gold standard", dunque lasciando i 7 soggetti analizzati (28 [27; 29] anni) senza alcuna costrizione per valutare anche l'usabilità e la capacità di engagement della app. Il "t-paired test" ha dimostrato la fattibilità del PPG ($p < 0.003$) e del SCG ($p < 0.02$) di catturare i cambiamenti posturali dei soggetti, estraendo gli HR medi tramite una semplice analisi in frequenza.

Dall'analisi dei questionari, il SUS ed il questionario ad-hoc suggerivano che la app è stata generalmente apprezzata in termini di usabilità, i quali hanno superato le rispettive soglie (68 e 50, rispettivamente), dimostrando esiti positivi. Riguardo al TWEETS, i punteggi relativi all'engagement comportamentale e cognitivo hanno ottenuto punteggi maggiori di quello ottenuto per l'engagement emotivo, dovuto al più forte apprezzamento riguardo la capacità dell'app nell'incoraggiare gli utenti ad interessarsi agli scopi biomedici della app e alla non invasività durante l'uso. In generale, la mediana del punteggio complessivo tra gli utenti di 23 [19; 27] è stata tradotta come un buon risultato nell'e-health engagement fornito dalla app, dimostrando che questo strumento potrebbe essere pensato come una potenziale tecnologia persuasiva.

L'analisi del secondo protocollo, eseguito ingaggiando solo un volontario femmina di 22 anni, è stata principalmente intesa per 2 scopi: 1) per validare la app come strumento di cattura del HR medio dagli spettri dei segnali PPG e SCG; 2) per una verifica teorica per testare la

possibilità di estrarre parametri fisiologici che presupponessero l'acquisizione simultanea di PPG e SCG, come ad esempio il PTT.

Il primo obiettivo è stato raggiunto confrontando gli HR medi dello smartphone, acquisiti simultaneamente dai segnali PPG e SCG, con quelli acquisiti dalle rispettive misurazioni standard del Nexfin, il PLT e l'ECG, rispettivamente. L'abilità dei segnali PPG e SCG nel misurare gli HR medi con un errore <5% rispetto ai "gold standard", quando i segnali non erano corrotti dal rumore ed utilizzando una semplice analisi in frequenza, ha permesso una prima validazione dell'uso della app nell'acquisire l'HR medio attraverso i suoi segnali, senza l'utilizzo di misurazioni cliniche standard. Questi risultati erano allineati con la letteratura attuale, la quale ha dimostrato la possibilità di estrarre l'HR da una semplice analisi in frequenza del PPG e del SCG, supportando l'idea di usare i segnali della app per questo scopo.

Per il secondo obiettivo, bassi valori di correlazione tra il PTT e il PAT ($r^2 = 0,13$) sono stati ricavati, probabilmente dovuti al ristretto numero di valori misurati da una singola acquisizione di 30 secondi, insieme ad un errore medio raffigurante una sottostima di 83 msec fornita dal PTT dello smartphone rispetto al PAT delle misurazioni "gold standard", le quali includevano il tempo di PEP. Comunque sia, il relativamente ristretto intervallo di confidenza delle misurazioni del PTT attorno al valore misurato ($CV \approx 10\%$) ha provato la potenziale coerenza nel tempo dei due sensori durante i 30 secondi di acquisizione, senza introdurre sfasamenti temporali lungo le acquisizioni.

Questi risultati hanno dimostrato la fattibilità della app nel misurare l'HR medio degli utenti con una semplice analisi in frequenza, la quale potrebbe essere implementata in futuro come strumento addizionale, offrendo la possibilità agli utenti finali di avere un parametro leggibile, e la potenzialità della app in termini di "eHealth engagement". Queste caratteristiche suggeriscono diversi utilizzi in contesti diversi, come ad esempio in ricerca e, magari, in nuovi scenari riguardanti l'engagement degli utenti per monitoraggio remoto e self-assessment, sfruttando la forma duttile della app per migliorare la sua capacità persuasiva. Maggiori sforzi devono essere ancora fatti per valutare la fattibilità e l'accuratezza della misurazione del PTT, ottenuta dall'acquisizione sincrona dei segnali PPG e SCG.

1 INTRODUCTION

1.1 SMARTPHONE AS A DIGITAL HEALTHCARE TECHNOLOGY

In the last years, people had more and more adapted their own life to smartphone technologies, augmenting their individual ubiquity and the possibility of using different smartphone applications during their normal daily life: at work, at home, during free time, etc.

Already in 2016, over the 28% of entire world population possessed at least a smartphone (1) and it was forecasted that this percentage would increase of 3% every year (2). Nowadays, the forecasts for the 2020 state that the worldwide number of smartphone owners will be around 37% (3). Just in Italy, the number of monthly active smartphone users is projected to reach the 47.57 million of individuals in 4 years (4), which means around 81% of Italian population will be a smartphone owner. In addition, in 2018 the Digital Observatory Innovation survey concluded that about 9 out of 10 Italian mobile owners believed that smartphones would become important or more important than a personal computer (5). These statistics suggest that effectively people are considering the smartphone as a basic commodity, increasingly more important than other common technologies.

In this scenario, technological business companies, research centers and other actors in the digital field had supported the grown of this new concept of life. In particular, the sector of digital health has attracted a specific interest by the app companies and healthcare systems, allowing the creation of a new health category called m-Health or mobile-Health, defined by The Global Observatory for eHealth (GOe) of the World Health Organization “...as a medical and public health practice supported by mobile devices, such as mobile phones, patient monitoring devices, personal digital assistants (PDAs), and other wireless devices;” and more: “mHealth involves the use and capitalization on a mobile phone’s core utility of voice and short messaging service (SMS) as well as more complex functionalities and applications including general packet radio service (GPRS), third and fourth generation mobile telecommunications (3G and 4G systems), global positioning system (GPS), and Bluetooth technology”. (https://www.who.int/goe/publications/goe_mhealth_web.pdf).

This panorama was confirmed by a study which investigated the most funded categories among health IT technologies since 2010 until 2017. As result, this analysis has positioned at the first place in this ranking the m-health apps category (6) (Figure 1.1.1). In the first half year of 2019, the sector of m-health apps was still within the first three places (7).

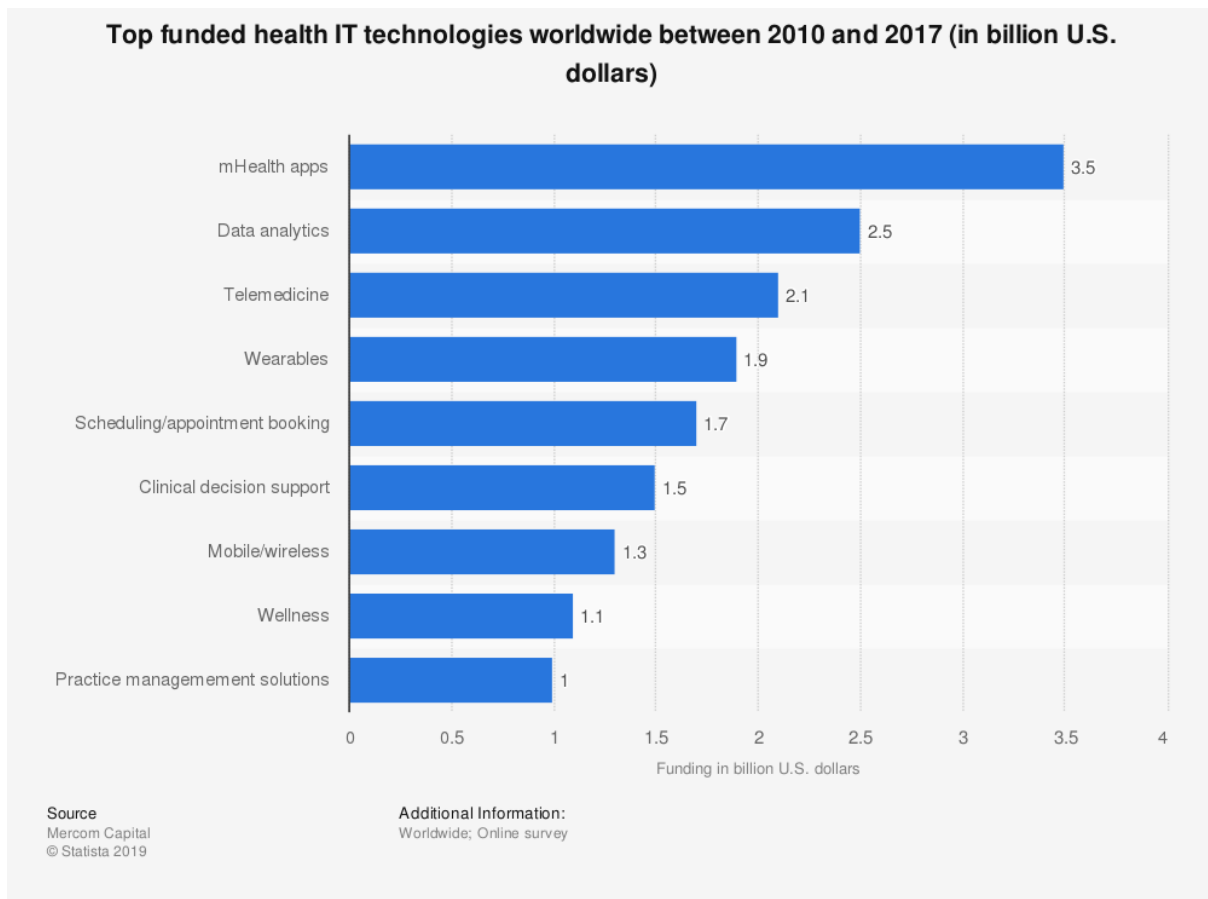


Figure 1.1.1 It shows the top funded health IT technologies worldwide since 2010. About 3.5 billion U.S. dollars of funding has been provided for mHealth apps which makes it the top most funded HIT technology in 2010-17.

This technological trend carries the opportunity of augmenting the user empowerment and his/her active role relevant to health, wellness, self-monitoring and self-care, by the support of smartphone well-established technologies (Yardley *et al.*, 2015).

1.2 SMARTPHONE FOR SENSING SIGNALS

The interest in m-Health is mainly due to the ability of smartphones of carrying different embedded or external sensors, which might allow their use as a standalone device for medical purpose, that could be useful for self-assessment and monitoring of common physiological parameters (Figure 1.2.1).



Figure 1.2.1 The Kardia Mobile App by AliveCor company transforms the smartphone in a standalone medical device for ECG and atrial fibrillation detection approved by the Food And Drug Administration (FDA). The results can be read by the user and also e-mailed to a physician. Image available on: <https://www.alivecor.com/kardiamobile>.

1.2.1 Smartphone embedded MEMS: accelerometer and gyroscope sensors

Thanks to the technological improvements that were made along the years by producing smaller, less obtrusive, and limited power consumption micro electro-mechanical systems (MEMS) that are widely accessible for their reduced costs, (Landreani and Caiani, 2017), smartphones can incorporate sensors such as accelerometers and gyroscopes in a single module called *inertial measurement unit* (IMU).

The MEMS accelerometers are composed by different mechanical elements, such as silicon cantilever and silicon membranes produced by micro-machining technique since 1980s (Minhang Bao, 2005), typically schematized as a silicon spring-mass system that moves with respect to the fixed housing and plates through springs, when there is a lateral acceleration (Figure 1.2.2).

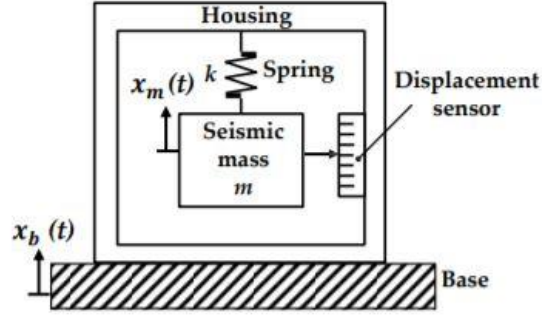


Figure 1.2.2 Mechanical model of a mono-axial accelerometer, schematized as a spring, a damping and a mass within a moving box (Li et al., 2018).

For the Newton's second law, taking as reference the model in the Figure 1.2.2:

$$Ma = -kx - b \frac{dx}{dt} \quad (1)$$

where a is the acceleration of mass with respect to the Earth (with $x = x + cost$):

$$a = \frac{d^2x}{d^2t} - \frac{d^2y}{d^2t} \quad (2)$$

by substituting equation (1) in (2), the equation of motion is obtained:

$$M \frac{d^2x}{d^2t} + b \frac{dx}{dt} + kx = M \frac{d^2y}{d^2t} \quad (3)$$

where $\frac{d^2y}{d^2t}$ is the box acceleration. Thus, neglecting the air friction inside the box frame and knowing the displacement of the mass x , it is possible to derive the acceleration of the smartphone, schematized as the box in this simplified model (Figure 1.2.2).

The typical MEMS accelerometer (based on the ADXL50 developed by Analog Devices and Siemens ((Minhang Bao, 2005))) structure can be divided into two modules:

- 1) the mechanical capacitive sensor (Figure 1.2.3), which is composed of a central mass plate, suspended over the substrate by four thin flexures (tethers), with fingers on both

sides. This central mass plate works as the seismic mass of accelerometer that can be displaced by an inertial force in the surface plane and in perpendicular to the beam flexures. For a finger of the central plate (“i” in Figure 1.2.3) there are two fixed strips (“A” and “B”), electrically connected to form a stationary electrode. The finger and the strips together form two mechanical capacitors (“ C_1 ” and “ C_2 ”). Thus, when the central plate is laterally accelerated, the capacitances “ C_1 ” and “ C_2 ” change in a push-pull way. The differential capacitance “ $C_1 - C_2$ ” can be used to measure the acceleration (Minhang Bao, 2005).

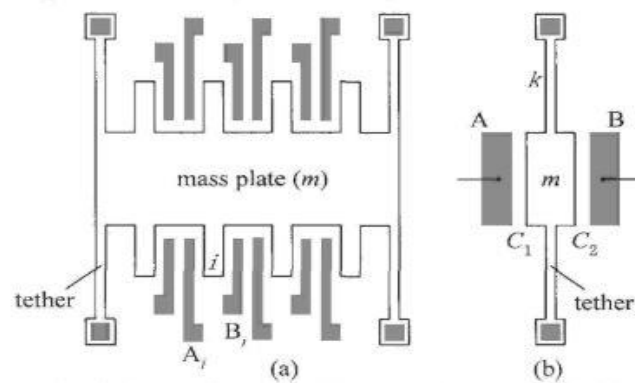


Figure 1.2.3 A micro mechanical capacitive sensor (Minhang Bao, 2005).

- 2) the signal detection circuit, consisting of a sensing circuit to capture the differential capacitance of the mechanical capacitive sensor related to the voltage output (Figure 1.2.4):

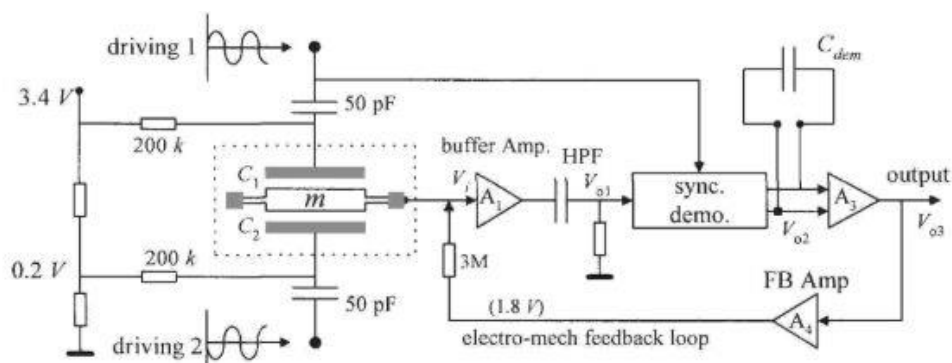


Figure 1.2.4 The signal detection circuit (Minhang Bao, 2005).

The signal detection circuit allows to extract the mass displacement x by sensing the voltage changes applied to V_i (Figure 1.2.4), due to the capacitance difference variation $C_1 - C_2$ (Figure

1.2.3). Thus, extracting the output voltage V_i as function of x , the following formula is obtained:

$$V_i = V_o \frac{c_1 - c_2}{c_1 + c_2} = \frac{x}{d} V_o \quad (4)$$

Now, by substituting x from equation (4) into equation (3) and considering negligible the air friction because small, the result is the acceleration of the smartphone as function of the output voltage V_i :

$$\frac{k d}{m V_o} V_i = \frac{d^2 y}{d^2 t} \quad (5).$$

Moreover, the seismic mass of the IMU (Figure 1.2.2) can be used as a sensing element to capture the angular velocity of the smartphone, transforming the sensor in a gyroscope. In fact, the MEMS gyroscopes don't need a rotating part which requires bearings, and this allows an easy miniaturization and the typical technique of MEMS manufacturing (Passaro *et al.*, 2017).

The physical principle behind the MEMS gyroscopes is based on the force F_z generated by the Coriolis' acceleration \mathbf{a}_c , respectively on Figure 1.2.5 (b) and (a), which causes an orthogonal displacement (along \mathbf{z} on Figure 1.2.5 (a) and (b)) of the mass with respect to the acceleration direction.

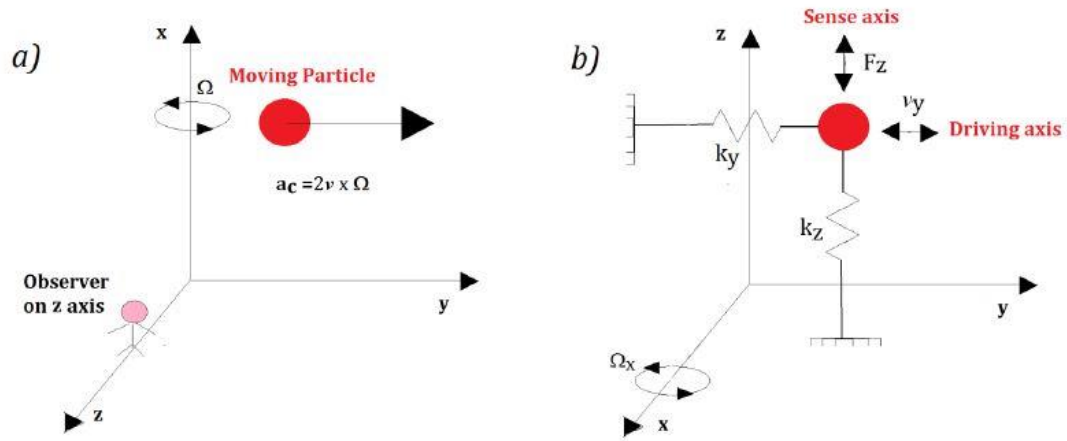


Figure 1.2.5 (a) Coriolis acceleration (a_c) acting on a moving particle; and (b) mass-spring model of a MEMS gyroscope (Passaro et al., 2017).

By retrieving this displacement using a sensing system that can capture this movement by exploiting for example the variations of capacitive plate capacitances (Figure 1.2.6), the gyroscope provides an indirect measurement of the angular velocity around a specific axis of the smartphone which embeds the sensing mass.

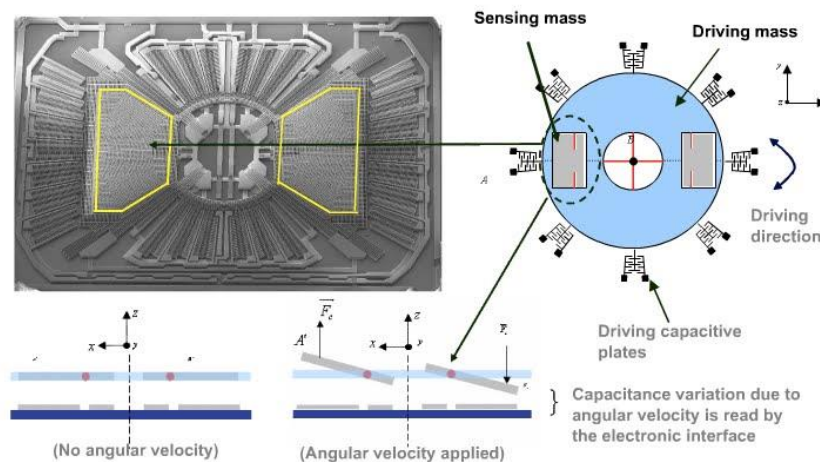


Figure 1.2.6 Example of capacitance variation of a MEMS gyroscope due to the Coriolis force F_c along the z axis, that is read by an electronic interface (https://www.eetimes.com/document.asp?doc_id=1313226#).

1.2.1.1 The smartphone SCG signal

The seismocardiographic (SCG) signal reflects mechanical heart activity during different cardiac phases by measuring the chest wall vibrations (Choudhary, Sharma and Bhuyan, 2018). The SCG has the capability to reflect different cardiac events called either fiducial points or characteristic points, as shown in Figure 1.2.7.

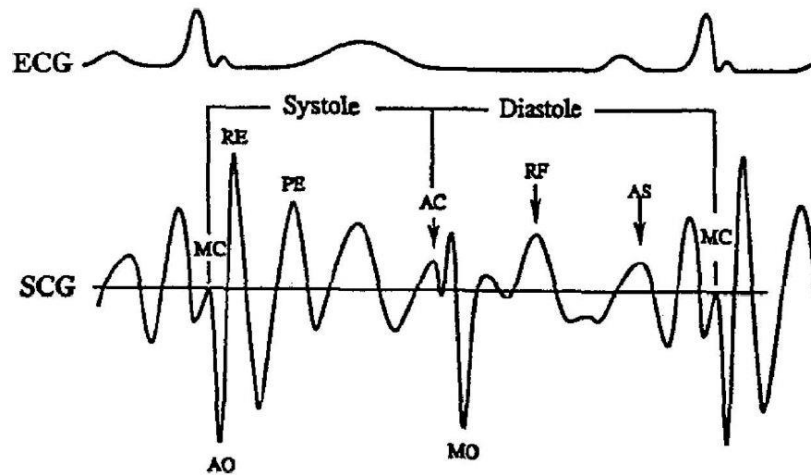


Figure 1.2.7 Simultaneous single channel electrocardiogram (ECG) and seismocardiographic (SCG) recordings (sampling rate, 250 Hz) with following points identified: MC = Mitral (Valve) Closure, AO = Aortic (Valve) Opening, RE = Rapid (Ventricular) Ejection, PE = Peak (Ventricular) Ejection, MO = Mitral (Valve) Opening, RF = Rapid (Ventricular) Filling, AS = Atrial Systole, AC = Aortic (Valve) Closure (Carson A. Wick, 2008).

Landreani and Caiani have recently reported a relevant review regarding the extraction of SCG by using different accelerometers, specifically exploiting embedded IMU sensors in the smartphones. From that work, it appears clear that acquiring SCG using the smartphone is feasible, just positioning the phone in different part of the thorax (sternum, cardiac apex, and navel) and from supine and standing postures, thus allowing extracting reliable measures of heart beat duration useful to determine daily resting heart rate (RHR), ultra-short heart rate variability for detection of stress and respiratory frequency (Landreani *et al.*, 2019).

1.2.2 The smartphone camera sensor

In addition to the MEMS sensors, the introduction of the complementary MOS (CMOS) active pixel sensor (CMOS sensor) "camera-on-a-chip" in 1990s by Eric Fossum and his team allowed putting on the market the actual modern smartphone built-in cameras. Actually, nearly all camera phones use CMOS sensors, due to the largely reduced power consumption compared to charge-coupled device (CCD) type cameras, which are also used, but in few camera phones.

In general, the smartphone digital built-in camera allows the conversion of the light reflected by the scene into a digital image, whose pixel values representing the intensity of light. This is

typically due to the capability of CMOS sensors of capturing intensity images. This conversion happens through a complex chain of operations schematized as in Figure 1.2.8.

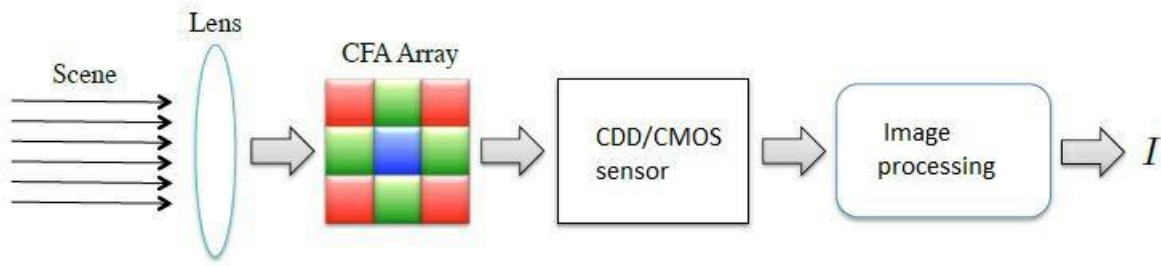


Figure 1.2.8 Digital image acquisition pipeline. Ray-lights reflected from the scene are focused by the lens on a Color Filter Array (CFA) superimposed to a CCD/CMOS sensor. The sensor output is processed and an RGB image is produced as output (Amerini *et al.*, 2016).

The camera acquisition pipeline starts with the light rays reflected by the scene, which are focused on a CCD/CMOS sensor after being mosaicked by a color filter array (CFA). At this level, each pixel is representing only the information regarding one color, i.e. red, green or blue (RGB). At the end, the RGB light intensity image is post-processed generally with pixel interpolation techniques.

Due to all these steps, the generated images will contain some traces left by these conversion operations that can be associated to the lens distortion, using de-mosaicking interpolation kernel, and other phenomena. In addition, each camera sensor has its peculiar noise artifact due to manufacturing process, known as photo response non-uniformity (PRNU).

Mathematically, the captured image I (Figure 1.2.8) by the camera considering the previous considerations can be defined as:

$$I = I^{(0)} + I^{(0)}K + N$$

where $I^{(0)}$ is the noiseless representation of the scene, N is the additive noise term and K is the multiplicative PRNU noise trace (Amerini *et al.*, 2016).

1.2.2.1 The smartphone PPG signal

Photoplethysmography (PPG) is a simple and low-cost optical technique that can be used to detect blood volume changes in the microvascular bed of tissue.

Usually, there are two main PPG operational configurations: transmission ('trans-illumination') mode where the tissue sample (e.g. fingertip) is placed between the source and detector, and reflection ('adjacent') mode where the LED and the detector are placed side-by-side (Figure 1.2.9).

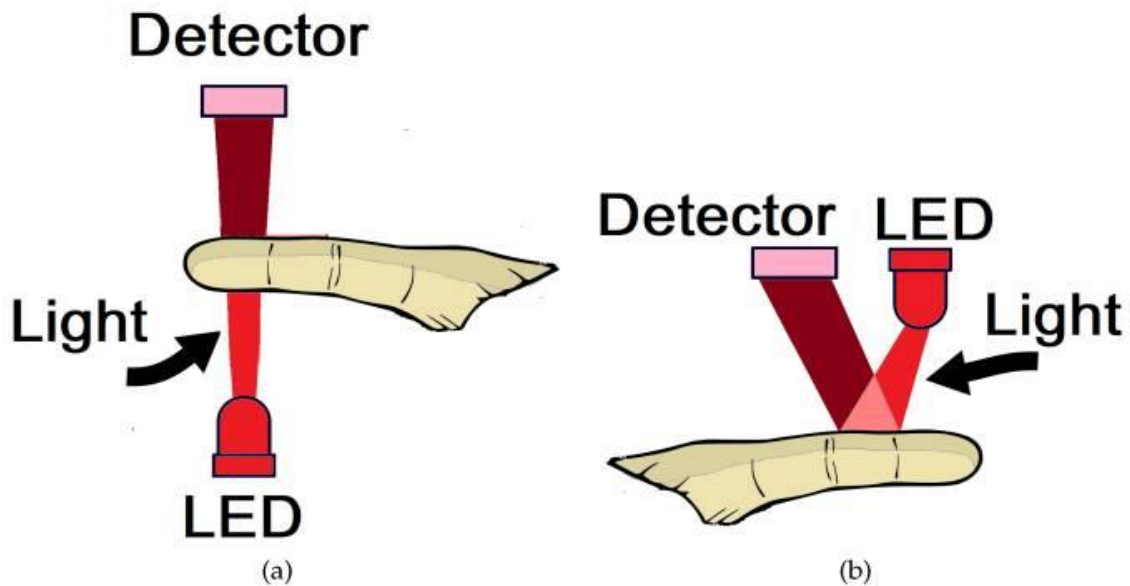


Figure 1.2.9 Example of photo detector and LED for transmission mode configuration (a) and photo detector and LED combination in reflection mode (b) (Moraes et al., 2018).

In particular, the reflection PPG is a technique which exploits the fact that blood absorbs more light than surrounding tissues, and variations in blood volume affect the reflected signal components of a suitable optical probe (Figure 1.2.10).

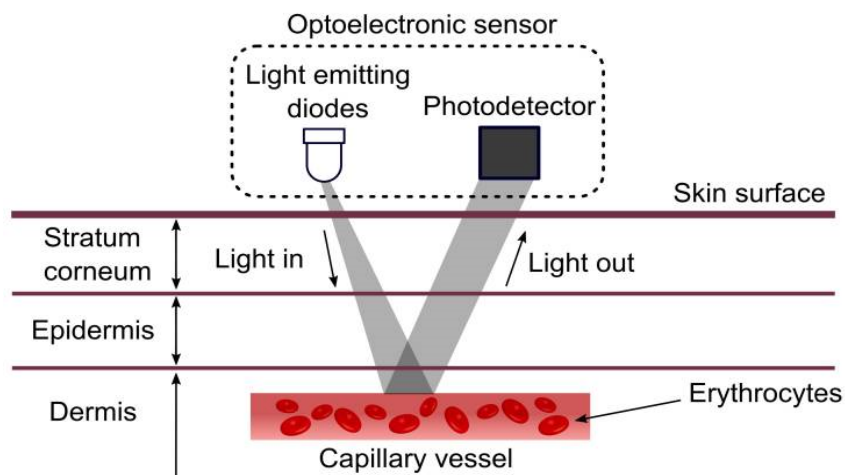


Figure 1.2.10 The photodetector captures the variations (Light out) of the light emitted by the LED (Light in) due to the blood volume changes (Moraes et al., 2018).

Thus, replacing the optical probe with a digital RGB camera (paragraph 1.2.2) and using a flashlight as light source, it is possible to acquire the PPG signal simply by the support of a smartphone (Figure 1.2.11). This new technique is called PPG imaging (Jonathan and Leahy, 2011).



Figure 1.2.11 An HTC hero used reflection mode for PPG acquisition (Abinaya, Prabhakaran and Jaisankar, 2014).

The PPG waveform includes a pulsatile ('AC') physiological waveform, attributed to cardiac synchronous changes in the blood volume within each heartbeat, that is superimposed on a slowly varying ('DC') baseline with various lower frequency components, attributed to respiration, sympathetic nervous system activity and thermoregulation. As shown in Figure 1.2.12, the AC component is superimposed on a much larger quasi-DC component that relates to the tissues and average of blood volume within the vessels. It represents the increase in light absorption (attenuation) associated with the increase in microvascular blood volume.

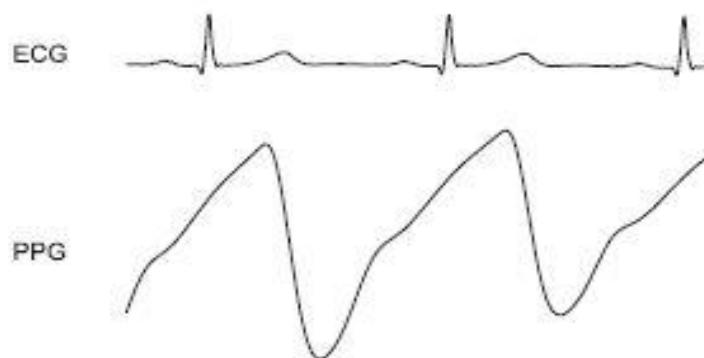


Figure 1.2.12 In the figure, the pulsatile (AC) component of PPG and the corresponding ECG are shown (Allen, 2007).

Therefore, the smartphone represents an attractive opportunity for developing biomedical applications aiming at the extraction of common medical biomarkers, taking the advantage of having both MEMS and C-MOS sensors embedded in a single device,

1.3 SMARTPHONE AS DEVICE FOR INVESTIGATING CARDIOVASCULAR SYSTEM

Statistically, one of the most emergent healthcare sectors among the mHealth app companies is that concerning the cardiovascular system, according to a survey conducted on mHealth app developers (Figure 1.3.1) (8).

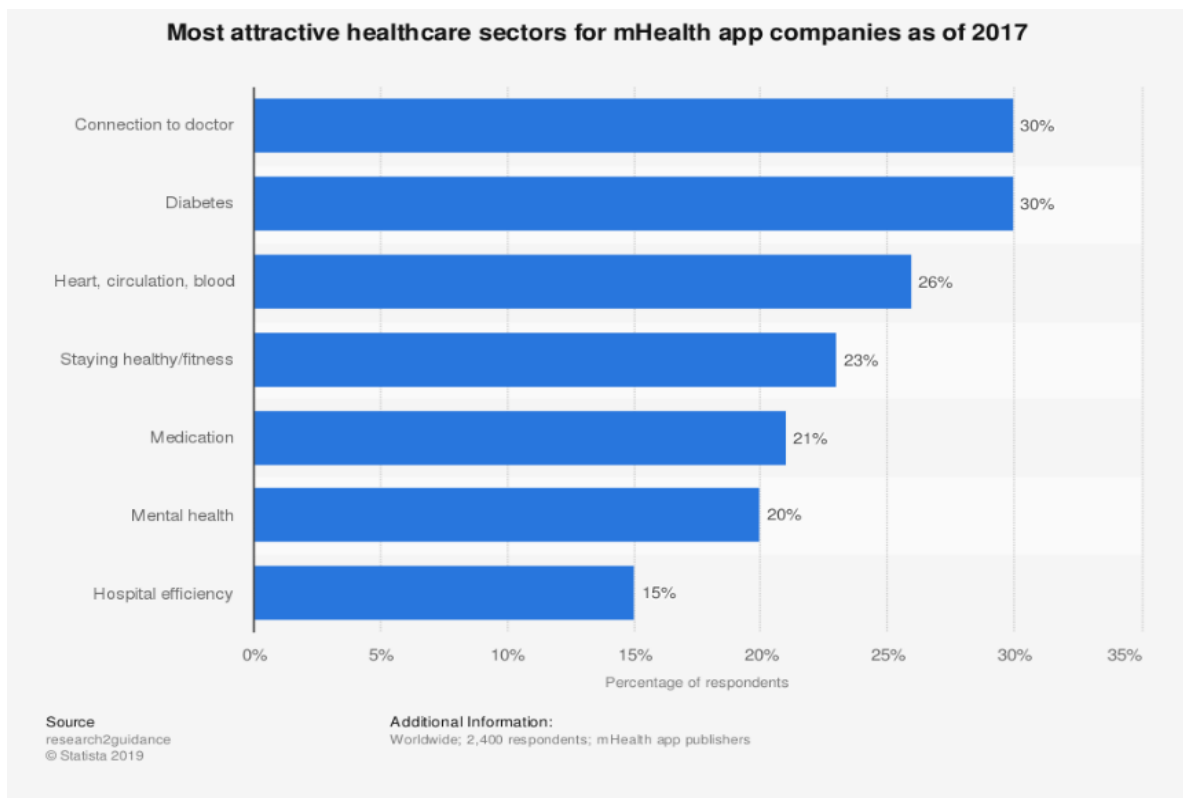


Figure 1.3.1 Statistic showing the most attractive healthcare sectors for mHealth app companies as of 2017.

An example of commercially available app in this field of application is “FibriCheck” (<https://www.fibrichk.com/>), which potentially could detect episodes of atrial fibrillation by scanning the user’s heart rate variability (HRV), exploiting the photoplethysmography (PPG) signal retrieved by the smartphone camera (Figure 1.3.2).



Atrial fibrillation

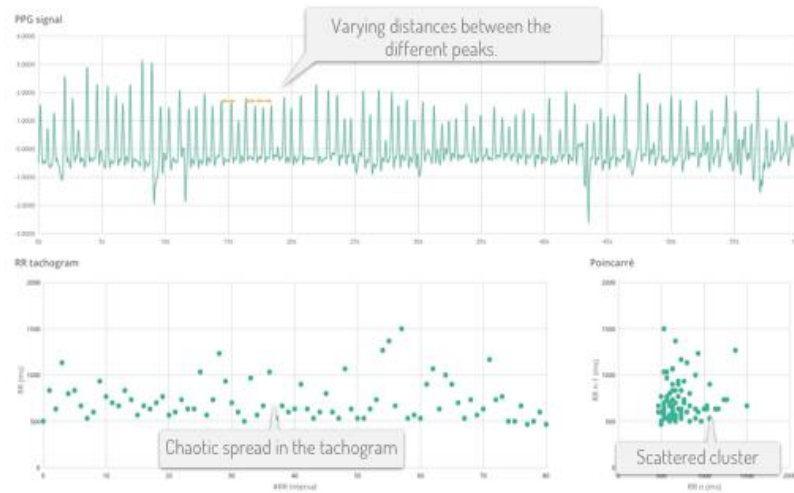


Figure 1.3.2 Commercial FibrCheck app: example of PPG, tachogram and poincaré signals analyzed to detect atrial fibrillation.

Another example is the “Instant Heart Rate” app by Azumio company (<https://www.azumio.com/s/instantheartrate/index.html>), which exploits the PPG signal to extract user’s heart rate (Figure 1.3.3).

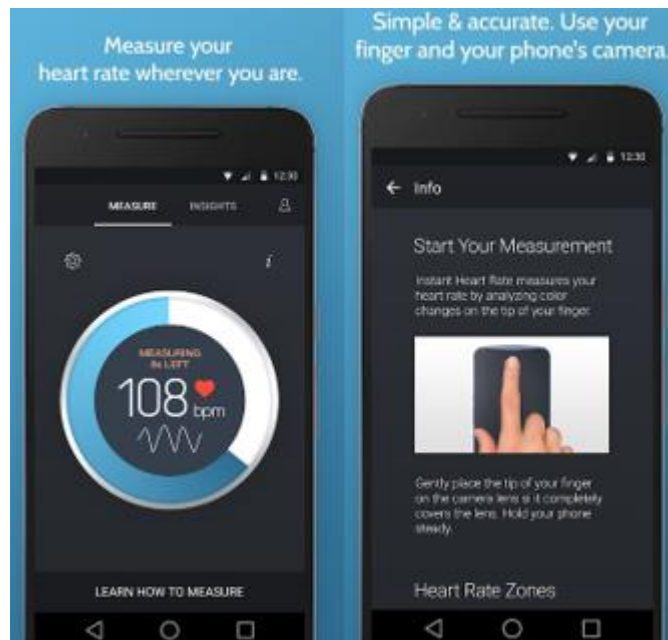


Figure 1.3.3 “Instant heart rate” app: heart rate detection using PPG signal through smartphone camera.

These apps show the potentiality of smartphones in obtaining physiological parameters, such as heart rate (HR) and heart rate variability (HRV) by the usage of smartphone camera.

The importance of the new prospective concerning the smartphone as biological sensors to track, monitoring and detecting biomarkers which are correlated to cardiovascular problems is underlined by a WHO study, which stated:

“ischaemic heart disease and stroke are the world’s biggest killers, accounting for a combined 15.2 million deaths in 2016. These diseases have remained the leading causes of death globally in the last 15 years.” (<https://www.who.int/news-room/fact-sheets/detail/the-top-10-causes-of-death>, update to 24 May 2018).

As matter of fact, physiological parameters such as HR, RHR (resting heart rate) and HRV, which could be detected as shown previously using a smartphone app (Figure 1.3.2 and Figure 1.3.3), are known for being strictly correlated to cardiovascular diseases (CVD) and useful predictors of CV problems. In this context, Zhang et al. demonstrated the correlation between the RHR with coronary artery disease and stroke (Dongfeng Zhang MD, Weijing Wang MD, 2012) and Caetano et al. showed the importance of a low HR through an epidemiologic study, where high RHR was found as independent predictor of CVD and general mortality (Caetano and Delgado Alves, 2015).

1.3.1 Smartphone for HR and HRV detection

The heart rate (HR) is defined as the number of heartbeats during a time period of one minute and it is measured as beat for minute (bpm). The heart rate variability (HRV) instead is the fluctuation in the time intervals between adjacent heartbeats (Shaffer and Ginsberg, 2017), which is a reliable reflection of the many physiological factors modulating the normal rhythm of the heart, particularly important to observe the interplay between the sympathetic and parasympathetic nervous systems (Acharya *et al.*, 2006).

Historically, these two physiological parameters to study human cardiovascular system and the response of the heart speed to hemodynamic and emotional changes are derived by the use of the electrocardiogram (ECG), which is considered the gold standard to assess HR and HRV. As anticipated in the previous paragraph, new technologies based on the use of a smartphone are focused on obtaining a feasible evaluation of these physiological measures, with a particular focus on the embedded sensors represented by the camera, to capture the PPG signal (paragraph 1.2.2.1), and the inertial sensors, to sense the SCG signal (paragraph 1.2.1.1).

1.3.2 Smartphone PPG for HR and HRV detection

Already in 2010, Orbac *et al.* tried to detect HR using an HTC Tatum Android smartphone, exploiting the smartphone PPG. A maximum error of 2 bpm, an accuracy over 91% and good consistency among 50 subjects were found (Pelegris *et al.*, 2010). One year later, Jonathan and Leahy tested the feasibility of obtaining the PPG with a Sony Ericsson model W705 and detecting the HR passing through the Fourier's transform, finding good consistency using the green channel, as shown in the Figure 1.3.4 (Jonathan and Leahy, 2011).

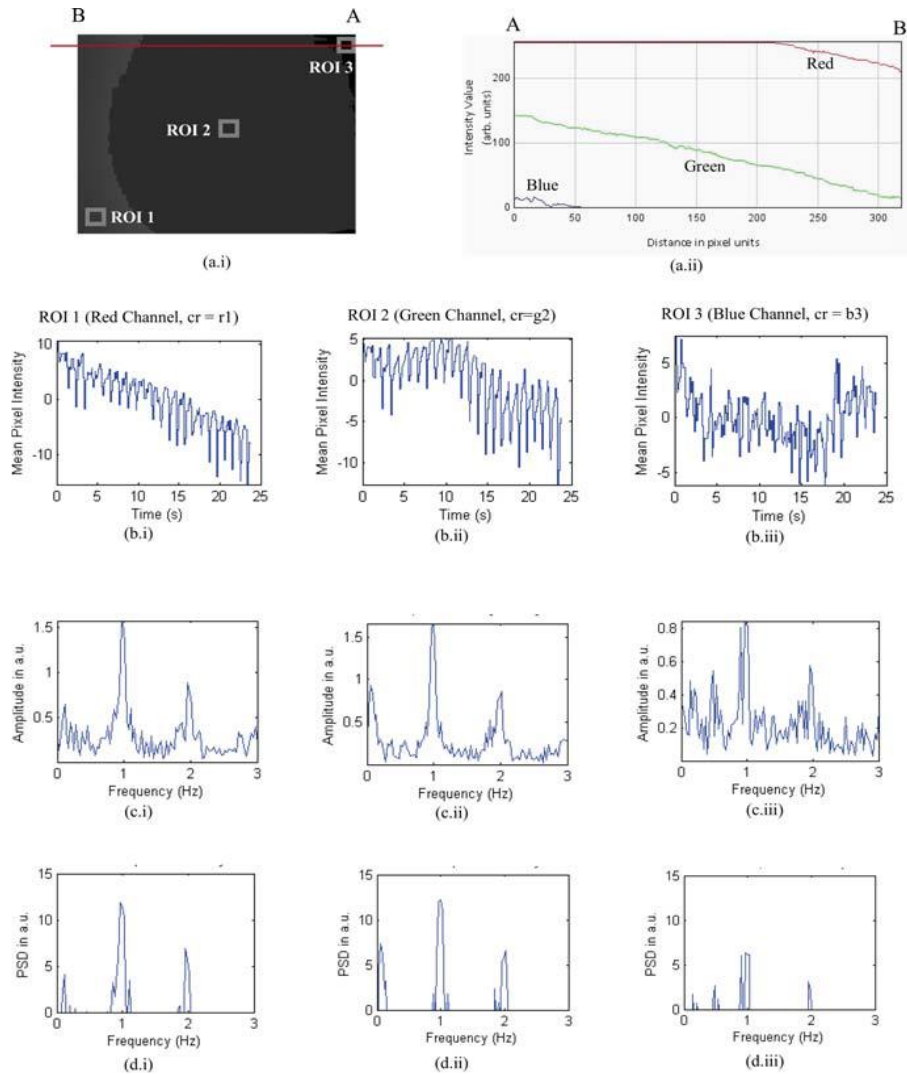


Figure 1.3.4 PPG ac signal processing results. (a.i) Typical single frame measuring 320x240 pixels showing selected 3 ROI's (grey squares) along a left diagonal. (a.ii) RGB profiling along observation line (in red) marked AB where A is towards the WLED position confirming green channel signal can be detected throughout the imaging area while red and blue channels detected in marked zones. (b) Raw PPG signal traces, (c) FFT spectra and (d) PSD spectra for (i) ROI 1 Red, (ii) ROI 2 Green and (iii) ROI 3 Blue channels (Jonathan and Leahy, 2011).

More recently, Matsumura et al. described the feasibility of using smartphone iPhysiometer app for a PPG beat-to-beat and frequency analysis to extract the HR, despite the presence of motion artifacts exploiting an iPhone 4 as represented in the Figure 1.3.5 (Matsumura *et al.*, 2014).

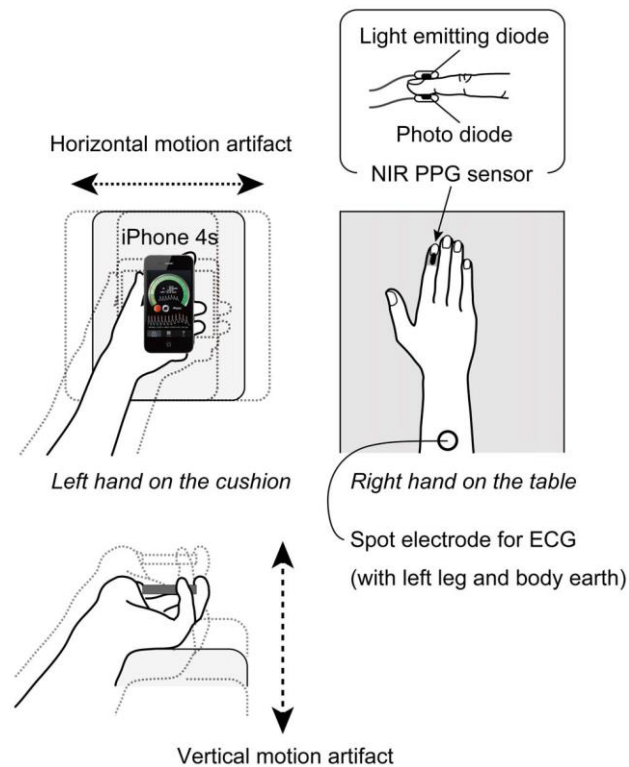


Figure 1.3.5 Schematic drawing of the experimental setup. The directions of the horizontal and vertical added motions are also shown. NIR = near-infrared, PPG = photoplethysmogram, and ECG = electrocardiogram (Matsumura et al., 2014).

In the 2015, Peng et al. concentrated their study on the possibility of retrieving the typical time domain and frequency domain-based parameters (Table 1.3.1) to analyze the HRV of 30 subjects (20 males and 10 females) from HTC S510e smartphone PPGs. Their results suggested that the smartphone can be a potential use for HRV measurement at resting and would be applied in low-cost healthcare applications, underlying the crucial importance of peak-detection phase for the parameter extraction (Peng *et al.*, 2015).

The Table 1.3.2 summarizes the literature in research of the last years regarding the use of smartphone PPG to investigate cardiovascular system. This insight carries out the real possibility of assessing the HR and HRV using different smartphone brands, accompanied by the proofs of feasibility and accuracy of a time and frequency domain analysis to extract the HR and HRV parameters.

Table 1.3.1 Commonly used HRV parameters.

Parameters to study HRV		Description (NN = “normal-to-normal intervals”)
Time-domain	AVNN	Average of all NN intervals
	CV	Coefficient of variation of NN intervals. The ratio of the standard deviation to the mean
	SDNN	Standard deviation of all NN intervals
	SDANN	Standard deviation of the averages of NN intervals in all 5-minutes segments of the entire recording
	RMSSD	Root mean square of successive differences between adjacent NN intervals
	SDSD	Standard deviation of successive differences between adjacent NN intervals
	NN50	Number of pairs of successive NN intervals that differ by more than 50 minutes
	pNN50	Proportion of NN50 divided by total number of NN intervals
Frequency-domain (5 minutes)	TP	Total power (≤ 0.4 Hz)
	VLF	Very low frequency power (≤ 0.04 Hz)
	LF	Low frequency power (0.04 – 0.15 Hz)
	HF	High frequency power (0.15 – 0.4 Hz)
	LF/HF	Ratio of LF to HF
	nLF	Normalized LF = $LF / (TP - VLF)$
	nHF	Normalized HF = $HF / (TP - VLF)$
Normalized HF = $HF / (TP - VLF)$	SD1	Standard deviation of short diagonal axis in Poincaré plot
	SD2	Standard deviation of long diagonal axis in Poincaré plot

Table 1.3.2 An overview of the works in literature to extract PPG signal through the smartphone camera.

Authors	Objective	Subjects	Smartphone	Camera fps	Resolution and ROI dimension (if present)	Chosen channel for PPG	Analyzed signal duration	Validation instrumentation	Results
Pelegris et al. 2010	Detect HR using smartphone PPG	50 people between 21 and 55 years old. Average 31,3 years.	HTC Tatum Android 1.6	11-12	-	-	9 seconds average	Commercially available pulse oximeter	2 BPM maximum error over 91% accuracy and good consistency. 4.3% average error
Adibuzzaman et al. 2014	Monitoring of HR, oxygen saturation and perfusion index using a smartphone camera	9 healthy subjects and between the age of 21 and 32. Seven of them are male and two of them are female	Galaxy Nexus	29.5	1280x720	Green	30 seconds	Commercially available pulse oximeter	Accuracy of the HR is related to the minimum peak to peak distance for peak detection and frame rate or sampling rate. New model approach for perfusion index and oxygen saturation.
Jonathan et al. 2011	Feasibility of Cellular phone-based PPG	1 healthy african descent volunteer	Sony-Ericsson model W705 with 4 GB memory card	30	300x240 and 8x8 ROI	Green	25 seconds	Commercially automatic blood pressure monitor(BPM1C, Kinetic Medical Devices, UK)	Green channel more consistent and best compromise between strength and localization in all frames and pixels for calculating FFT and PSD of PPG
Gregoski et al. 2012	Smartphone-based PPG for HR detection	14 adults aged 18–59 (11 females, 6 non-Hispanic Whites, 3 Hispanic Whites, and 5 Non-Hispanic AfricanAmericans)	Motorola Droid	20	176x144	YUV PLANE	15 minutes	Nonin Onyx II model 9560BT ambulatory finger pulse oximeter and ECG	HRs obtained from smartphone and ECG correlation $r > .99$ and $< .1$ bpm the SEEs and between smartphone and Nonin $r > .99$ and SEEs < 2.09 bpm. $\geq 95\%$ data points in the limits of agreement for Bland-Altman.
Abinaya et al. 2014	Measurement of HR using smartphone	--	HTC Hero	25	820x400	Red channel	10 seconds	--	FFT plot of fingertip video has been achieved
Di Santo et al. 2018	Smartphone-based PPG for assessment of ulnar artery patency	Patients from the hospital's coronary care unit, inpatient cardiology service and Regional Referral Centre/Day Unit	iPhone 4s running Instant-heart rate app	--	--	--	2 minutes	Conventional plethysmography	smartphone heart rate-monitoring application to assess ulnar artery patency had superior diagnostic accuracy than the clinical standard (modified Allen test)
Scully et al. 2012	Physiological parameter monitoring using smartphone-based PPG	--	Motorola Droid	25	720x480 and 50x50 ROI	Green	2 minutes	ECG recordings, 5-lead electrode configuration. A respiration belt to monitor breathing rate (Respirace Systems, Ambulatory Monitoring Inc.) Sampling rate of 400 Hz. A commercial reflectance pulse-oximeter (Radical SET™, Masimo) was placed on the left ring finger to record SpO2 at a sampling rate of 1 Hz.	Estimation of HR and breathing rates using intensity changes in the green band of the video signal provided results that were accurate compared to their respective standards. HRV measurements derived from an ECG and the mobile phone were also shown to agree favorably. Decreases in oxygen saturation from the breath holding test led to similar decreases in our SpO2 computation from the mobile phone data.
Kurylyak et al. 2012	Smartphone-based PPG	10 subjects between 26 and 60 years old	HTC HD2, Nokia 5800, iPhone4, Samsung Galaxy S i9000	25, 29, 30, 30	352x288, 640x480, 480x272, 720x480	Red channel	10 seconds	CMS50DL Finger Pulse Oximeter SPO2 Monitor using two fingers of left hand	1.03% error in HR with 4 different smartphones using red channel and ad-hoc algorithms to extract PPG and verify correct finger contact with the camera.
Ferrer-Mileo et al. 2015	HRV estimation using smartphone-based PPG	10 healthy subjects	Motorola MOTO x or SAMSUNG s5 (Chosen randomly)	30	640x480	Green	100 seconds	ECG electrodes, using the standard I lead, were attached to the subjects. A Biopac SS4LA photoplethysmograph probe was attached to the right or left index finger chosen at random. These two signals were acquired at 5 kHz using a BIOPAC MP36E acquisition system.	Fiducial point E the best. sPPG not suitable due to low resolution and not stable fps.
Matsumura et al. 2013	HR detection and Normalized Pulse Volume using iPhysiometer app in the	12 undergraduate male volunteer students, recruited through flyers, aged 20.6 ± 0.76	iPhone 4s	30	192x144	Green	72 data points (three conditions, two repetitions, 612)	Pulsioximeter and ECG of laboratory	Green light is the best against motion artifact to detect HR and lnNPV

	presence of motion artifacts	(SD) years					participants)		
La'zaro et al. 2015	Respiratory rate derived from smartphone camera PPG	30 healthy subjects (22 men and eight women, between 20 and 26 years old)	iPhone 4S, iPod 5, HTCOneM8	--	ROI 50x50	Green	60 seconds	--	Normal ranges of spontaneous respiratory rates (0.2–0.4 Hz) can be accurately estimated from smartphone-camera-acquired pulse photoplethysmographic signals based on pulse width variability or pulse rate variability. Up to 0.6 Hz when using the iPhone 4S or iPod 5 devices.
Krivoshei et al. 2016	Smartphone detection of atrial fibrillation	80 consecutives in- and outpatients at the University Hospital Basel.	iPhone 4s	--	--	Green	From 2 to 5 minutes	HR monitor chest belt (Wahoo TICKR, Model SHRMI1G)	The highest sensitivity and specificity was achieved using the combination of the indices nRMSSD and SD1/SD2 with the tachogram filter. By prolonging the analyzed interval from 2 to 5 min, we reached a sensitivity and specificity of 95%
Liu et al. 2015	Smartphone PPG for PPT estimation	14 adults aged 18–59. 11 females, 6 non-Hispanic Whites, 3 Hispanic Whites, and 5 Non-Hispanic AfricanAmericans	--	30	1280x800	Green channel for fingertip and red channel for temple	10 seconds	Experiment 1: PTT obtained using two PPG modules (both TP-TSD200A from BIOPAC). Experiment 2: used one TP-TSD200A PPG module and one TP-TSD155C ECG system, both from BIOPAC	High-performance in detection of maxima and minima in PPGi signal with 98% SE and 97% PPV. SFP algorithm is more time-consuming compared to other techniques. Therefore, to be implemented in the form of a smartphone application, the SFP algorithm needs to be optimized

1.3.3 Smartphone SCG for HR and HRV detection

In the 2011, Kwon et al. tested the possibility of extracting the HR through the SCG signal, using the embedded MEMS accelerometer in the iPhone 4. They demonstrated the capability of the smartphone in estimating HR, obtaining good consistency and correlation after a linear regression analysis compared to ECG reference signal (Kwon *et al.*, 2011). During the following years, this preliminary study was confirmed by other works which demonstrated the capability of the accelerometers to detect heart rhythm parameters strongly correlated with the gold standard measures (Laurin, Blaber and Tavakolian, 2013; Jafari Tadi *et al.*, 2014).

In the 2015, Landreani et al. used two iPhone 6 smartphones to retrieve the SCG signals exploring two different subject positions, standing and supine, with the aim of measuring beat-to-beat HR. In the supine pose, one smartphone was placed on the belly above the navel (POS2) and the other placed on the thorax in correspondence of the midclavicular line and fourth intercostal space (POS1). During the standing position, the subjects hold only one smartphone at the POS1 (Figure 1.3.6).

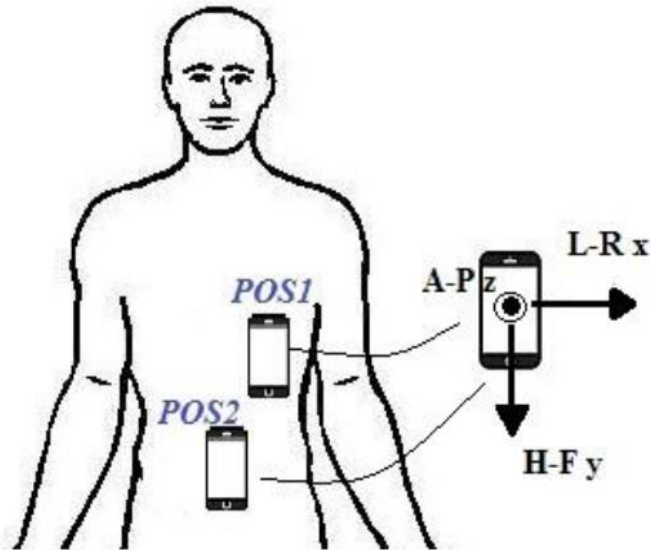


Figure 1.3.6 Schematization of the two positions and orientation of the mobile devices used during acquisition: in supine, two smartphones were simultaneously placed in POS1 and POS2; in standing, the smartphone was kept by the subject in POS1 (Landreani et al., 2015).

For the beat-to-beat analysis of the SCGs obtained from the POS1, an ad-hoc algorithm was developed in order to detect the local minima during each heartbeat, that in the POS1 SCG represent the isovolumetric contraction of the heart (IVC, Figure 1.3.7). After the algorithm application, they obtained a feasibility of 100% for the supine position with the phone on the POS1, which meant all acquired signals were processable, with an accuracy of fiducial points detection of 98.6% (calculated as the ratio between number of detected peaks over the total peaks). For the standing position, two signals were discarded, with a resulting feasibility of 78% and an accuracy of 94.6 %. From the IVC-IVC beat extraction, they derived a strong correlation ($r^2 > 0.99$) with the RR series of the ECG for the POS1 during supine condition, with no significant bias with respect to the RR measurements and narrow limits of agreement ($\pm 2SD$: POS1 ± 20 msec). For the standing posture, they obtained a linear correlation coefficient of 0.989, no significant bias and larger limits of agreement ($\pm 2SD$: ± 38 msec) than in supine. These results showed the feasibility of using the smartphone SCG for the HR beat-to-beat analysis, substantially for both standing and supine condition.

Although the possibility to use the accelerometer signals as an alternative instrument to investigate HR or HRV without the use of the current gold standard measures was well-established, what seems to lack is a standard methodology to acquire the SCG signal. The quality of the signal and the analysis type is strongly dependent on the waveform shape assumption and on the position of the accelerometer sensor on the body for the acquisition.

Moreover, the smartphone SCG signal feasibility is strictly related to the hardware, which embeds the sensor (Landreani and Caiani, 2017).

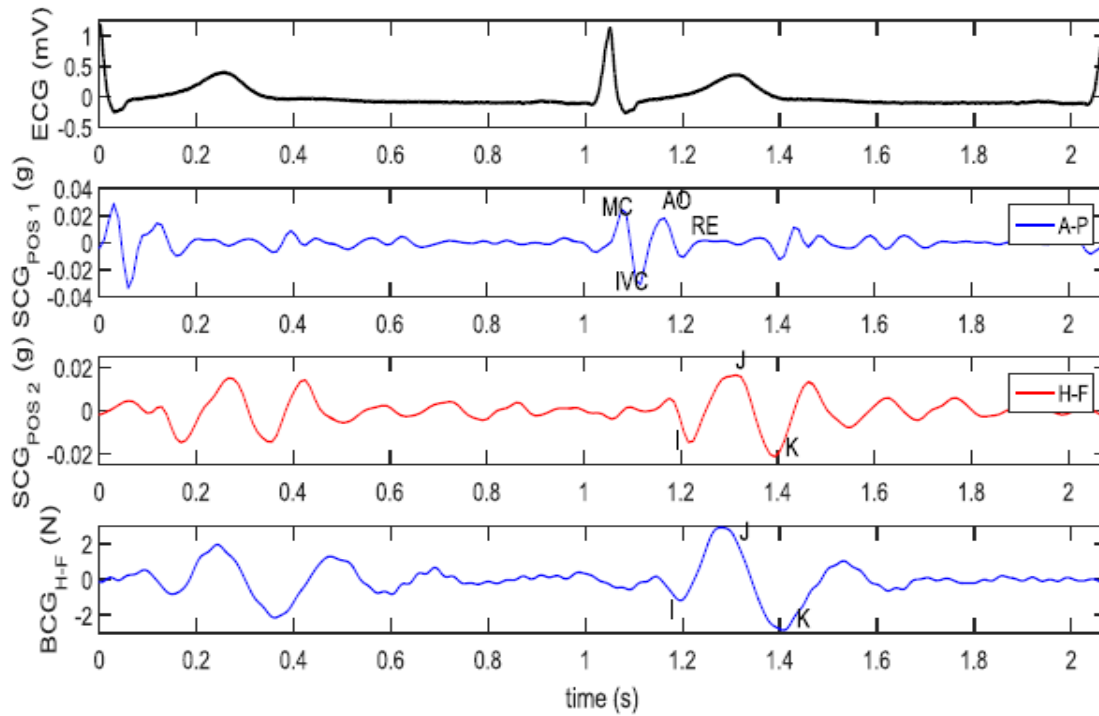


Figure 1.3.7 Example of the ECG, simultaneous filtered SCG signals, obtained from POS1 (A-P) and POS2 (H-F), and BCG (H-F), with the relevant adopted nomenclature (Landreani *et al.*, 2015).

Besides the HR and HRV, another important parameter which can be used to investigate cardiovascular problems is the so-called pulse transit time (PTT). As the HRV, the PTT parameter needs a beat-to-beat analysis of two synchronized signals, one proximal and one distal, such as the SCG and PPG (Figure 1.3.8), thus underlining the importance of having signal waveforms that allow fiducial point detection (Zhang and Zhang, 2005; Shin, Lee and Lee, 2009). Thus, to derive the PTT signal by the use of the smartphone technology, an app which senses simultaneously the PPG and the SCG signal is necessary (Wang *et al.*, 2018).

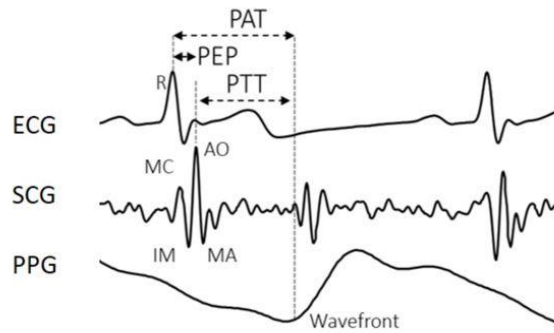


Figure 1.3.8 PTT measurement from SCG and PPG using Seismo app on Google Pixel smartphone. The temporal result of PAT differs from PTT due to the inclusion of PEP time (Wang et al., 2018).

1.4 APPS FOR ACQUISITION OF SCG AND PPG

In the app portals, a specific application available to transform the smartphone in a dedicated tool to acquire the SCG and/or PPG signal seems actually to be missing. For a non-biomedical purpose, there are different apps that allow the visualization of the signals coming from the 3-axis MEMS accelerometer or gyroscope, serving for various scopes. An example is the freely available “Hamm Seismograph” app (Figure 1.4.1), that allows visualizing singularly or altogether the acquired signals.

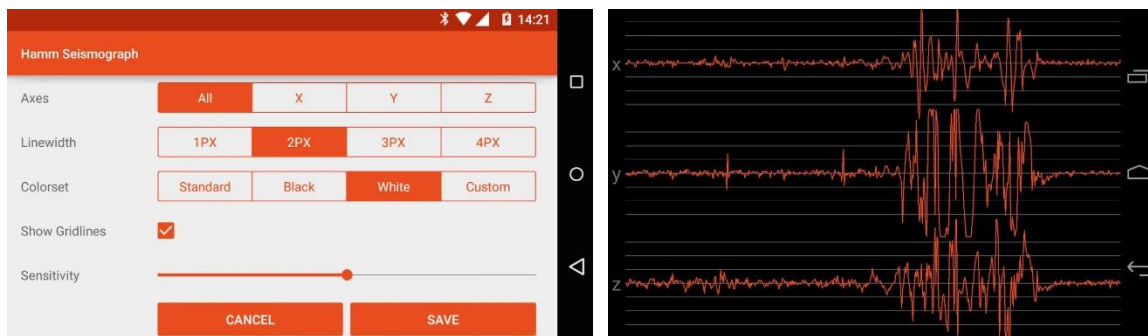


Figure 1.4.1 Hamm Seismograph app: the app allows the real-time visualization of 3-axis of smartphone accelerometer. The app ratings amounts to 4.4 out of 5 total, with 128 reviews on the Google Play Store (<https://play.google.com/store/apps/details?id=de.inovation>).

Another commercially available app to sense the smartphone motion is “Sensor Kinetics” (Figure 1.4.2). This app allows the user to verify what kind of motion sensors are inside the smartphone unit and to test and visualize them a in real-time graph, as shown in the Figure

1.4.2. The paid version Sensor Kinetics Pro gives the user the ability to save and share sensor data and to apply filters to the data stream.

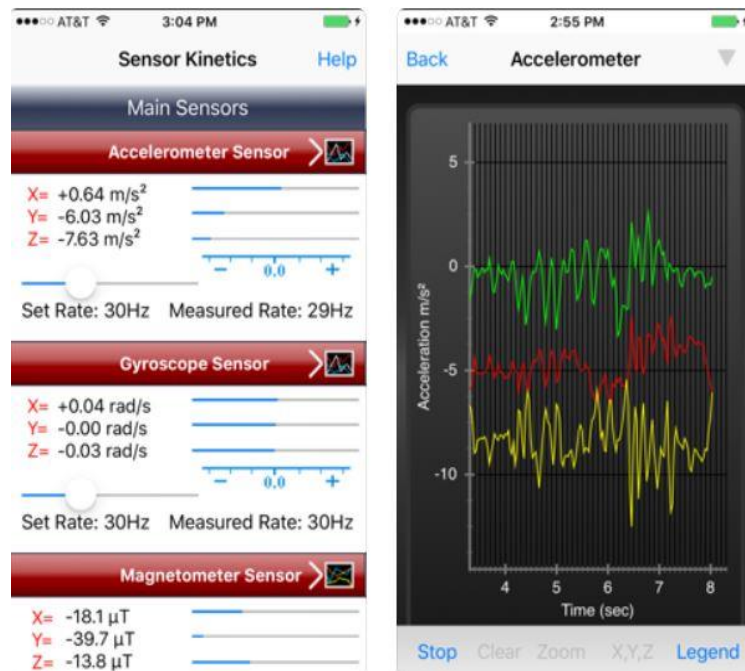


Figure 1.4.2 The Sensor Kinetics app screenshots. This app has a rating of 4.2 out of 5 total with 13 reviews <https://apps.apple.com/us/app/sensor-kinetics/id579040333>.

Actually, the number of commercially available apps which take advantage on the smartphone motion sensors seems to be considerably higher respect to the apps for displaying and save simply the PPG signal, without aiming to the typical HR or HRV screening (Figure 1.3.2 and Figure 1.3.3). Indeed, there is no trace of well-known available apps on the different stores for this purpose.

The same considerations can be done for mobile applications for the simultaneous acquisition and visualization of SCG and PPG, perhaps with the opportunity of collecting the acquired data as well.

Thus, what seems actually to be lacking is an app to acquire biological signals which is nearer as idea of usage to the final user. In practice, the applications found on the general app stores are restricted to the use imposed by the developers, without the possibility for the end user to “move freely” inside the application, except for paid versions. Similarly, in research the implemented apps are concentrated typically on one of the cited acquisition methods, such as either PPG or SCG, or SCG and PPG simultaneously, without separated modules for each of

these, perhaps inside a single application, and generally no huge efforts appear being done about app usability design and accuracy testing.

1.5 AIM OF THE THESIS

As emerged from the literature, the smartphone has the capability to be transformed into a mobile standalone device to capture different physiological signals by the availability of its embedded sensors, such as the camera and the IMU subsystems. From these signals, several clinical biomarkers, such as HR, HRV, and further the PTT, can be studied in an easy way, in an attempt to widen the possibility for self-monitoring thus providing the basis for increased patient empowerment. Lacking a specific application that allows acquiring both SCG and PPG and targeted to a usability design approach, the aim of this thesis was to develop such a versatile, user-friendly and multi-purpose mobile smartphone application for the acquisition of SCG and PPG, both singularly or simultaneously, flanked by the design analysis from the user point of view, to enhance the persuasive capability of this new biomedical technology in familiar environments (e.g. at home, during normal routine, etc...). The tool resulting from this study will provide the researcher with an incredible opportunity to conduct research in various experimental protocols in order to validate the biomarkers that can be obtained by the analysis of SCG and PPG signals (alone or in combination) and to analyze the potentiality of this technology in the e-health patient engagement.

In the next section (*2. Materials and methods*), the hardware and software components for this app framework are explained, from a practical and design point of view, while in the third chapter (*3. The experimental protocols and outcome analysis*) two different experimental protocols for a first app evaluation will be exposed. Successively, the experiment results will be shown (*4. Results*) together with their discussion in the final section (*5. Discussions and conclusions*), that will also consider possible limitations and future implications of this work.

2 MATERIALS AND METHODS

To design a mobile app, a common tool consists in an integrated development environment (IDE) that combines with a software development kit (SDK) and a smartphone to run the developed app.

In this section, the work behind the fulfillment of this point will be described through two principal paragraphs. The first one will cover the hardware and software components used for the realization of the mobile app able to acquire the PPG and SCG signals, whereas the second paragraph will explain the design of the application combined with the description of the planning choices.

2.1 MATERIALS: SMARTPHONE HARDWARE AND THE INTEGRATED DEVELOPMENT ENVIRONMENT (IDE)

A mobile application, commonly called “*app*” (a term which was popularized by Apple in 2008), is “... *a type of application software designed to run on a mobile device, such as a smartphone or tablet computer. Mobile applications frequently serve to provide users with similar services to those accessed on PCs. Apps are generally small, individual software units with limited function.*” (<https://www.techopedia.com/definition/2953/mobile-application-mobile-app#:~:targetText=A%20mobile%20application%2C%20most%20commonly,to%20those%20accessed%20on%20PCs.>).

Starting from this definition, an app is therefore a software composed of limited set of actions that the user can benefit by the means of the smartphone as actuator. Thus, the smartphone is technically the physical interface between the user and the application.

Particularly for a biomedical application, the smartphone entity covers a fundamental role, because it has the responsibility of acquiring signals from a physiological system, which implies the need of accurate and different sensors. Moreover, the feasibility of this task implies higher responsibility than other general applications, because it is focused on capturing important biomarkers (paragraph 1.3, chapter 1) such as HR and PTT, which could be related to the health of the user.

2.1.1 The smartphone hardware

As stated in the previous paragraph, to run a mobile app a smartphone device is required. For this thesis, the choice of using a Xiaomi smartphone Redmi note 7 (4 + 64 GB) was done (Figure 2.1.1).



Figure 2.1.1 Smartphone: Android Xiaomi Redmi Note 7. Image available on: <https://www.androidpit.com/redmi-note-7-review>.

The Redmi Note 7 is an Android smartphone device produced by Xiaomi Company, actually covering a large segment of the smartphone market (9). This model assembles a memory of 64 GB, a 4 GB RAM and an Octa-core 4 + 4 cores as CPU (Table 2.1.1). Actually, the Redmi Note 7 is available on the market at 199,90 euro, cheaper than other smartphones of the last generations.

Table 2.1.1 Redmi Note 7 (64GB + 4) specification. Data available from: https://en.wikipedia.org/wiki/Redmi_Note_7.

Redmi note 7 (4+64 GB) general specification	
CPU	Octa-core 4 + 4 cores (4x 2.2 GHz Kryo 260 Gold – Cortex-A73 derivative) (4x 1.8 GHz <u>Kryo 260</u> Silver – Cortex-A53 derivative)
GPU	650 MHz Adreno 512
Storage option	4+64GB
	RAM: Dual channel LPDDR4x, ROM: eMMC 5.1
Screen	6.3" 19.5:9 "dot notch" 2340x1080 FHD+ LCD; 409ppi
Battery	4000mAh non-removable
Fast charge	Quick Charge 4
Cellular network: GSM	Band 2/3/5/8
Cellular network: WCDMA	Band 1/2/4/5/8
Cellular network: CDMA	N/A
Cellular network: TD-SCDMA	N/A
Cellular network: LTE-FDD	Band 1/2/3/4/5/7/8/20/(28)
Cellular network: LTE-TDD	Band 38/40
Wi-Fi	2.4/5 GHz IEEE 802.11a/b/g/n/ac
Radio	FM
Bluetooth	Bluetooth 5.0
VoLTE	Yes
3.5mm Jack	3.5mm jack
USB	Type C
Navigation	GPS, A-GPS, GLONASS, BeiDou
Expansion card	Dual sim DSDS 3-choose-2 4G+4G hybrid card tray; expandable storage with Micro SD card up to 256GB
Dimension	159.21 mm x 75.21 mm x 8.1 mm
Weight	186g
Software	MIUI 10; Android 9

2.1.1.1 The smartphone hardware: Redmi Note 7 sensors

The smartphone Redmi Note 7 embeds different sensors in a single unit. In particular, two sensors are described in this paragraph: the mobile digital camera, strictly connected with the smartphone video specifications, and the IMU module, which are embedded on the Redmi Note 7 (Table 2.1.2).

Table 2.1.2 Redmi note 7 embedded sensors with specifications. Data available from: <https://www.devicespecifications.com/en/editor-review/91b096/8>.

Redmi Note 7 sensor	Sensor technical specification
Back main camera	48MP 0.8µm Samsung ISOCELL GM1 f/1.8
Back secondary camera	5MP (f/2.4) (depth sensor)
Front camera	13MP (f/2.0)
Infrared	Yes
Accelerometer and gyroscope	BOSCH 2062701. Accelerometer: max range:156.906 m/s ² ; resolution: 0.002 m/s ² ; current: 0.18 mA. Gyroscope: max range: 2000°/s; resolution: 0.06°/s; current: 0.9 mA
Magnetometer	AKM 1. Max range: 4912.0 uT; resolution: 0.1 uT; current: 1.1 mA
Proximity sensor	Sensortek 2. Max range: 5 cm; resolution: 0.05 cm. Current 0.mA.
Orientation sensor	Yes
Rotation vector	QTI 2. Max range 1; resolution: 0.00000006; current: 2 mA.
Game rotation vector	QTI 2. Max range 1; resolution: 0.00000006; current: 2 mA.
Fingerprint	Fingerprint Cards FPC1511
Ambient light sensor	Sensortek 1. Max range: 4096.0 lx; resolution: 0.5 lx; current: 0.09 mA.
Linear acceleration	QTI 2. Max range: 156.906 m/s ² ; resolution: 0.002 m/s ² ; current: 1.0799866 mA
Gravity sensor	QTI 2. Max range: 156.906 m/s ² ; resolution: 0.002 m/s ² ; current: 1.0799866 mA
Significant motion	QTI 2. Max range -; resolution -; current: 0.18 mA.
Step detector	QTI 2. Max range -; resolution -; current: 0.18 mA.
Step counter	QTI 2. Max range 1; resolution 1; current: 0.18 mA.
Geomagnetic rotation vector	QTI 2. Max range 1; resolution 1; current: 0.13 mA.

2.1.1.2 The smartphone hardware: camera sensor and video for PPG acquisition

The smartphone Redmi Note 7 camera module is composed of a main back camera with 48 MP of resolution accompanied by a low-resolution secondary back-camera (5 MP), which functions as depth sensor (Table 2.1.2). Below this dual camera, the flashlight is present, as shown in Figure 2.1.2.

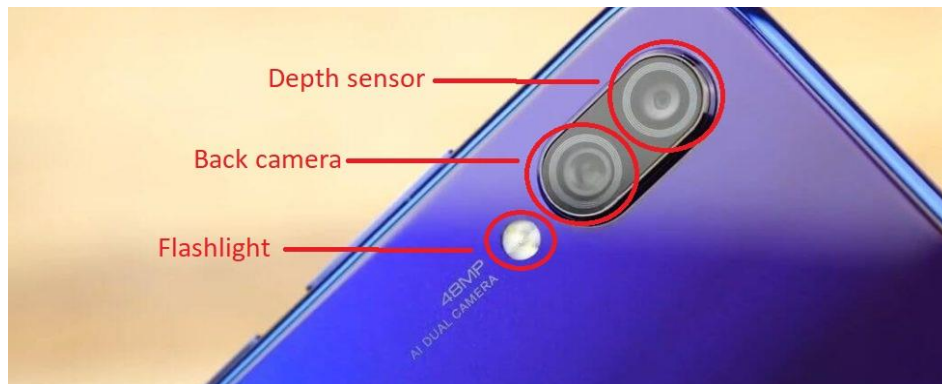


Figure 2.1.2 Xiaomi Redmi Note 7 dual camera: this module is composed of the principal 48 MP back camera, the 5 MP camera depth sensor and the flashlight. Image available on: <https://www.awaqa.com/xiaomi-redmi-note-7-review-test-low-price-buy/>.

For the purpose of PPG extraction, the video specifics have a key role as well (Table 2.1.3), being dependent on the smartphone hardware offered by the developer.

Table 2.1.3 Redmi Note 7 video specification: resolution with the corresponding frame rates and the possible video-audio format. Data available from: <https://www.mi.com/global/redmi-note-7/specs>.

Redmi note 7 (4+64 GB) video specification	
resolutions and frame rates	1080p, 60fps/30fps 720p, 30fps 720p slow motion, 120fps 1080p slow motion, 120fps
Video-audio formats	H.264 (Baseline / Main / High profile), MPEG4 (Simple profile / ASP). Supported audio formats: PCM, AAC / AAC + / eAAC +, MP3, AMR - NB and WB, FLAC, WAV.

The Redmi Note 7 allows video acquisition at different frame rates: 30 fps, 60 fps and 120 fps. At each sampling rate, a specific frame temporal resolution is imposed by the developers,

such as 720p or 1080p for video at 30 fps, 1080p at 60 fps, and 720p or 1080p at 120 fps, where the number follows by the p indicates the number of pixels along the vertical axis of the standard frame coordinate system (Figure 2.1.3). However, by software programming, it is possible to change the frame resolution.

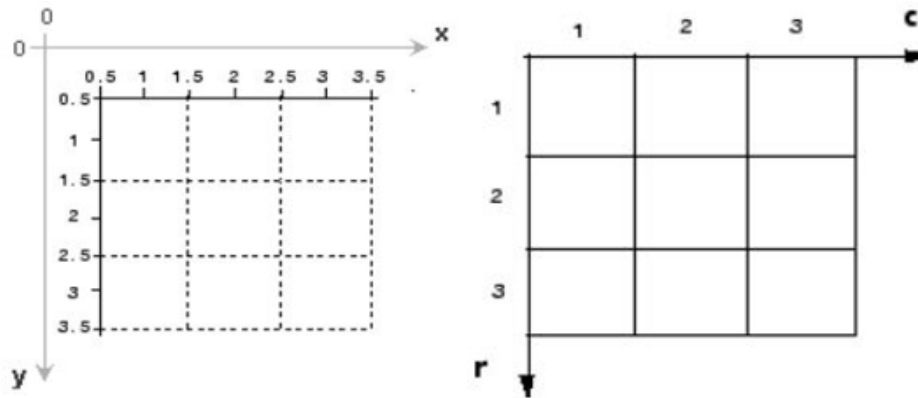


Figure 2.1.3 Standard image coordinate system: the coordinate of a pixel can be described with the typical cartesian notation (x, y) (on the left) or using the corresponding row and column position of the same pixel (r, c) (on the right).

Other important features are the format and the codec of the video, as well as the corresponding audio. A program (or hardware) that can decode compressed video or audio is called a codec; playing or encoding a video file will sometimes require the user to install a codec library corresponding to the type of video and audio coding used in the file.

This last fact becomes important when a software is used to process the images and audio inside the video file. Thus, the knowledge about the different available video format is needed for the developer. In this respect, Redmi Note 7 offers two video formats H.264 and MPEG4, with PCM, AAC / AAC + / eAAC +, MP3, AMR - NB and WB, FLAC, WAV corresponding audio formats (Table 2.1.3).

2.1.1.3 The smartphone hardware: accelerometer and gyroscope sensors for SCG acquisition

The Redmi Note 7 IMU module includes the accelerometer and gyroscope sensors (Table 2.1.2). These two sensors are represented by a BOSCH 2062701 3 axial accelerometer and gyroscope. The maximum range of the accelerometer measurements arrives to 156.906 m/s^2 , with a resolution of 0.002, while the gyroscope as a range until $2000 \text{ }^\circ/\text{s}$ with a resolution of 0.06.

The typical Android smartphone accelerometer axis orientation is shown in Figure 2.1.4. This information is fundamental to investigate the SCG, in order to understand in which direction

the heart vibrations are affecting the inertial signal. In particular, the x and y axes represent the acceleration forces on the plane formed by the smartphone orthogonally with respect to the other, while the z axis represents the acceleration perpendicular to this plane. For the gyroscope, there are three types of rotations around the 3 axes of orientation: the pitch, which represents the rotation around the x axis, the roll around the y axis and the yaw around the z axis.

No information about the nominal sampling frequencies for the accelerometer and gyroscope are provided.

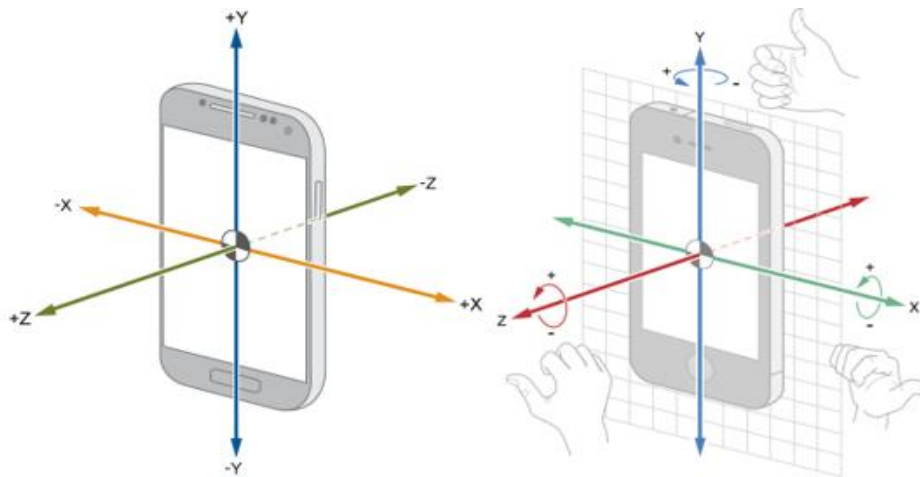


Figure 2.1.4 Android smartphone 3 axial accelerometer orientations (on the left), whose rotations around their axes are sensed as angular velocities by the gyroscope (on the right).

2.1.2 The integrated development environment

An integrated development environment (IDE) is defined as “... a software application that provides comprehensive facilities to computer programmers for software development. An IDE normally consists of at least a source code editor, build automation tools, and a debugger.” (https://en.wikipedia.org/wiki/Integrated_development_environment), and the choice of the IDE strictly depends on the operating system running on the smartphone.

The choice of a Redmi Note 7 (paragraph 2.1.1) with installed an Android 9 operating system (Table 2.1.2) implies the use of the Android IDE, called “Android Studio” (Figure 2.1.5). Android Studio is the official integrated development environment (IDE) for Google's Android operating system, built on JetBrains' IntelliJ IDEA software and designed specifically for Android development. The Android IDE presents embedded features useful for the development of smartphone applications, for example to automatically build the projects (the Gradle), to run or debug the apps on a virtual smartphone (Android Virtual

Device Emulator) or the built-in support for Google Cloud Platform, enabling integration with Firebase Cloud Messaging. The standard programming languages are all supported, but typically the most used is Java, because it derives from IntelliJ IDEA, which is a Java integrated development environment.

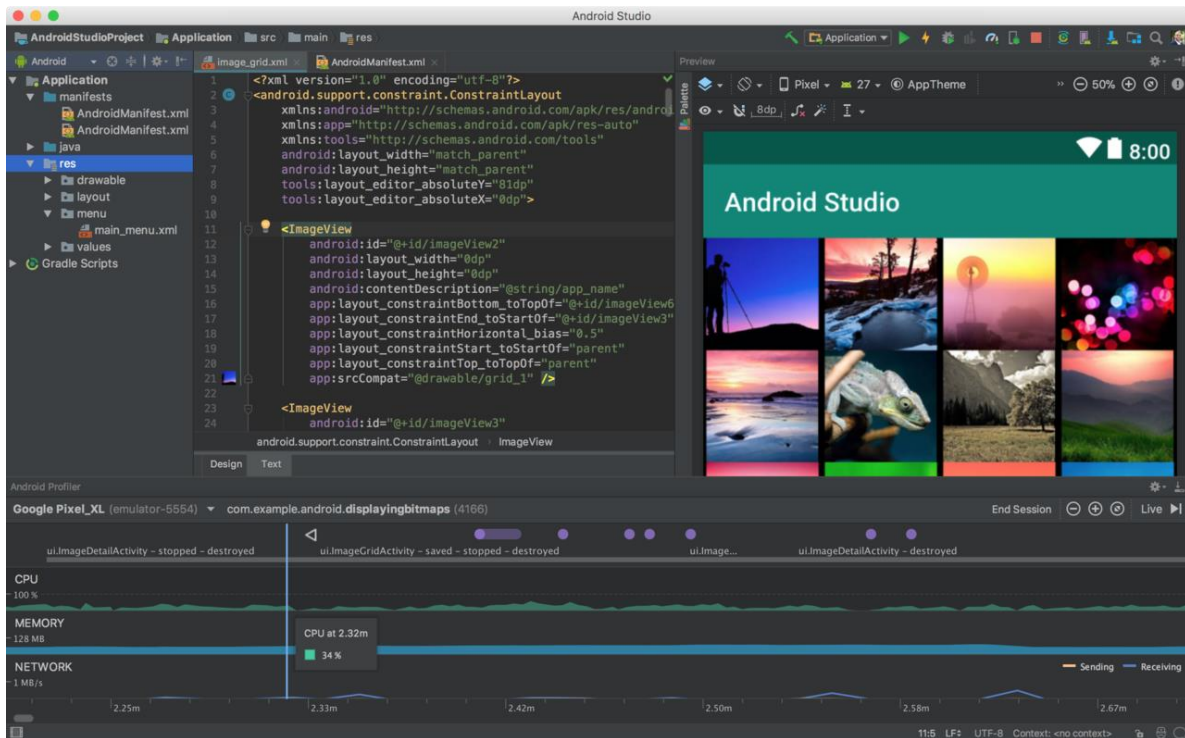


Figure 2.1.5 Android official IDE screenshot for Google's Android operating system.

The Android IDE needs the integration of the Java Development Kit (JDK), which is a software development kit (SDK), that is a collection of tools in one installable package, that makes easier the app development by having a compiler, a debugger or sometimes a software framework.

Android Studio is freely available on the official developer Android website (https://developer.android.com/studio/?gclid=CjwKCAiAzanuBRAZEiwA5yf4uibDhyPd7pplugmI4UOevBOYnr3YXyyfDfGu2jLc-h2aPUNY8_ZIGhoCJ3wQAvD_BwE).

2.2 METHODS: THE APPLICATION DESIGN

After having introduced the software and hardware tools for this framework, in this paragraph the design choices for the application development will be described, together with the explanation of the different scenarios offered to the end user during the app utilization and with the fundamental Android tools to derive the app code.

2.2.1 The design of an Android smartphone 3 module-based app for retrieving biological markers by using PPG and SCG signals

Android is a mobile operating system based on a modified version of the Linux kernel and other open source software, designed primarily for touchscreen mobile devices such as smartphones and tablets. Android is developed by a consortium of developers known as the Open Handset Alliance, with the main contributor and commercial marketer being Google (<https://www.makeuseof.com/tag/android-really-open-source-matter/>). In the first quarter of 2019, the Android operating system covers around the 88% of all smartphone sold to the end users (1).

Combining these facts, a smartphone which is equipped with the open source and widely used Android system seems to be compatible for being used as actuator of a mobile application. Moreover, for a biomedical purpose the smartphone ability of acquiring different physiological signals is one of the requirements that is strictly dependent on the sensors embedded in the mobile device itself.

For all these reasons, the Xiaomi Redmi Note 7 (paragraph 2.1.1) was chosen as the hardware to run the presented app, and the official android IDE Android Studio (paragraph 2.1.2) was selected to write the Java code behind the mobile application.

2.2.1.1 The design concept: a ductile, flexible and noninvasive app

The main choices within this project were finalized to build an app that can capture two specific biological signals: the PPG and the SCG (chapter 1).

Conceptually, the app design aimed to offer a fast, noninvasive and unobtrusive experience to the end user, overcoming the discomfort derived by the traditional measurements for common biomarkers like HR and HRV, including wearing electrodes and lasting the acquisition for some minutes. As consequence, the purpose of this app was to allow the highest possible usage flexibility, having as much as possible a ductile form which can be modeled by the user reflecting its needs, opening the doors both to self-monitoring and to research purposes.

Consequently, the app was structured in 3 different modules, activated singularly by the user: the first one to acquire the PPG signal by the use of the smartphone digital camera; the second one to capture the SCG by the support of the IMU embedded sensors, and the last module which combines the first two, offering the possibility of simultaneously acquiring the PPG and SCG signals, that together can be used to extract important biological biomarkers, such as the PTT (chapter 1, paragraph 1.3).

2.2.1.2 First scenario: from the initial activity to the choice of one of the 3 app modules for capturing PPG and SCG

When the user runs the application on the smartphone, the screen displays the initial page (Figure 2.2.1), which is represented on Android Studio by the Java class “InitialActivity.java” (Figure 2.2.2).

InitialActivity

This activity is the first page the user can interact with:

1. Button for setting acquisition frame rate for the camera (30, 60 or 120 fps);
2. Button for setting acquisition times as seconds (from 1 to 30 seconds);
3. Button to choose the user's weight;
4. Button to choose the user's age;
5. Toggle button to choose user's gender (M or F);
6. Button to choose the user's height;
7. Button to clear all written texts on the page;
8. Button to pass at the acquisition activity, without saving the user's info on the cloud;
9. Button to pass at the acquisition activity, saving the user's info on the cloud;
10. The user can write in the editable label free notes.

IMPORTANT: make sure the device was connected to internet for saving the txt file on cloud.

Figure 2.2.1 The InitialActivity is the first page which the user can interact with when the application is run. On the left, the possible actions that can be made by using the objects indicated by the arrows (on the right).

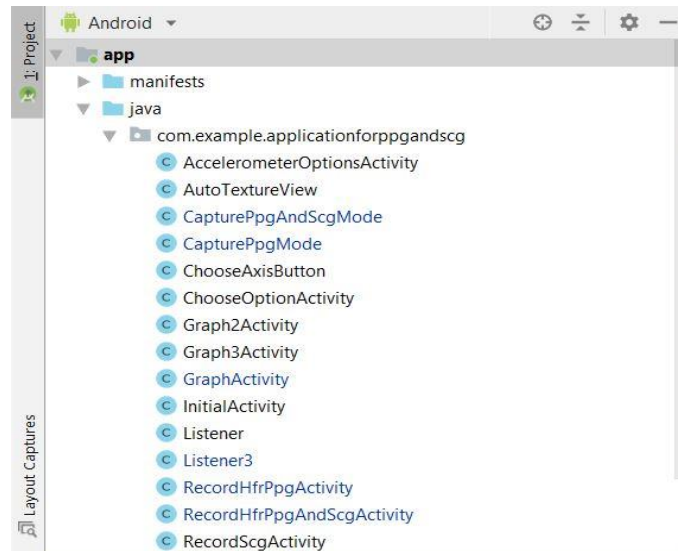


Figure 2.2.2 Android Studio IDE: the list of the different java classes created for this project.

The layout presents different buttons, each one with its specific function, as shown by the Figure 2.2.1

This activity allows the insertion of the user parameters (e.g. height and weight that could be used for the computation of body mass index (BMI)), and the setting relevant to the data acquisition: duration and frame rate of the video for the PPG. It is important to underline the possibility of acquiring at three different frame rates, 30, 60 or 120 fps, and to set the length of the acquisition from a minimum of 1 second to a maximum of 30 seconds. This last choice is limited to the RAM capability in collecting data for a longer time, “stressing” the CPU. However, acquisitions of 30 seconds represents a common standard for this kind of evaluation (Table 1.3.2, (Landreani and Caiani, 2017)).

After having provided the required information (the free notes indicated by arrow 10 in Figure 2.2.1 are optional), three options are given to the user. The first one, indicated by the arrow 9 in the Figure 2.2.1, to save all inserted information on the smartphone internal storage (Figure 2.2.3) and on the Google Firebase Cloud (Figure 2.2.4) as .txt file, whose name is uniquely identified by the inserted information together with the date and the time of the storage operation. When the file is stored, the root folder that will contain the file is created on the Google Cloud, with the same encoded name (Figure 2.2.3 and Figure 2.2.4). The Cloud URL is inserted via software inside the code.

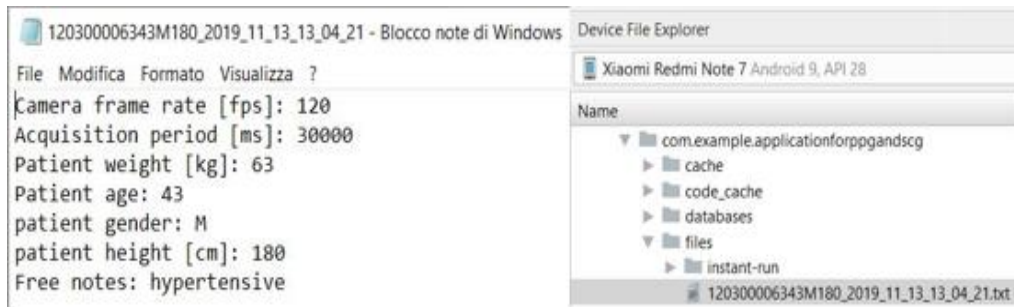


Figure 2.2.3 The .txt file with the acquisition information and the personal user parameters is shown on the left. The file is extracted by using the Device File Explorer of Android Studio from the smartphone internal storage (on the right).

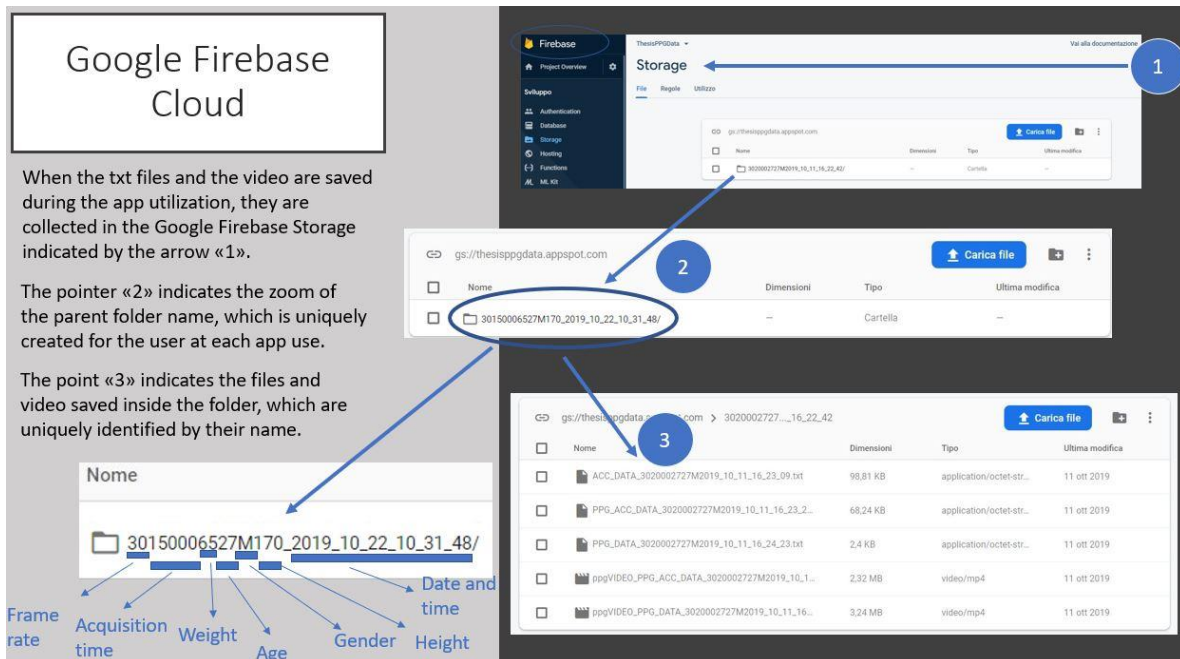


Figure 2.2.4 Google Firebase Cloud storage (arrow 1). The arrow 2 indicates the folder created at the moment of the information saving. The root folder that contains the .txt file shown in fig. 2.2.3 has the same univocal name. The arrow 3 indicates the folder content.

The second choice (arrow 8, Figure 2.2.1) allows the user to pass to the next activity, without storing the .txt file. The third choice simply erases all previously inserted information to restart the process, as shown by arrow 7 in Figure 2.2.1. In any case, the information containers must be filled-in to pass to the next activity called “ChooseOptionActivity”, from which the user can come back simply by using the back button on the smartphone touch screen.

All these steps are summarized in the flowchart of Figure 2.2.5.

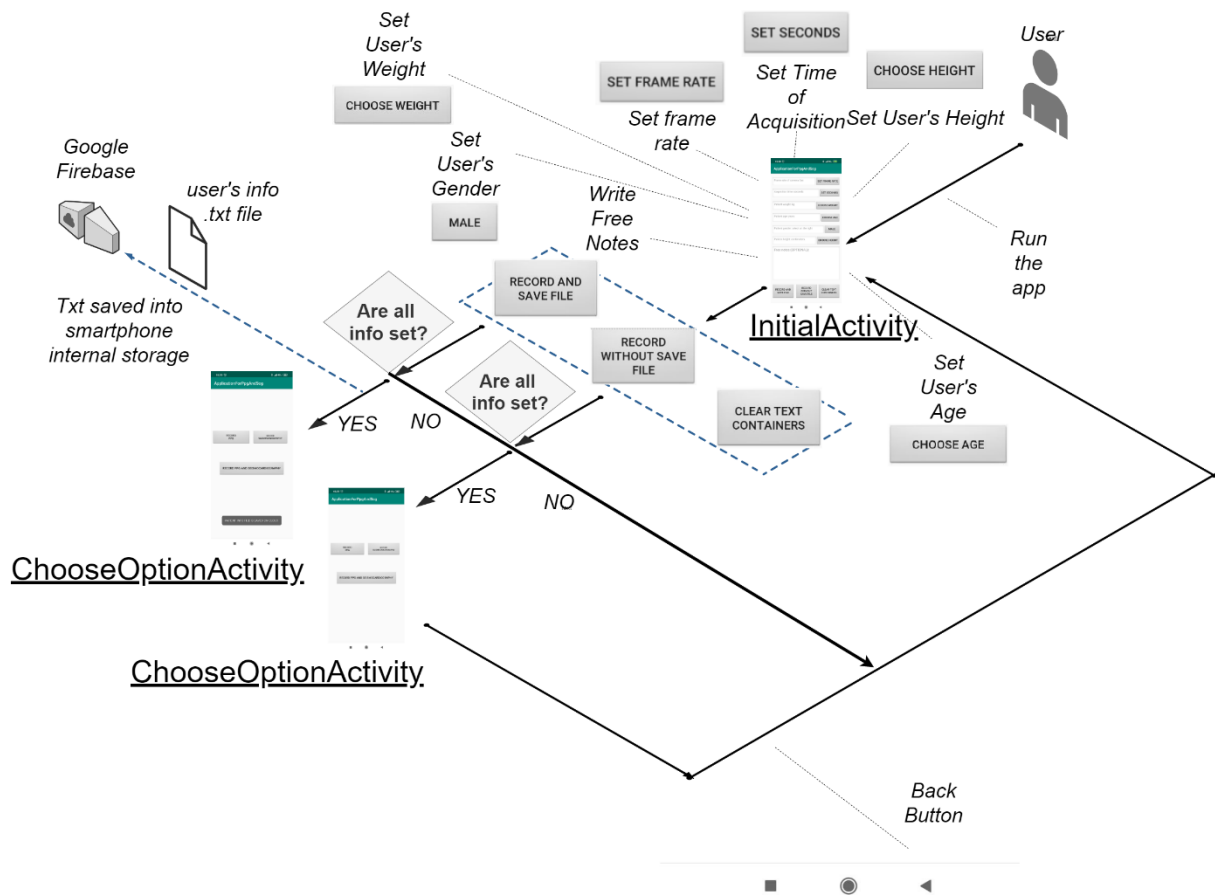


Figure 2.2.5 Flowchart of the first app activity, from the "InitialActivity" to the "ChooseOptionActivity".

2.2.1.3 Second scenario: the choice for one of the 3 app modules for capturing PPG and SCG signals

At the end of the steps explained in the previous paragraph (Figure 2.2.5), the user will interface with the second principal activity (Figure 2.2.6), which corresponds to the "ChooseOptionActivity" class on Android Studio (Figure 2.2.2).

Here, the user can choose among three buttons: the first one (arrow 1, Figure 2.2.6) that will open the module to capture the PPG signal; the second one (arrow 2, Figure 2.2.6) to start the acquisition of the SCG signal, and the third one (arrow 3, Figure 2.2.6) that will open the module to simultaneously acquire the SCG and PPG signals.

As shown in Figure 2.2.6, the arrow 4 indicates the message appearing in case the user has pressed the button "SAVE AND RECORD FILE" in the previous activity (Figure 2.2.1), otherwise no message will pop up.

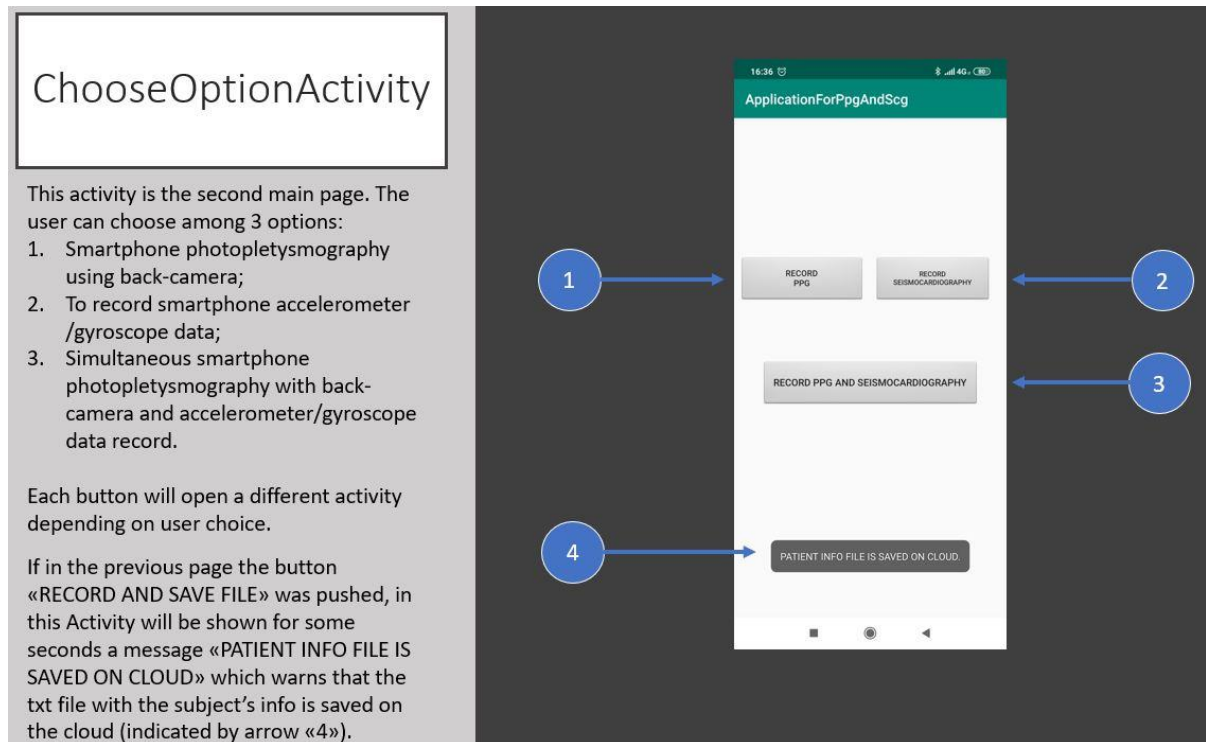


Figure 2.2.6 ChooseOptionActivity allows the user to choose among 3 different modules using the indicated buttons. The first one (indicated by arrow 1) will open the activity to capture the PPG signal; the arrow 2 indicates the button to pass to the activity for sensing the SCG signal, and the third one (indicated by arrow 3) will open the activity to simultaneously record the SCG and PPG signals.

2.2.1.4 Third scenario: the PPG module

As anticipated in the previous paragraph, if the user presses the button “RECORD PPG” (indicated by arrow 1, Figure 2.2.6), the activity to acquire the PPG signal (Figure 2.2.7, screenshot on the left side) will be opened, which is represented by “RecordHfrPpgActivity” class on Android Studio (Figure 2.2.2).

RecordHfrPpgActivity

Here, the ppg is recorded exploiting the back-camera of the smartphone.

This activity is opened by the button «1» in the previous «ChooseOptionActivity».

After having selected the option indicated by arrow «1», when the user has positioned the fingertip of the index finger on the camera, he/she can run the acquisition of the PPG simply pushing the button «4»

1. This pop-up is used to choose if the ppg signal will be computed on-board (NO) or if only the acquired video will be saved without computation (YES);
2. The arrow «2» indicates the activity in the background;
3. This arrow indicates the activity in the foreground, after the first selection;
4. This button will run the acquisition (read the advice on the button).

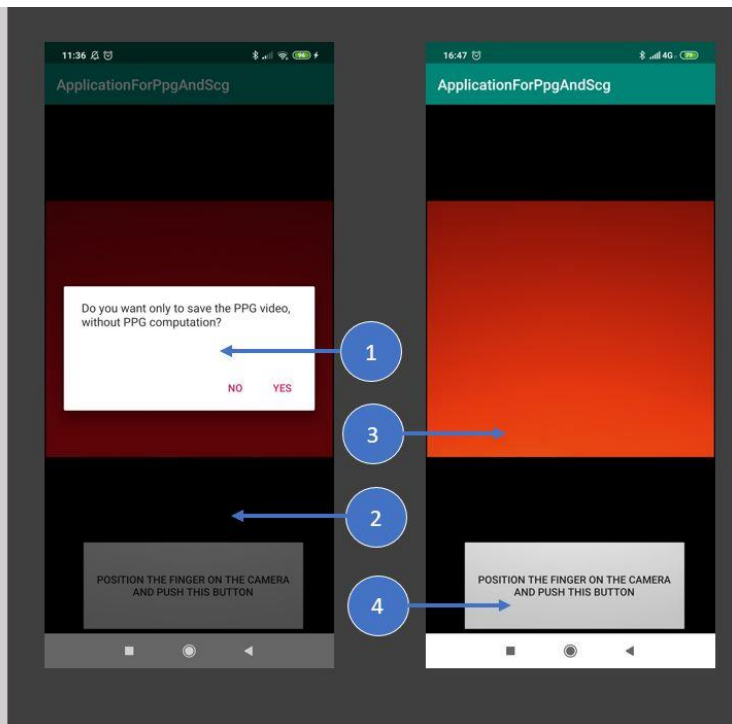


Figure 2.2.7 The RecordHfrPpgActivity first visualization. Before starting the acquisition, the user chooses if the PPG will be computed on-board or not (arrow 1), in the meanwhile the activity run on the background (arrow 2). After this choice, the images acquired by the smartphone camera are shown on the page center (indicated by arrow 3), while the user positions the finger on the camera objective. The arrow 4 indicates the button to start the acquisition.

To begin the acquisition, the user must choose either if to compute the PPG on board or if to export only the acquired video for an external processing. This can be done through the buttons of the dialog window shows by the arrow 1 in the Figure 2.2.7 (the arrow 2 indicates the activity in background, while the arrow 3 the activity in foreground after the decision).

Before acquiring the PPG signal, the text on the button indicated by the arrow 4 in Figure 2.2.7 suggests positioning the finger on the smartphone camera objective, as shown in fig. 2.2.8. In the meantime, the frames acquired by the camera are shown in real-time, as indicated by the arrow 3 in the Figure 2.2.7, in a customized *AutoTextureView* class on Android Studio (Figure 2.2.2) as container.

When the user presses the button to run the acquisition, a 5 seconds-countdown synchronized with 5 beep sounds starts, while the button becomes orange (Figure 2.2.9) and not clickable until the acquisition (and on board PPG processing, if selected) is completed.

RecordHfrPpgActivity

Here, the ppg is recorded exploiting the back-camera of the smartphone. This activity is opened by the button «1» in the previous «ChooseOptionActivity».

In these pictures is explained how to position the finger on the camera to achieve the best acquisition.

The finger has to cover the flash as vertical as possible, while the fingertip is positioned on the camera.

The depth sensor on the top of the camera must be free.

1. The arrow «1» indicates the depth sensor;
2. The arrow «2» indicates the camera;
3. The third arrow «3» points to flash.

IMPORTANT: in this case is shown a Redmi note 7 smartphone.

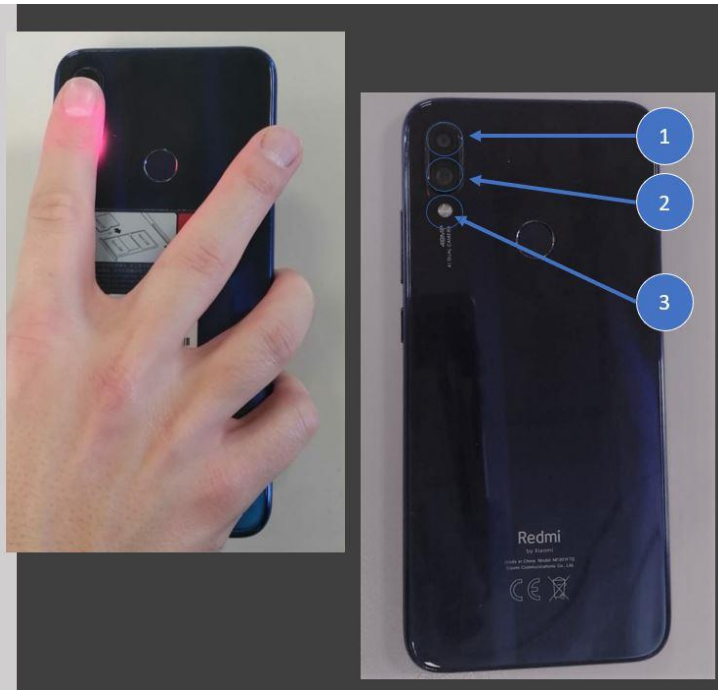


Figure 2.2.8 Before starting the acquisition, the user positions the fingertip of the index finger in vertical position on the camera objective (indicated by arrow 2), covering the flashlight (arrow 3), but leaving uncovered the depth sensor (arrow1).

RecordHfrPpgActivity

Here, the ppg is recorded exploiting the back-camera of the smartphone.

If the button «2» was pushed, before the signal acquisition a 5 second countdown will start associated to 5 beep sounds.

In this phase the button becomes orange.

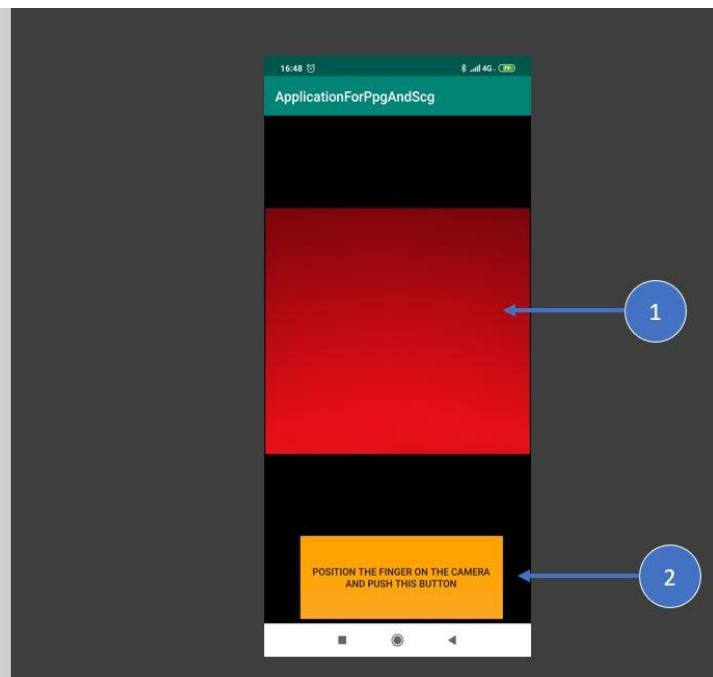


Figure 2.2.9 RecordHfrPpgActivity after the user has pushed the button to run the acquisition: a 5 seconds-countdown will start, and the button will be visualized as orange (arrow 2).

After the 5 seconds-countdown, the effective acquisition starts, together with a message “Frame acquisition is run!” (Figure 2.2.10) visualized. During this phase, the video (arrow 1, Figure 2.2.10) is acquired by the smartphone camera at the frame rate initially set by the user (paragraph 2.2.1.2), for the duration selected (paragraph 2.2.1.2).

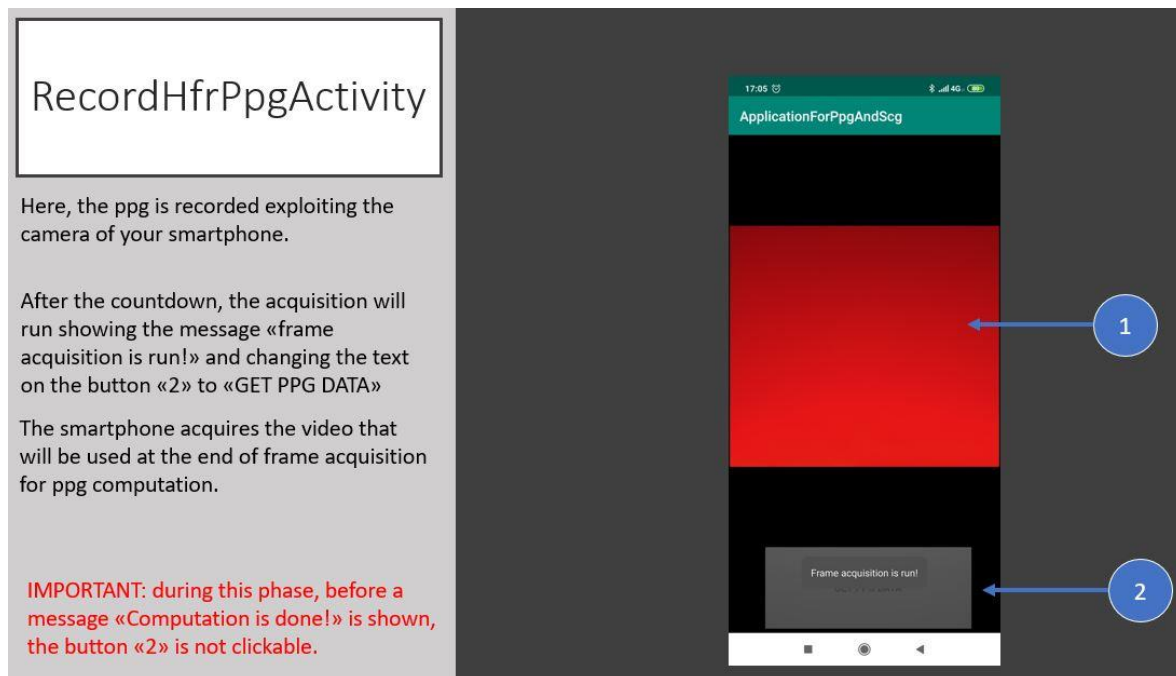


Figure 2.2.10 RecordHfrPpgActivity: a message “Frame acquisition is run!” will be pop-up over the button after the 5 seconds-countdown (arrow 2). During this phase, a video at the set frame rate is acquired for the extraction of PPG. The video is shown where the arrow 1 indicates.

At the end of the acquisition, a message “Frame acquisition is done and video saved!” will pop-up on the screen, followed by two beeps (Figure 2.2.11). In that moment, depending on the initial choice of computing or not the PPG signal on board, different events will be triggered: the acquired video is saved in the internal storage of the smartphone and , if selected (if not it will pass to the scenario described by Figure 2.2.12), the PPG computation starts for each frame of the acquired video.

Once the PPG on board computation is completed, , a sequence of beeps is produced, together with a message on the screen “Computation is Done!” and the text “GET PPG DATA” on the button, that suggests the user to press it to save the desired signal (Figure 2.2.12).

RecordHfrPpgActivity

Here, the ppg is recorded exploiting the back-camera of the smartphone.

When the frame acquisition (to collect the frames for the PPG signal) is finished, a message «Frame acquisition is done and video saved!» will be shown followed by two beep sounds.

When the frame acquisition is finished, the video is saved on the internal storage and the ppg computation starts, if this option was chosen at the beginning.

IMPORTANT: during this phase, before a message «Computation is done!» is shown, the button «2» is not clickable»

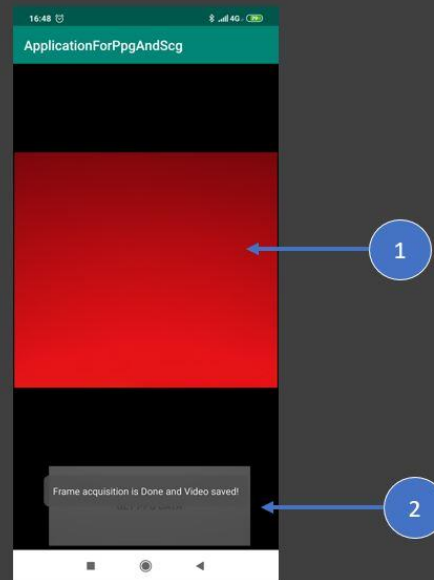


Figure 2.2.11 RecordHfrPpgActivity after the video acquisition: a message “Frame acquisition is done and video saved!” is shown, followed by two beeps. In this moment, the PPG computation (if set) starts using the frames of the acquired video.

RecordHfrPpgActivity

Here, the ppg is recorded exploiting the camera of your phone.

When also the PPG signal is computed, a message «Computation is done!» will be shown followed by some beep sounds. The button «2» now is clickable.

Now, to save the PPG data on cloud and show the result on a graph, click the button «2» to get the PPG data and pass to the «GraphActivity»

IMPORTANT: make sure the device was connected to internet for saving the txt file on cloud.

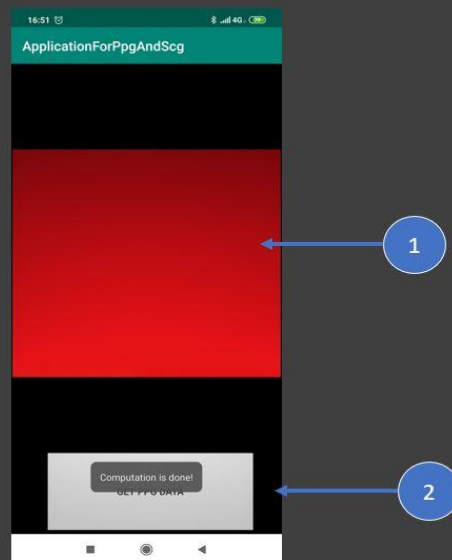


Figure 2.2.12 RecordHfrPpgActivity: when the PPG computation is complete, a message “Computation is done!” is shown. In the meantime, a sequence of beeps warns the user and the button becomes clickable again with the text “GET PPG DATA” (arrow 2) on it. If the on-board PPG computation was not activated, the button would be clickable without the message “Computation is done!”.

When the user presses the button “GET PPG DATA”, if the on-board PPG computation was initially selected, a new activity will be opened (Figure 2.2.13), called as Android Studio class “GraphActivity” (Figure 2.2.2); otherwise, the “ChooseOptionActivity” will be opened (Figure 2.2.6). Simultaneously, a .txt file and the video are sent to the storage on Google Cloud root folder (arrow 3, Figure 2.2.4) and the .txt is saved in the smartphone internal storage as well. The .txt file contains the on-board computed PPG values (if this option was not selected, this array will not be present), the mean frame rate during the acquisition, the timestamp vector calculated using a fixed time interval ($1/\text{mean sampling rate}$) between two frames, the real camera system timestamps (in nsec) associated to each frame acquisition event, the system absolute time of the acquisition beginning (in nsec) and the effective time duration of the acquisition (in nsec), calculated from the system time as reference (Figure 2.2.14).

When the “GraphActivity” is opened, a message with the internal storage path information appears (Figure 2.2.13, arrow 1): this activity allows the user to visualize the result of the PPG signal computation, with the possibility of scrolling and zooming the graph for a better view (Figure 2.2.13, arrow 2). The user can go back to the previous “ChooseOptionActivity” simply using the back button on the screen. To create the graph, the library 'com.jjoe64:graphview:4.2.2' was used.

All these steps are summarized in the flowchart shown in Figure 2.2.15.

GraphActivity

Here, a graph of the raw ppg data is drawn.

If the on-board ppg computation was selected in the previous «RecordPpgActivity» and the button «GET PPG DATA» was clicked:

- a message (indicated by arrow «1») in this activity, describing the internal storage directory for the txt file, containing the ppg data, will be shown;
- the plot should show a signal indicated by the arrow «2».

IMPORTANT: make sure the device was connected to internet for saving the txt file on cloud.

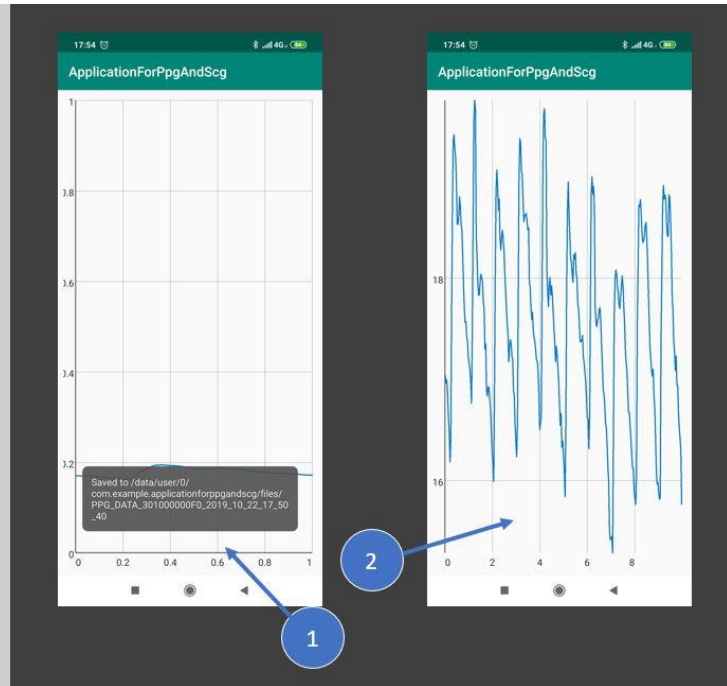


Figure 2.2.13 GraphActivity shows the plot of the obtained signal. The arrow 1 indicates the message when activity is opened, which refers to the internal storage path of the .txt file, while the arrow 2 indicates the graph of the computed PPG, after the user having zoomed the graph.

```
*PPG_DATA_3010006027F170_2020_02_27_10_49_04 - Blocco note di Windows
File Modifica Formato Visualizza ?
PPG signal values [au]:
[0.5906243137254902,0.5914117647058823,0.5884941176470588,0.5919858823529411,0.5914070588235294,0.5929835294117647,0.5911027450980393,0.5936454901960784,0.5930556862745098,0.5914352941176471,0.590881568627451,0.5903545098039216,0.592158431372549,0.5947827450980392,0.5950572549019608,0.5921113725490196,0.5919419607843137,0.5949176470588236,0.5906243137254902]

Mean frame rate [frames/sec]: [29.0]

Timestamp values (calculated by mean frame rate) [sec]:
[0.0,0.034482758620689655,0.06896551724137931,0.10344827586206896,0.13793103448275862,0.17241379310344827,0.20689655172413796,0.24137931034482762,0.2758620689655173,0.31034482758620696,0.34482758620689663,0.379310344827,0.41379310344827,0.44827586206896551723,0.48275862068965515,0.517241379310344827,0.5517241379307,0.586206896551723,0.620689655172413793099]

Camera system timestamp [ns]:
[1.4736107E7,4.8049107E7,8.1368107E7,1.14670107E8,1.48002107E8,1.81297107E8,2.14614107E8,2.47923107E8,2.81236107E8,3.14547107E8,3.47882107E8,3.81389107E8,4.14497107E8,4.47796107E8,4.81127107E8,5.14424107E8,5.47745107E8,5.81062107E8,6.14371107E8,6.47676107E8,6.80988107E8,7.14315107E8,7.47613107E8,7.80941107E8,8.14268107E8,8.47550107E8,8.80870107E8,9.14186107E8,9.47490107E8]

Acquisition beginning time of ppg (system abs. time) [ns]: [3.59602253795636E14]
Acquisition end time of ppg (respect to startTime ref.) [ns]: [1029806405]
```

Figure 2.2.14 When the “GET PPG DATA” is pressed, the .txt file relevant to the PPG data is saved on the smartphone internal storage and on Google Cloud (fig. 2.2.4, indicated by arrow 3). The .txt file name begins with the words “PPG_DATA_ ...” followed by the info inserted initially and the date and time of the moment of the button pressing to save the file.

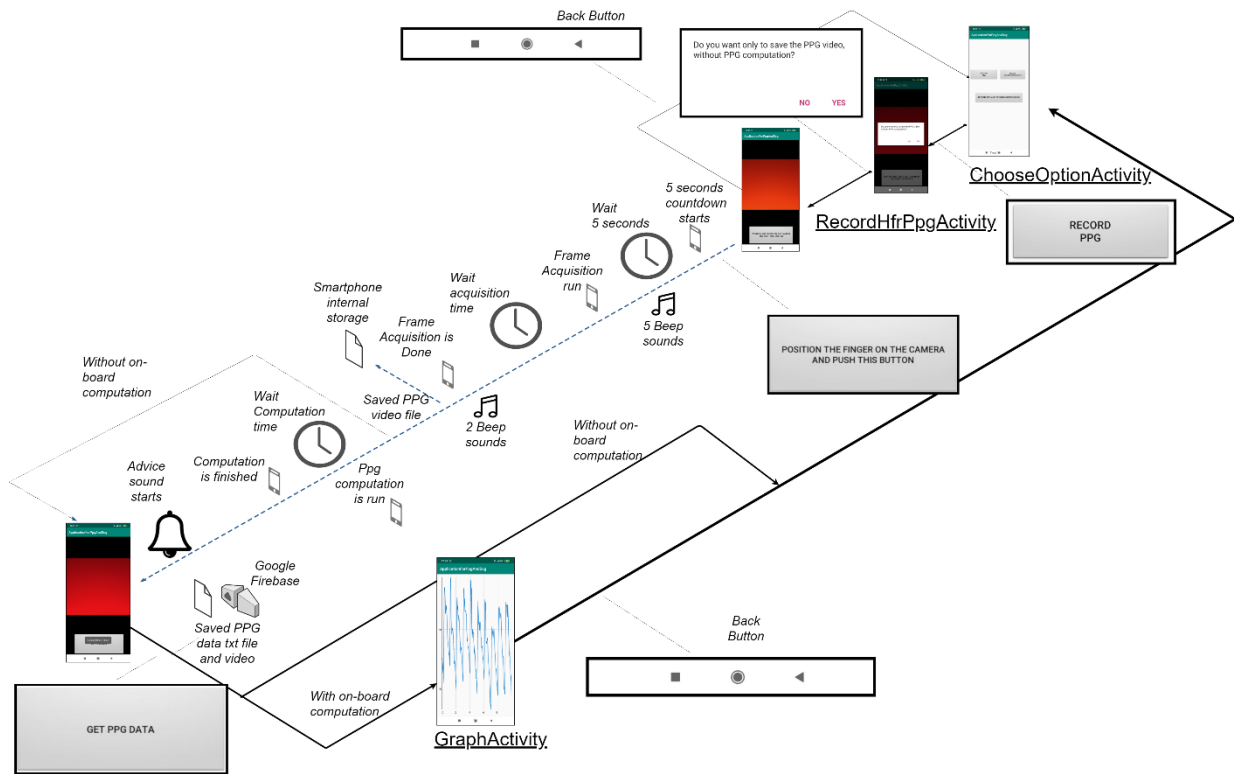


Figure 2.2.15 Flowchart of the possible operations that the user can perform, from the choice of the “RecordHfrPpgActivity” to the graph of the PPG signal on “GraphActivity”.

2.2.1.4.1 Behind the PPG acquisition module design: the CameraDevice class and the MediaRecorder class

The described “RecordHfrPpgActivity” class operates as container of a fragment called on Android Studio “CapturePpgMode” (Figure 2.2.2). Inside this fragment, there is the code for implementing the PPG acquisition.

The main Android Java classes to allow the recording of the video, from which the PPG is computed, are called *CameraDevice* and *MediaRecorder*.

The *CameraDevice* class allows to assess by software the camera hardware through *createCaptureRequest*, which in turn uses the class *CaptureRequest* to set important hardware features, such as the *FLASH_MODE* and the *CONTROL_AF_MODE*. The first one is used to set the flashlight modality, which was set as *FLASH_MODE_TORCH* to have a fixed flashlight on throughout the video acquisition. The second feature *CONTROL_AF_MODE* allows switching off the autofocus with the setting *CONTROL_AF_MODE_OFF*, in order to not change the digital focus during the video acquisition, thus affecting the PPG waveform.

Another important feature of the class *CameraDevice*, which makes innovative the way of acquiring the PPG signal, is the *createConstrainedHighSpeedCaptureSession*. This method forces the camera hardware to create a video acquisition session at a high frame rate modality, such 60 or 120 fps. This method works only with smartphone devices with this capability, as the Redmi Note 7, otherwise to capture at 30 fps, the activity *createCaptureSession* is used.

The *CameraDevice* class in combination with the *MediaRecorder* class allows the app to directly access the camera hardware and acquire the video for the PPG. In particular, the *MediaRecorder* has a collection of attributes for setting the specifications of the video to be acquired, such as the video size, the video encoder and output format, the video frame rate and the audio source and encoder. For the purpose of this work, the video size was scaled to 360x480 pixels to safeguard RAM for PPG computation, the .mpeg4 format was chosen and the AAC and H64 audio and video encoders were set.

To obtain the camera system timestamps (Figure 2.2.14) as the time at which the frames are acquired, the class *CameraCaptureSession.CaptureCallback* was implemented. This class creates a callback function that allows to grab some parameters as a result of each frame acquisition, in particular the *CaptureResult.SENSOR_TIMESTAMP*, encoded with the *elapsedRealtimeNanos* and defined as “*time since the system was booted, and include deep sleep. This clock is guaranteed to be monotonic, and continues to tick even when the CPU is in power saving modes, so is the recommended basis for general purpose interval timing.*”, measured in nanoseconds. (from: <https://developer.android.com/reference/android/os/SystemClock>)

2.2.1.4.2 Behind the PPG acquisition module design: the PPG computation

Once the video is acquired and saved in the internal storage of the smartphone (Figure 2.2.15), if the user chose the option to activate the on-board PPG computation, the video will be used for extracting the PPG signal as follows.

The “CapturePpgMode” fragment implements a code to find the video file on the internal storage by saving its path when the file was created. When the file is retrieved, the method *getFrameAtTime* of the *MediaMetadataRetriever* class allows to access the acquired images of size (360x480) in the video file frame by frame. Each image is saved as Bitmap, by mapping automatically each frame pixel value to the sRGB (IEC 61966-2-1:1999) space. The Bitmap stores each pixel into a 32-bit variable: the first byte corresponds to alpha channel, the transparency; the second byte to the red channel; the third byte to the green channel and the

fourth byte to the blue channel. A byte for every channel means a range of pixel intensity values between 0 and 255 for each color. For this app, the red channel was chosen to extract the PPG signal, taking advantage of its consistency and robustness (Kurylyak, Lamonaca and Grimaldi, 2012; Abinaya, Prabhakaran and Jaisankar, 2014).

Then, a region of interest (ROI) of 50 pixels x 50 pixels is considered in the image, as big enough to obtain the signal intensity for the PPG computation (Jonathan and Leahy, 2011; Scully *et al.*, 2012; Lázaro *et al.*, 2015). Calling *frameHeight* and *frameWidth* the two dimensions of the extracted frames and taking as pixel position reference the (x, y) coordinates (Figure 2.1.3), the algorithm positions the ROI over the frames with the upper-left corner at $(\text{frameWidth}/2 - 25, \text{frameHeight}/2 - 25)$ coordinates on the image, which means at frame center (Figure 2.2.16).

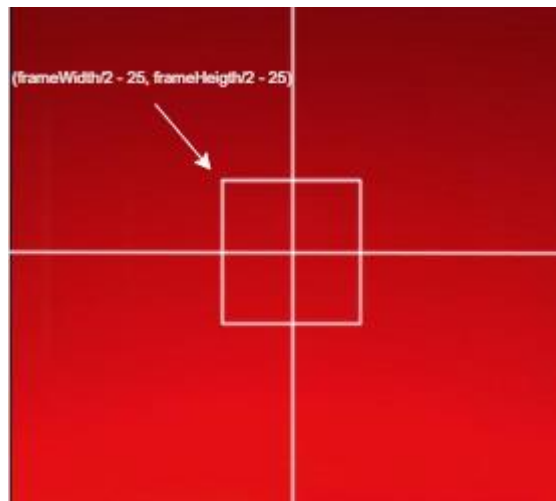


Figure 2.2.16 The algorithm for on-board PPG computation placed the 50x50 ROI on the frame center, which presupposes the ROI left-upper corner positioned at $(\text{frameWidth}/2 - 25, \text{frameHeight}/2 - 25)$ coordinate.

Finally, the mean of the pixel values in the ROI for each frame is computed and the obtained series is normalized in a range between 0 and 1 by dividing for 255. After, the signal is inverted deriving the smartphone PPG of the user (Kurylyak, Lamonaca and Grimaldi, 2012), which can be visualized and saved (Figure 2.2.13 and Figure 2.2.14) as described through the previous steps.

2.2.1.4.3 Behind the PPG acquisition module design: the camera frame rate jitters and stability

To evaluate the stability of the sampling frequency of the camera sensor and its variations along the acquisition, 9 trials at different possible camera frame rates (30, 60 and 120 fps) and at different acquisition durations (10, 20 and 30 seconds) have been performed. Table 2.2.1 summarizes the results of these tests, reporting the mean sampling frequencies obtained in different trials.

Table 2.2.1 Camera mean sampling frequencies evaluated at three different possible frame rates (30, 60 and 120 fps) at three different acquisition time (10, 20 and 30 seconds).

Camera sampling frequency median [25 th ; 75 th] (Hz)			
Acquisition time duration	Camera fps (Hz)		
	30	60	120
10 seconds	30.02 [30.00; 30.04]	59.74 [59.55; 58.92]	120 [119.47; 120.53]
20 seconds	30.02 [29.99; 30.05]	59.74 [59.61; 59.87]	120 [114.58; 125.42]
30 seconds	30.02 [29.99; 30.05]	59.74 [58,39; 61.08]	120 [113.34; 126.66]

The Table 2.2.1 suggested a high stability during all acquisition durations and for 30 Hz and 60Hz frame rates, which is confirmed by a low standard deviation around the mean frequency for each trial. The higher fluctuations of the sampling frequency at 120 Hz were due to some jump in frame rate along the acquisition, as shown in Figure 2.2.17, where the missing of frames for a narrow time interval is visible (Figure 2.2.17, on the bottom). At a certain instant, corresponding to the missed frame, the sampling frequency presents a dramatic decrease below 114 Hz.

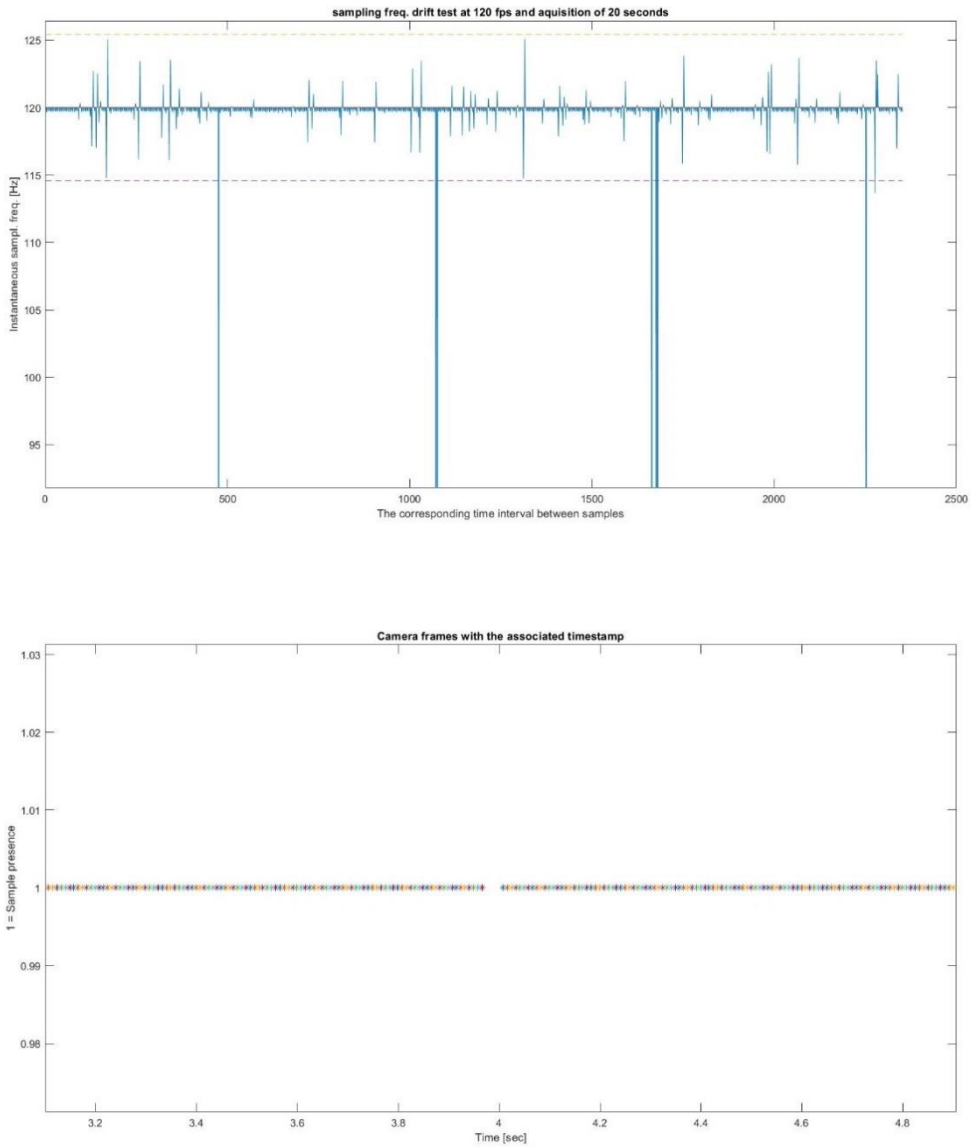


Figure 2.2.17 On the top, the instantaneous sampling frequency of the camera sensor, calculated as the inverse of time interval between 2 consecutive frames. The decreased value represented by the peaks corresponds to the skip in frame acquisitions shown in the picture on the bottom, which results in an increase of the time interval between those 2 consecutive frames.

In particular, the Figure 2.2.18 shows the worst case at 120 fps for an acquisition of 30 seconds.

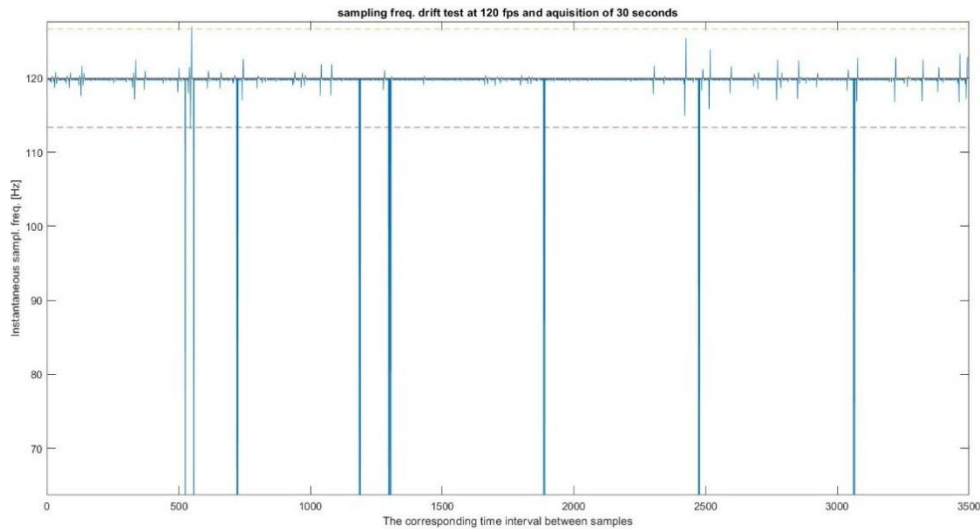


Figure 2.2.18 The plot represents the instantaneous sampling frequencies in a single trial, calculated as the inverse of the time interval between two consecutive frames. The peaks below 110 Hz are due to the missing of frame acquisition, which implies a decrease of sampling frequency. The dotted lines represent the 1st and 3rd quartiles of the distribution. This trial was done setting the app at 120 fps with an acquisition duration of 30 seconds.

2.2.1.4.4 Behind the PPG acquisition module design: the method to position the index finger on the smartphone camera

The choice of positioning the index finger to cover the activated flashlight, thus leaving uncovered the depth sensor (Figure 2.2.8), was derived by some tests, also considering all the color channels (red, green and blue), testing different possibilities offered by the Redmi Note 7. For this purpose, the vertical position of the finger parallel to the highest side of the smartphone was taken as suggested position (Figure 2.2.8), because it allows a natural grip of the smartphone and to correctly position the fingertip on the camera lens, without exercising a high pressure against the camera. In addition, the use of the flashlight during the acquisition was tested. The raw PPG signal was computed as pixel mean of the overall image and the lowest frame rate was used (30 fps).

In these tests, the different combination between using or not the flashlight, and covering or not the depth sensor, using the left or the right hand for each configuration, were verified. In Figures 2.2.19-2.2.26 the results of these trials are shown. The high consistency and robustness among the 3 different color channels, for both hands, was visible in the Figure 2.2.19 and Figure 2.2.20, covering the flashlight and leaving uncovered the depth sensor, compared to other possible combinations. For this reason, for the use of this app the final suggested position is that shown in Figure 2.2.8.

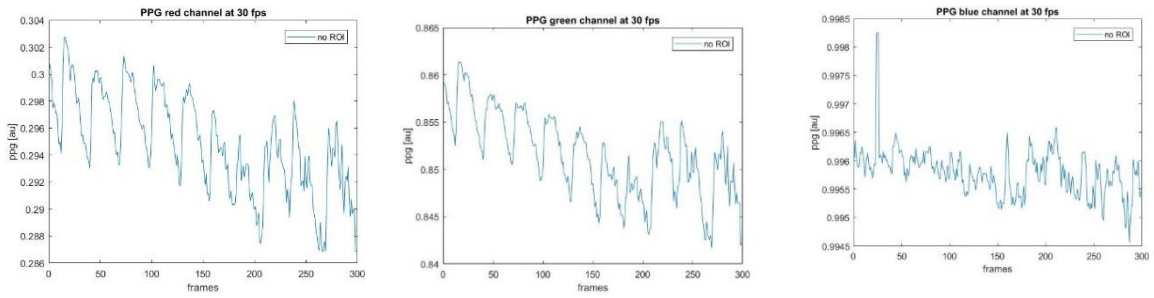


Figure 2.2.19 Right hand finger position: without cover the depth sensor and covering the flashlight.

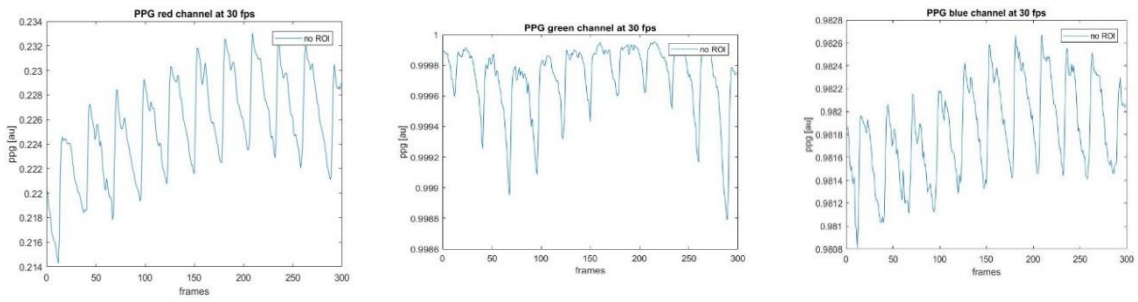


Figure 2.2.20 Left hand finger position: without cover the depth sensor and covering the flashlight.

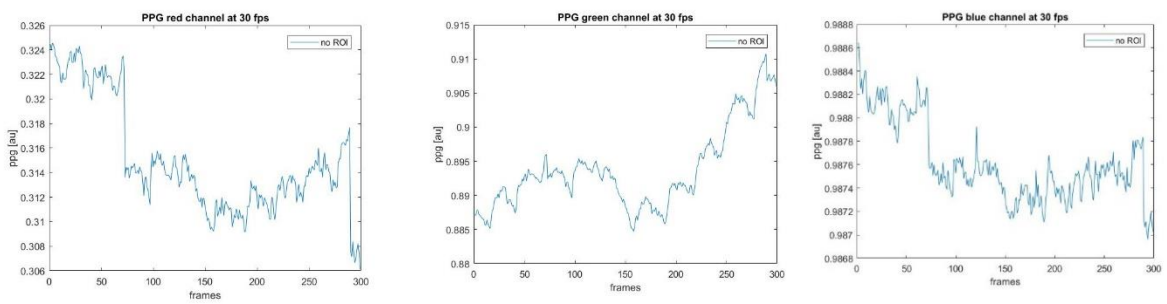


Figure 2.2.21 Right hand finger position: covering the depth sensor and covering the flashlight.

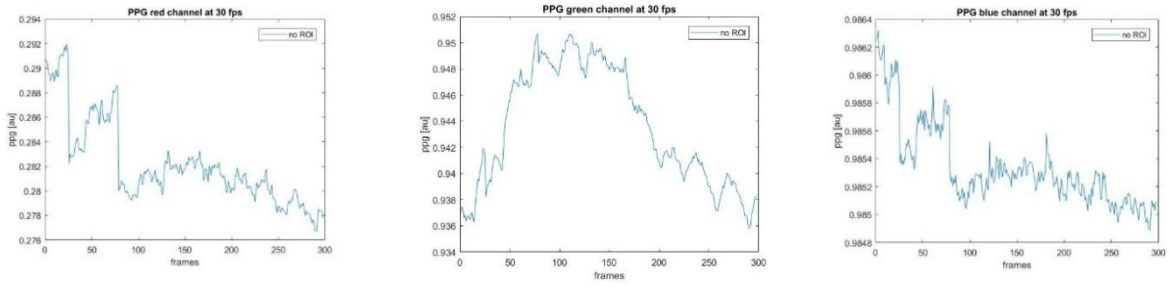


Figure 2.2.22 Right hand finger position: covering the depth sensor and covering the flashlight.

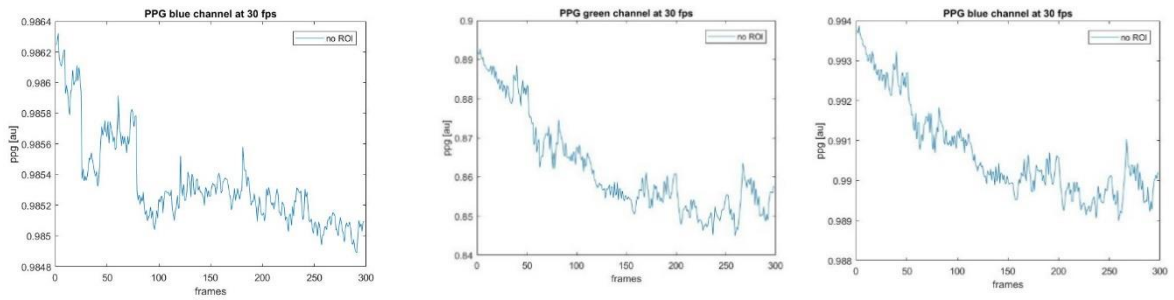


Figure 2.2.23 Right hand finger position: covering the depth sensor, without using the flashlight.

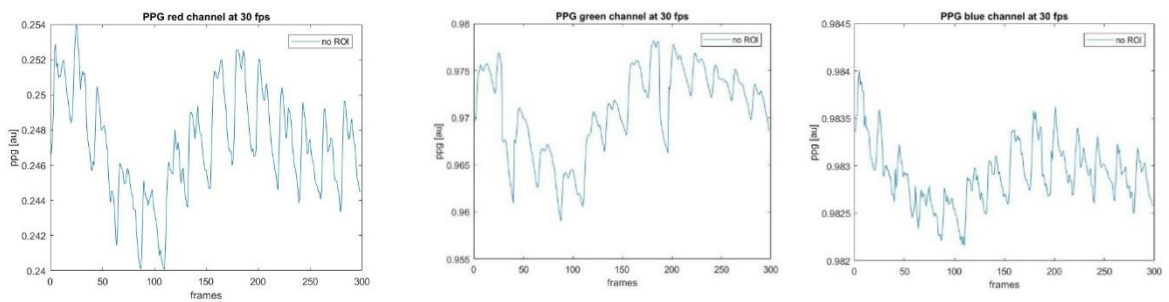


Figure 2.2.24 Left hand finger position: covering the depth sensor, without using the flashlight.

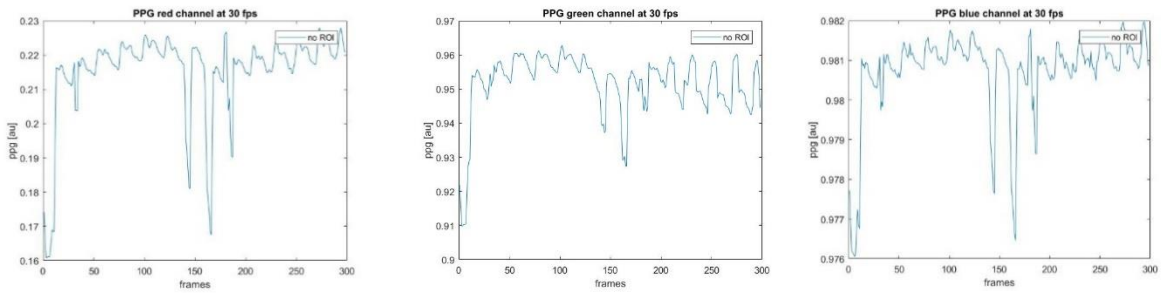


Figure 2.2.25 Right hand finger position: without covering the depth sensor and without using the flashlight.

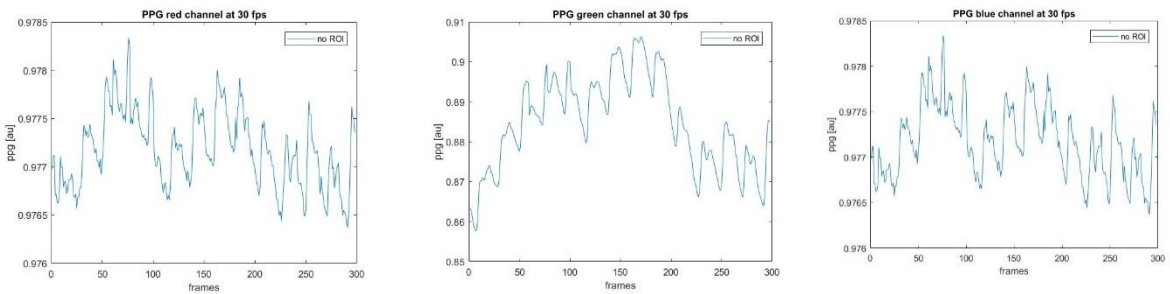


Figure 2.2.26 Left hand finger position: without covering the depth sensor and without using the flashlight.

2.2.1.5 Fourth scenario: the SCG module

On the second “ChooseOptionActivity” app main page, when “RECORD SEISMOCARDIOGRAPHY” button (arrow 2, Figure 2.2.6) is selected, the SCG module (Figure 2.2.27) called “RecordScgActivity” on Android Studio (Figure 2.2.2) will be opened.

The “RecordScgActivity” includes as its core a real-time graph (Figure 2.2.27, arrow 1) to visualize the data from one of the accelerometer axis directions, created using the library 'com.jjoe64:graphview:4.2.2'. The accelerometer and gyroscope sensors acquire signals along all possible directions and around all the 3 axes in background (Figure 2.1.4). The user can choose which axis is currently visualized (arrow 4, Figure 2.2.27) by using a button on the graph to change to the next axis in a rotating sequence (Figure 2.2.27, arrow 3).

RecordScgActivity

Here, the seismocardiography is recorded exploiting the accelerometer/gyroscope of the smartphone.

This activity is opened by the button «2» in the previous «ChooseOptionActivity».

1. The accelerometer data with respect to the chosen axis are shown in the real-time graph indicated by arrow «1»;
2. Arrow «2» indicates the button to run the acquisition (read the advice on the button);
3. The button indicated by arrow «3» changes the accelerometer axis shown on the graph;
4. Arrow «4» indicates the text which shows what axis is actually shown on real time graph.

When the user has positioned the smartphone on the chest, he/she can run the acquisition of the accelerometer/gyroscope data simply pushing the button «2».

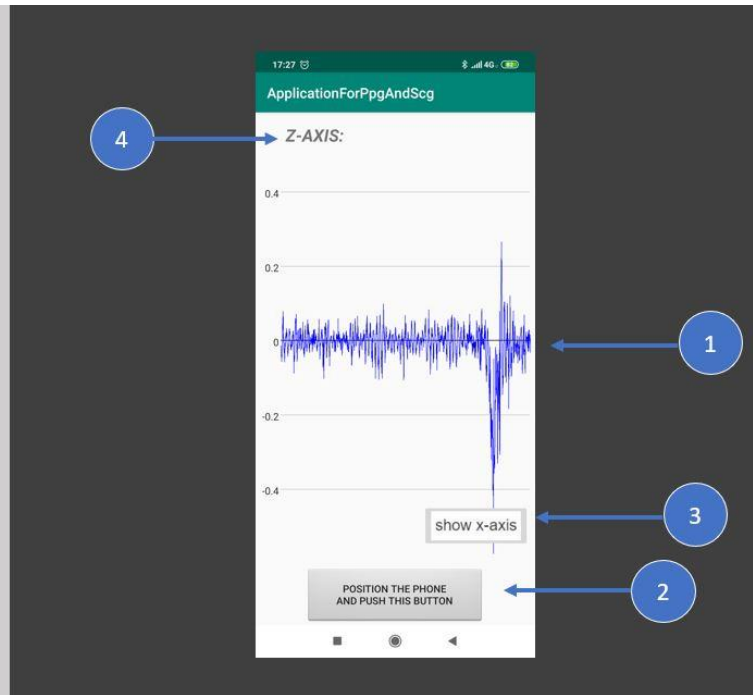


Figure 2.2.27 RecordScgActivity contains a real-time graph (arrow 1) to visualize the data from the accelerometer axis direction indicated by arrow 4. The button to change the visualized axis is indicated by arrow 3, while the arrow 2 indicates the button to run the acquisition.

Always on the same layout, the user can find a button (Figure 2.2.7, arrow 2) suggesting positioning the smartphone on the chest, typically on lower or upper sternum (Landreani and Caiani, 2017), and to push it to start acquiring the SCG signal. In this case, the SCG acquisition will start after 5-seconds countdown accompanied by 5 synchronized beeps, while the button becomes orange and not actionable for the duration of the acquisition (Figure 2.2.28), set initially by the user (paragraph 2.2.1.2).

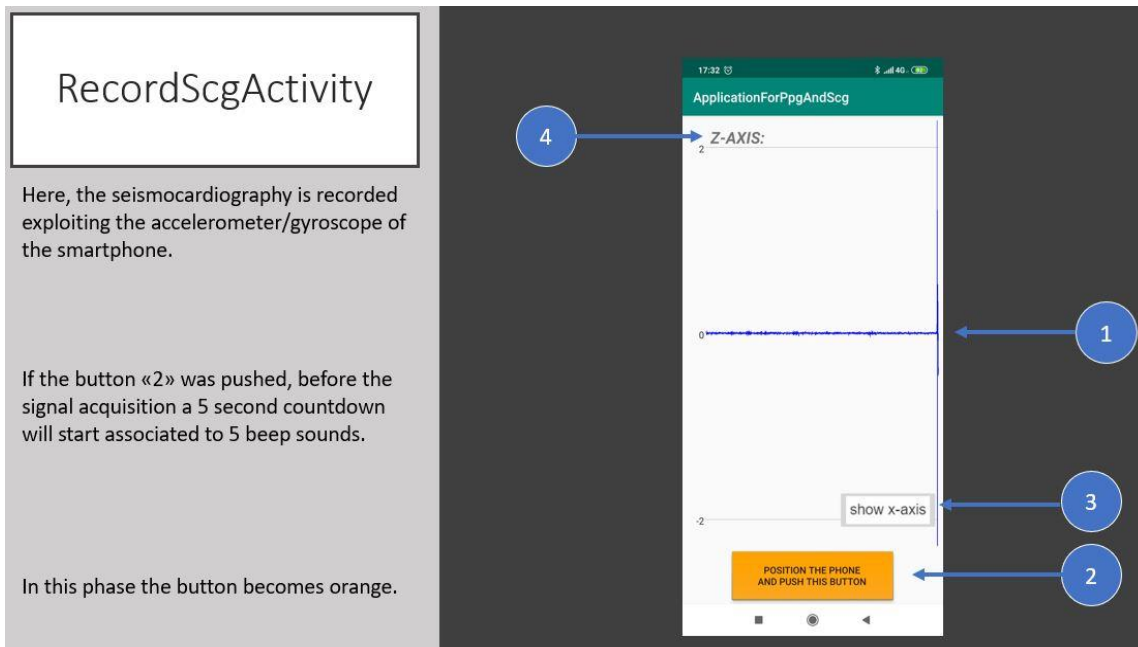


Figure 2.2.28 “RecordScgActivity” after the user has pressed the button indicated by arrow 2. The button becomes orange (arrow 2) and not clickable for all the acquisition duration, while the graph is frozen (arrow 1) during the 5-seconds countdown together to 5 synchronized beeps.

During the acquisition, the user can visualize the acquired signal on the real-time graph (Figure 2.2.29, arrow 1) along the direction chosen previously (Figure 2.2.29, arrow 4). In the meantime, all the data are stored in background.

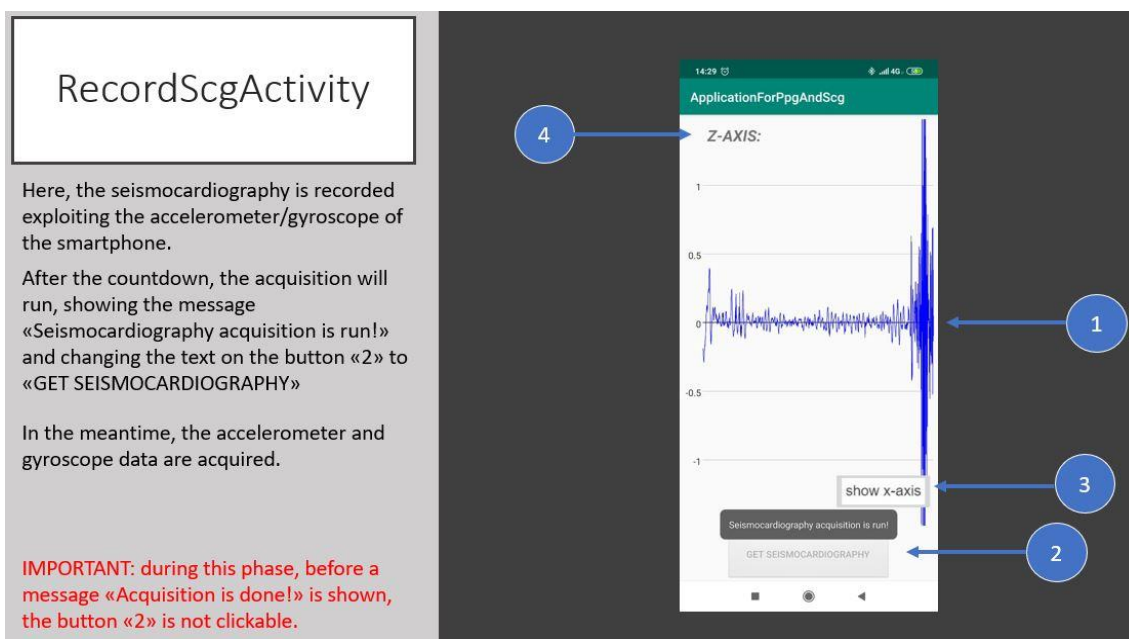


Figure 2.2.29 RecordScgActivity during the acquisition. When the detection of SCG signal starts, a message “Seismocardiography acquisition is run!” is shown over the button (arrow 2). The real-time graph shows the acquired data along the direction indicated by arrow 4.

At the end of the acquisition, 2 beeps are generated and the message “Acquisition is done!” is visualized (Figure 2.2.30).

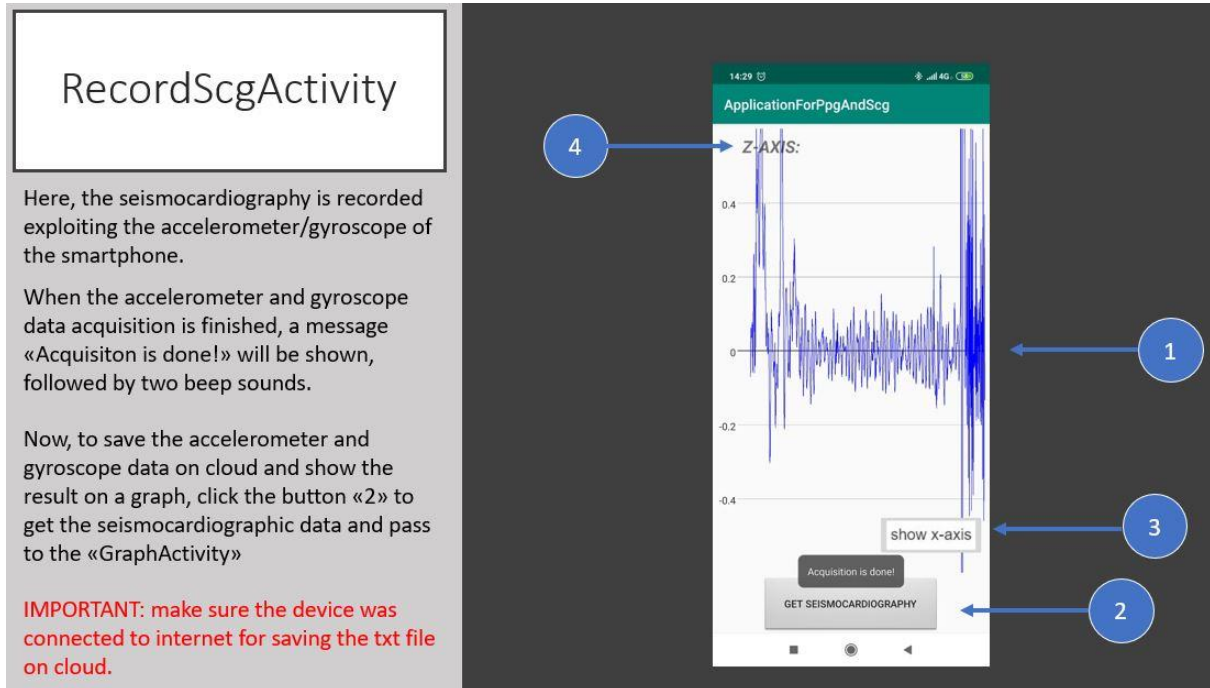


Figure 2.2.30 “RecordScgActivity” at the end of acquisition: the real-time is once again frozen (arrow 1), while the button is now clickable with the hint “GET SEISMOCARDIOGRAPHY” (arrow 2). A pop-up “Acquisition is done!”, which warns the user about the acquisition end, is also shown, followed by 2 beeps.

By clicking the button with “GET SEISMOCARDIOGRAPHY” text, the user launches the “GraphActivity” for visualizing the acquired data (Figure 2.2.31) in the same direction previously set during the real-time visualization. This “GraphActivity” is the same described in the previous scenario for the PPG visualization (paragraph 2.2.1.4), as well as the library to create the graph.

GraphActivity

Here, a graph of the raw accelerometer data is drawn.

If in the previous «RecordScgActivity» the button «GET SEISMOCARDIOGRAPHY» was pressed:

- a message (indicated by arrow «1») in this activity, describing the internal storage directory for the txt file containing the accelerometer data, will be shown;
- the plot should show a signal as indicated by the arrow «2».

IMPORTANT: make sure the device was connected to internet for saving the txt file on cloud.

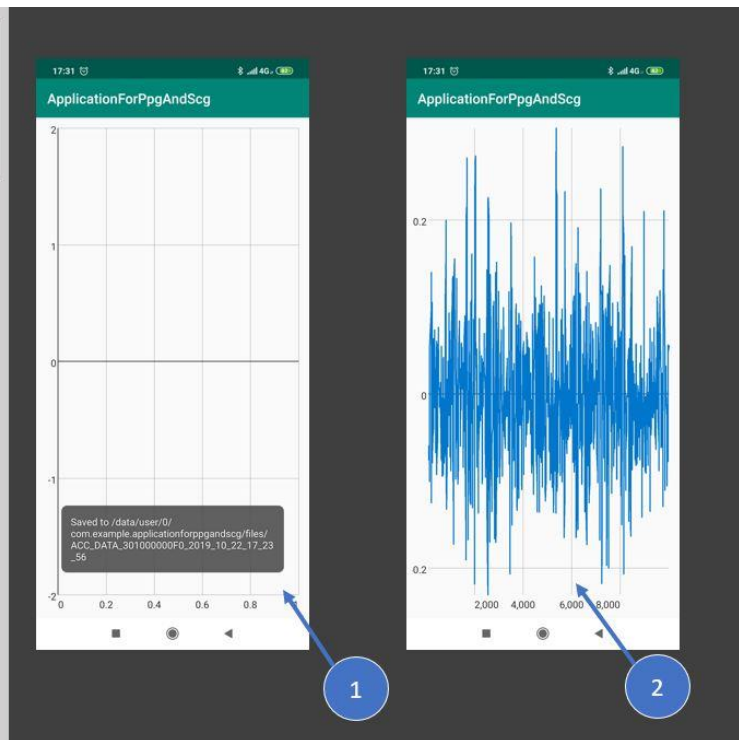


Figure 2.2.31 “GraphActivity” shows the SCG signal along the direction visualized previously on the “RecordScgActivity”. When the “GraphActivity” is opened, a message which indicates the internal storage path of the .txt containing the SCG data is shown (arrow 1). By scrolling and zooming the graph with the touch screen, the user can appreciate the acquired signal (arrow 2).

Passing from the “RecordScgActivity” to the “GraphActivity”, the SCG data are saved on a .txt file and stored in the internal storage path and on the Google Cloud service, as shown in Figure 2.2.4. The .txt file name begins with “ACC_DATA_”, followed by the same coding of the root folder and the date and time of the button press event (Figure 2.2.4). The .txt file contains the following information: the values sensed by the accelerometer along its 3 axis (x, y, z); the gyroscope data about the rotation among the 3 accelerometer axis; the timestamp vectors of the accelerometer and of the gyroscope computed using the mean sampling rate; the system timestamp vectors associated to each data acquisition event (in nsec); the mean sampling rates of the sensors during the acquisition; the vector of the sampling rates calculated for each second; the beginning absolute system time and the effective temporal duration of the acquisition (Figure 2.2.32).

All these user possible actions are summarized in the Figure 2.2.33.

```

*ACC_DATA_3010006027F170_2020_02_27_15_02_50 - Blocco note di Windows
File Modifica Formato Visualizza ?
Seismocardiogram x-axis values [m/s^2]:
[0.049274325370788574, 0.0872613787651062 0.10883504152297974,... 0.23879393935203552]

Seismocardiogram y-axis values [m/s^2]:
[0.01571035385131836, 0.020016193389892578, ... 0.10555052757263184,0.14562439918518066]

Seismocardiogram z-axis values [m/s^2]:
[-0.16876983642578125, -0.1532440185546875, -0.14742183685302734,... -0.10146713256835938]

Acceleromet mean sampling rate [samples/sec]: [191.0]

Timestamp of Accelerometer (calculated using mean sampling rate) [sec]:
[0.005235602094240838,0.02617801047120419,...,0.9947643979057549,0.9999999999999957]

Accelerometer means sampling rate list [samples/sec]:
[191.0]

Accelerometer system timestamp [ns] :
[1954873.0, 7051309.0, 1.2117227E7, 1.7213662E7, 2.227958E7,... 9.66371377E8]

Angular rate around x-axis values [rad/s]:
[0.015838623046875, 0.013702392578125, 0.0115814208984375,... 0.0115814208984375]

Angular rate around y-axis values [rad/s]:
[0.0133514404296875,..., 0.0112152099609375, 0.005889892578125, 0.0016326904296875]

Angular rate around z-axis values [rad/s]:
[0.01715087890625, 0.0128936767578125, 0.0150146484375,... 0.0118255615234375]

Gyroscope mean sampling rate [samples/sec]: [384.0]

Gyroscope sampling rate list [samples/sec]:
[384.0]

Timestamp of Gyroscope (calculated using mean sampling rate) [sec]:
[0.0078125,0.010416666666666666,0.013020833333333332,...,0.9999999999999942]

Gyroscope system timestamp [ns]:
[673135.0, 3206094.0, 5769571.0, 8302530.0, 1.0835489E7, 1.3368448E7,| ..., 9.72719033E8]

Acquisition beginning time of scg(system abs. time) [ns]: [3.74828456051842E14]

Acquisition end time of scg (respect to startTime ref.) [ns]: [1027293698]

```

Figure 2.2.32 The .txt file containing the accelerometer and gyroscope data, with the corresponding timestamp vectors, the mean sampling rates during the acquisition, the vector of the sampling rate calculated at each second, the acquisition beginning system time and the effective acquisition end time. The .txt file name saved by the "RecordScgActivity" begins with the words "ACC_DATA_" followed by the parameters inserted initially by the user and the date and time at the moment of the storage.

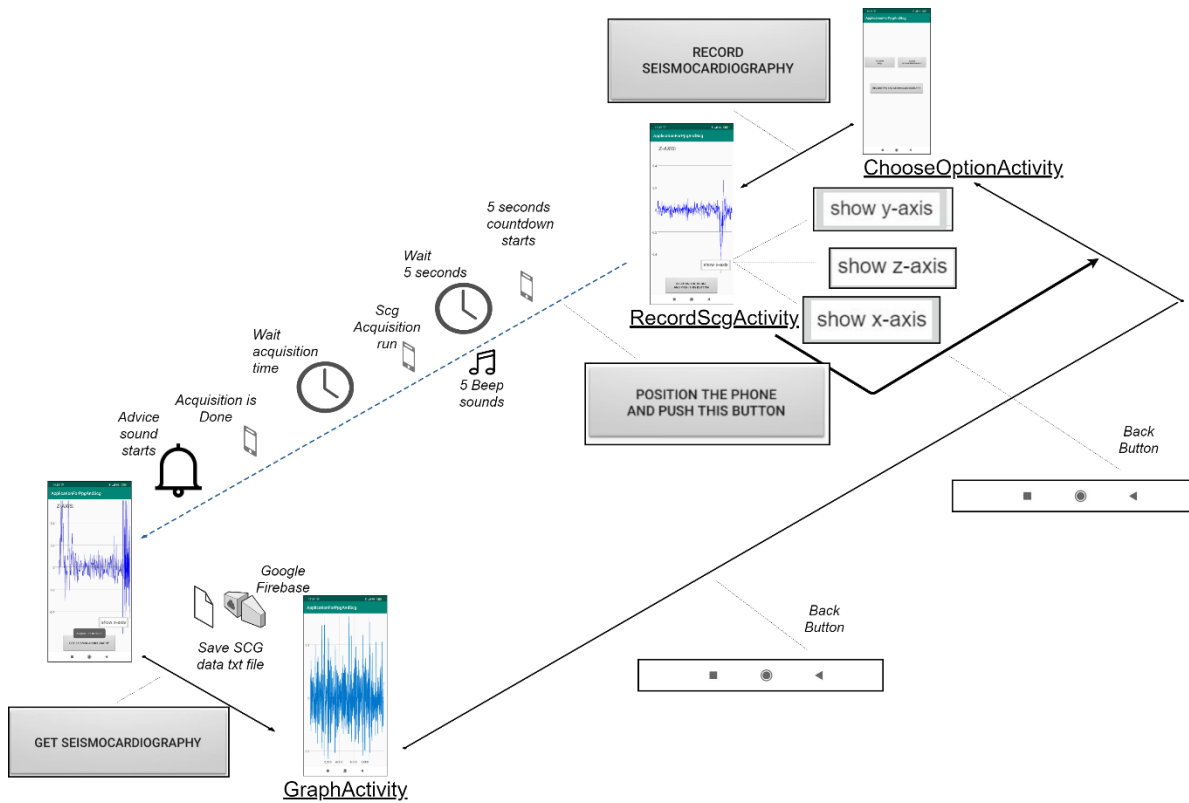


Figure 2.2.33 Flowchart of the possible operations that the user can act, from the choice of the “RecordScgActivity” to the graph of the SCG signal on “GraphActivity”.

2.2.1.5.1 Behind the SCG acquisition module design: the SensorManager class and its methods

The Android SDK provides a class to set and manipulate the IMU sensors, called *SensorManager*. The *SensorManager* has a collection of methods that the developer can exploit to interact with the smartphone accelerometer and gyroscope. The first fundamental methods are the *getSystemService* and *getDefaultSensor* that open the communication between the smartphone and its embedded accelerometer and gyroscope hardware. The *TYPE_LINEAR_ACCELERATION* attribute of the *getDefaultSensor* method allows the possibility of using the accelerometer to capture the 3D acceleration with the compensation of the gravity force, while the *TYPE_GYROSCOPE* parameter allows the use of the gyroscope sensor.

After having opened the communication with the IMU sensors, the second principal *registerListener* method of *SensorManager* class imposes the smartphone to listen to the sensors, capturing the events that are sensed by the IMU. This method needs as parameter a *SensorEventListener* class. For this reason, the “Listener” Java class on Android Studio was created (Figure 2.2.2). Inside the “Listener” class, the code to capture the accelerations along

the x, y and z axes and the angular rotations is implemented, combined with the customized methods to calculate the sampling rate every second during the acquisition and to store in a vector the timestamp computed by the system time as reference.

Moreover, the *registerListener* method allows to suggest to the smartphone system the sampling rate that the developer needs to achieve, expressed as microsecond delay between the samples captured by the accelerometer or the gyroscope. To force the system to use the maximum sensor sampling rate, the *SENSOR_DELAY_FASTEST* parameter is used, which is set for the gyroscope and the accelerometer in the “RecordScgActivity”.

2.2.1.5.2 Behind the SCG acquisition module design: the accelerometer and gyroscope jitters of the sampling rate

To evaluate the stability of the accelerometer and gyroscope sampling rates along the SCG acquisition, the possibility of retrieving the system timestamp vectors identified by the *elapsedRealtimeNanos* (Figure 2.2.32) of the Android systems, and consequently the sampling frequency during the signal acquisition, was exploited. For this purpose, 6 trials were done for 3 different acquisition durations: 10, 20 and 30 seconds, while the sampling frequency was set to the maximum with the *SENSOR_DELAY_FASTEST* parameter, as explained before.

To evaluate the performances, the mean of the inverse of the time interval between each couple of consecutive samples was calculated (Table 2.2.2) for both accelerometer and gyroscope, together with the respective jitter interval. The results are reported with respect to the acquisition duration of the test.

Table 2.2.2 Summary of accelerometer and gyroscope sampling frequency stability and jitters evaluation. For every acquisition time period, the values represent the median sampling frequency among the trials with the associated 1st and 3rd quartiles.

Test sampling frequency drift: median [25 th ; 75 th] (Hz)	
Acquisition time duration	Accelerometer sampling frequency (Hz)
10 seconds	250.14 [249.34; 250.94]
20 seconds	250.14 [249.34; 250.94]
30 seconds	250.14 [249.34; 250.94]
Test sampling frequency: median [25 th ; 75 th] (Hz)	
Acquisition time duration	Gyroscope sampling frequency (Hz)
10 seconds	250.14 [249.34; 250.94]
20 seconds	250.14 [249.34; 250.94]
30 seconds	250.14 [249.34; 250.94]

As shown in the Table 2.2.2, the accelerometer and the gyroscope sampling frequencies demonstrated an optimum stability and a very narrow range of jitter along all the durations.

To appreciate this behavior, a plot representing the sample-by-sample instantaneous sampling frequency of the accelerometer and gyroscope sensors, during a trial of 30 second, is shown in the Figure 2.2.34.

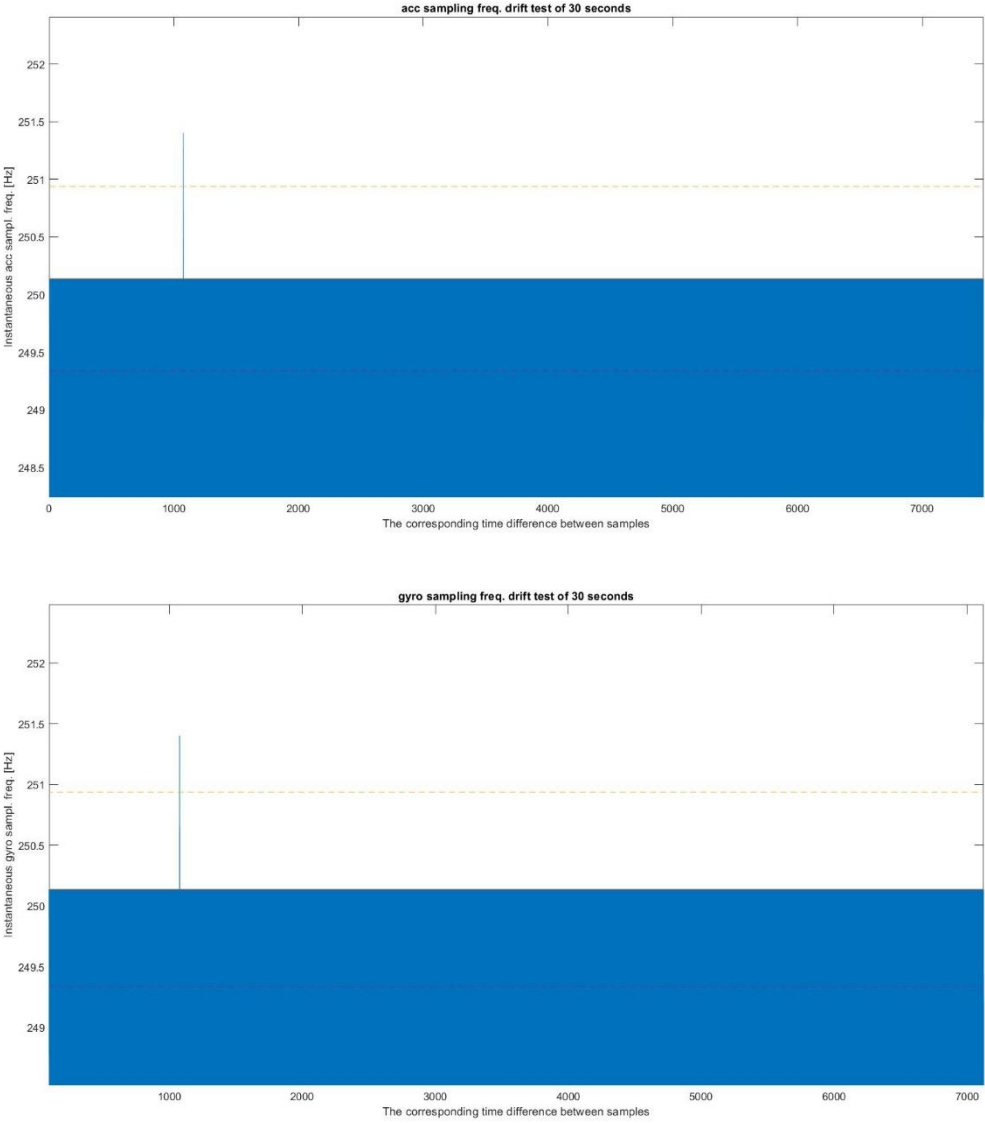


Figure 2.2.34 The inverse of time intervals calculated for each couple of consecutive samples, along the entire acquisition of 30 seconds, are shown on the top for the samples acquired by the accelerometer sensor, while on the bottom the for gyroscope samples. The dotted lines represent the 1^s and 3rd quartiles around the median value.

These results demonstrated a high stability and robustness of the IMU sensor for sensing external events driven by the Redmi Note 7 smartphone for durations of acquisition until 30 seconds, which are fundamental for the app purpose.

2.2.1.6 Fifth scenario: the SCG and PPG module

As described in the paragraph 2.2.1.3, if the button “RECORD PPG AND SEISMOCARDIOGRAPHY” (indicated by arrow 3, Figure 2.2.6) is selected, the activity to acquire simultaneously both the PPG and SCG signals (Figure 2.2.35) will be opened, represented by “RecordHfrPpgAndScgActivity” class on Android Studio (Figure 2.2.2).

Initially, a window dialog is shown (Figure 2.2.35, arrow 1), where the user must choose if the PPG will be computed on board or not (the arrow 2 in the Figure 2.2.35 points to the activity in background). After this operation, another dialog window, indicated by arrow 3 in the Figure 2.2.35, allows the user to set separately the acquisition duration of the two signals, scrolling the column on the left for the PPG time and the column on the right for the SCG signal.

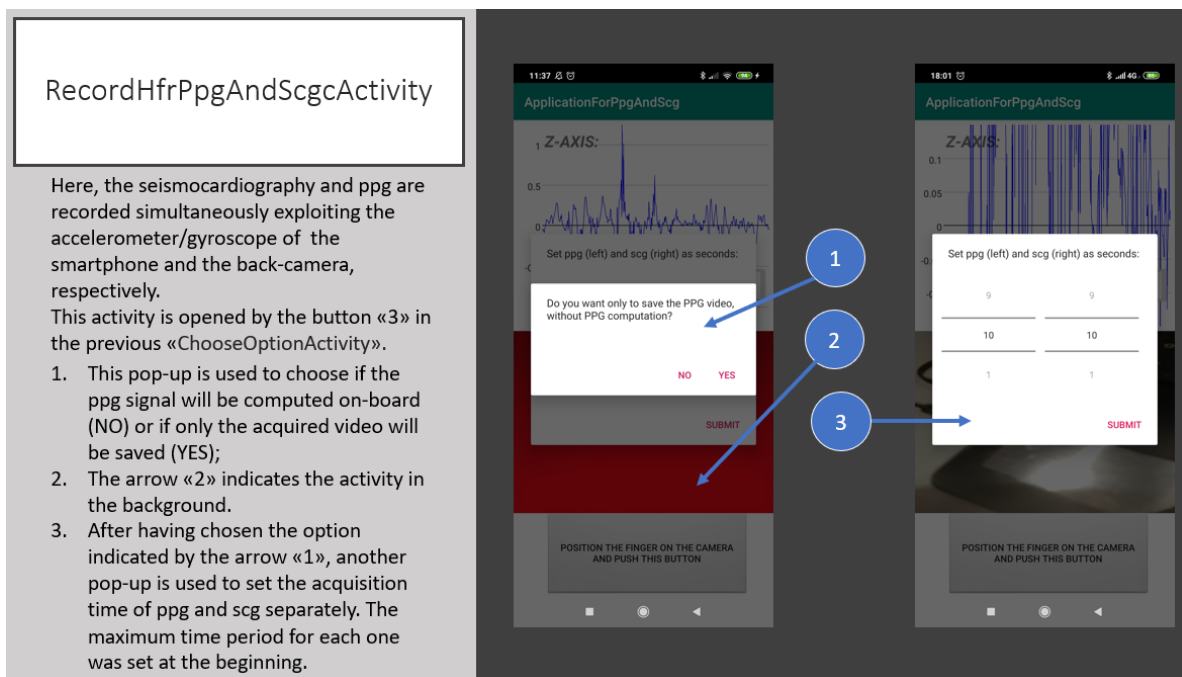


Figure 2.2.35 “RecordHfrPpgAndScgActivity”: when this activity is launched, a window dialog is pop-up (arrow 1) to choose if the PPG on-board computation will be run or not. After this operation, a second pop-up will be shown (arrow 3), which allows the user to set different acquisition time for PPG and SCG, respectively on the left and on the right of the window columns. The maximum time was set at the beginning through the “InitialActivity”. In the meanwhile, the activity is working in background (arrow 2).

After having selected the two acquisition durations, the activity will appear in the foreground (Figure 2.2.36). Here, the data acquired by the accelerometer and the frames captured by the camera are shown on a real-time graph and on a video container, respectively (Figure 2.2.36, arrow 1 and 2, respectively). These java objects for the visualization with their functions are the same used in the “RecordScgActivity” and in “RecordHfrPpgActivity”.

RecordHfrPpgAndScgcActivity

Here, the seismocardiography and ppg are recorded simultaneously exploiting the accelerometer/gyroscope of the smartphone and the back-camera, respectively:

1. The accelerometer data with respect to the chosen axis are shown in the real-time graph indicated by arrow «1»;
2. The arrow «2» indicates the acquired frames on the page centre;
3. The arrow «3» indicates button that will run the acquisition (read the advice on the button).
4. Button indicated by arrow «4» changes the accelerometer axis shown on the graph;
5. Arrow «5» indicates the text which shows what axis is actually shown on real time graph.

User can run the acquisition of the accelerometer and camera data simply by pushing the button «3».

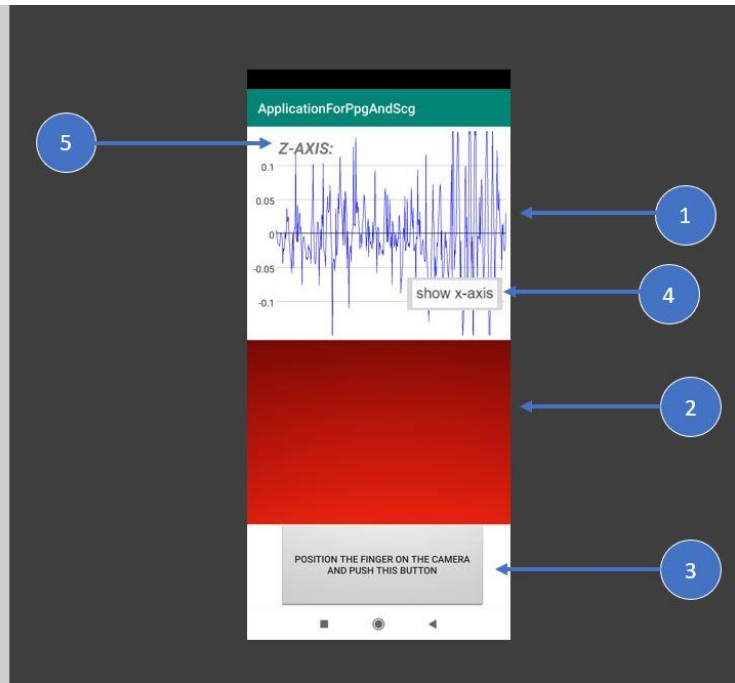


Figure 2.2.36 “RecordHfrPpgAndScgcActivity”: after the chosen of the acquisition times for the PPG and SCG, the main activity appears in the foreground. Here, the visualization of the data given by the accelerometer (arrow 1) and the frames captured by the smartphone camera (arrow 2) are shown. The button indicated by arrow 3 is used to run the simultaneous acquisition of the two signals. The button 4 allows to change the visualized accelerometer axis, which is indicated by arrow 5.

As suggested by the button indicated by arrow 3 in Figure 2.2.36, the user can position the index fingertip on the camera objective and the smartphone on the chest, with the smartphone screen placed towards the body. The app leaves to the user 5 seconds, synchronized to 5 beeps, to do this operation, during which the app is frozen, and the button will become orange (Figure 2.2.37).

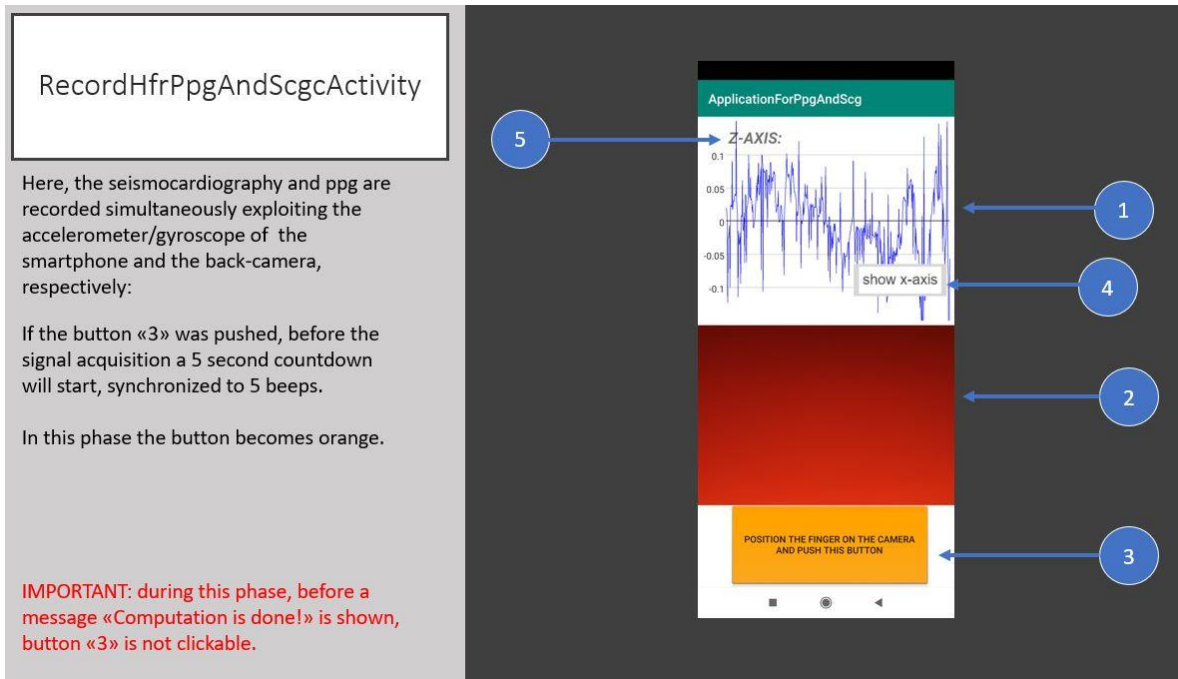


Figure 2.2.37 “RecordHfrPpgAndScgcActivity”: when the button is pressed to run the acquisition, this latter becomes orange (arrow 3) and not clickable for all the acquisition and PPG computation (if set). The real-time graph (arrow 1) and the video visualization (arrow 2) are frozen and a 5-seconds countdown will start, synchronized with 5 beeps.

Then, the effective acquisition of the signals begins and a message “Period of acquisition is run” is visualized (Figure 2.2.38). During this phase, the accelerometer and gyroscope data are collected by the smartphone simultaneously with the video recording from the camera.

RecordHfrPpgAndScgcActivity

Here, the seismocardiography and ppg are recorded simultaneously exploiting the accelerometer/gyroscope of the smartphone and the back-camera, respectively:

After the countdown, the acquisition will run, showing a message «Period of acquisition is run!» and changing the button text to «GET PPG AND SCG DATA»

During the acquisition phase, a video is recorded for computing (if selected) the ppg signal, while the inertial sensor data are stored in background.

IMPORTANT: during this phase, before a message «Computation is done!» is shown, button «3» is not clickable.

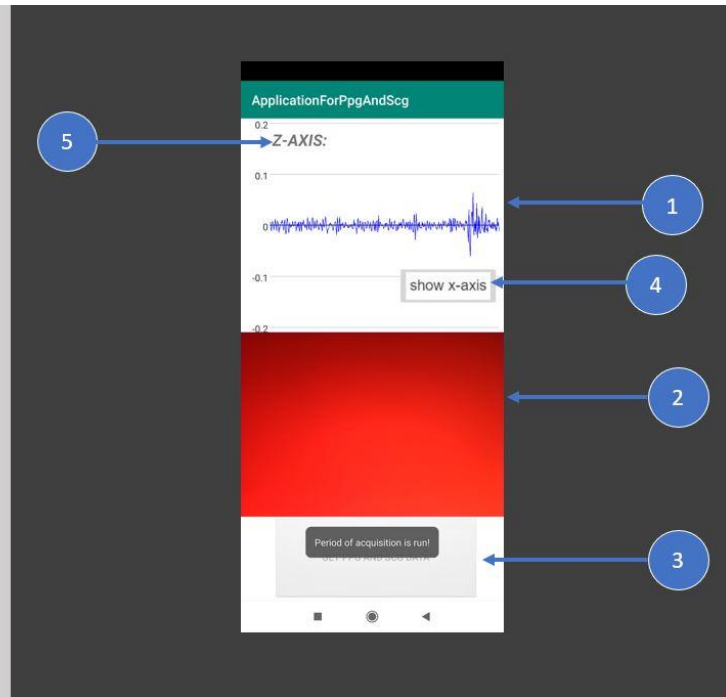


Figure 2.2.38 “RecordHfrPpgAndScgcActivity”: after the 5 beeps and the 5-seconds countdown, a message “Frame and scg acquisition is run!” is shown, which indicates the beginning of the accelerometer and gyroscope data collection and of the video recording.

When the acquisition duration of both IMU and camera sensors is finished, a message “All acquisition are done and video saved!” is shown together with two beeps (fig. 2.2.39). These events underline the storage of the video inside the internal memory of the device and, if set at the beginning (Figure 2.2.35), the start of PPG calculation from the video in background. When the PPG computation is finished, a sequence of beeps accompanies the visualization of the button with the text “GET PPG AND SCG DATA”, and the message “Computation is done!” will be shown (Figure 2.2.40).

RecordHfrPpgAndScgcActivity

Here, the seismocardiography and ppg are recorded simultaneously exploiting the accelerometer/gyroscope of the smartphone and the back-camera, respectively.

When the acquisition phase of the video and accelerometer/gyroscope data is completed, a message «All acquisitions are done and video saved» will be shown and the video is saved into the smartphone storage, followed by two beep sounds. At this moment, the computation of the ppg values starts, if this option was selected at the beginning .

IMPORTANT: during this phase, before a message «Computation is done!» is shown, button «3» is not clickable.

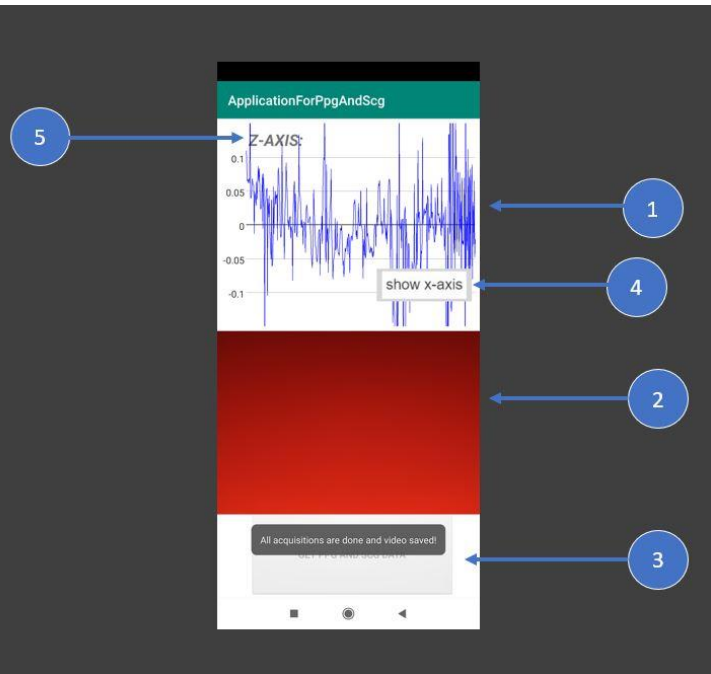


Figure 2.2.39 “RecordHfrPpgAndScgActivity”: when both IMU and camera sensor acquisitions are completed, a message “All acquisition are done and video saved!” (arrow 3) is shown, followed by 2 beeps, which indicates the beginning of PPG computation in background (if selected). In the meantime, the real-time graph (arrow 1) and video (arrow 2) visualizations are stopped and the acquired video is saved in the internal storage.

RecordHfrPpgAndScgcActivity

Here, the seismocardiography and ppg are recorded simultaneously exploiting the accelerometer/gyroscope of the smartphone and the back-camera, respectively.

When also the PPG signal is computed (if this option was chosen), a message «Computation is done!» will be shown, followed by some beep sounds.

Now, to save the PPG and accelerometer data on cloud and on smartphone internal memory and to show the results on graphs, click the button and pass to the «Graph3Activity»

IMPORTANT: make sure the device was connected to internet for saving the txt file on cloud.

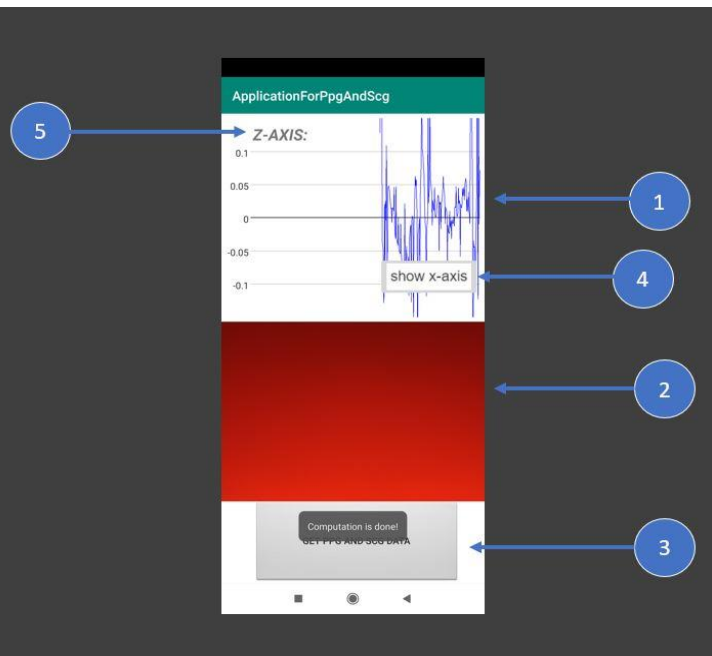


Figure 2.2.40 “RecordHfrPpgAndScgActivity”: when the PPG computation in background is concluded, a message “Computation is done!” is shown simultaneously to a sequence of beeps to warn the user. The button (arrow 3) will be newly clickable.

Once the user has pressed the button (Figure 2.2.40, arrow 3), three events are triggered: 1) the storage in the smartphone internal memory and 2) on Google Cloud service (Figure 2.2.4) of a .txt file with the information of the PPG data and of inertial sensor data, as described in the paragraphs 2.2.1.4 and 2.2.1.5 (Figure 2.2.14 and Figure 2.2.32) in the same order, starting from the PPG information, and 3) the start of the next activity “Graph3Activity” (Figure 2.2.41) as Android Studio class (Figure 2.2.2).

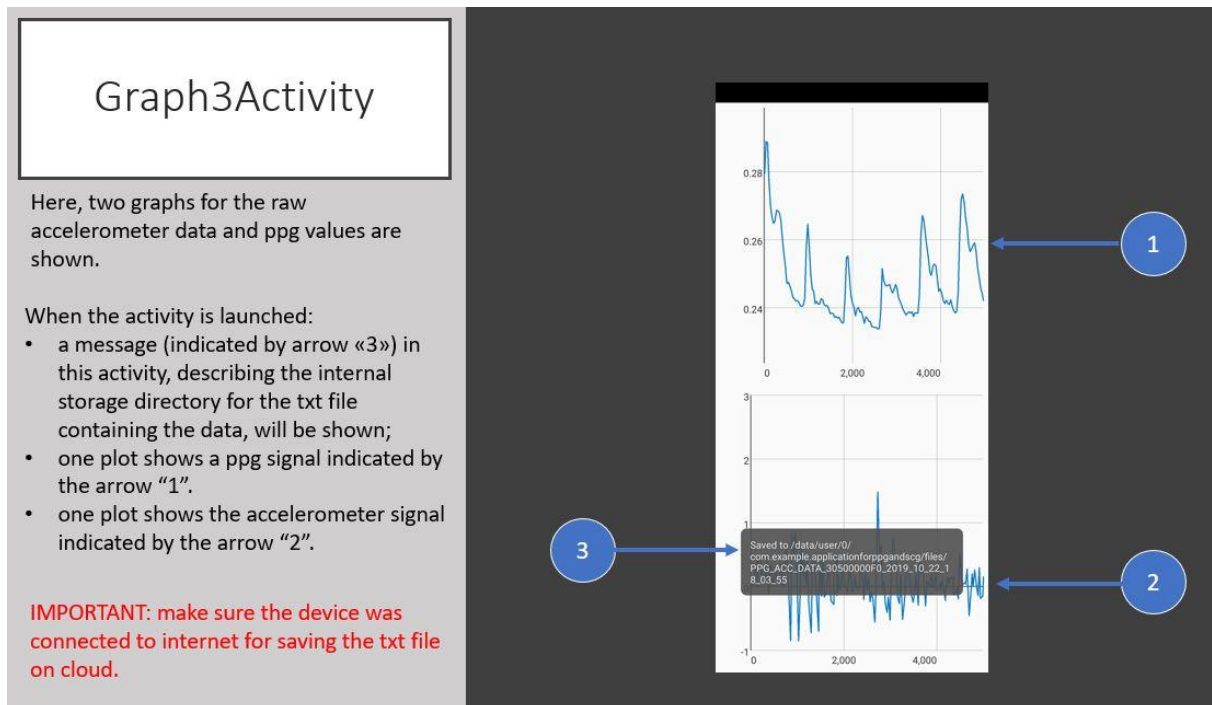


Figure 2.2.41 “Graph3Activity” shows the resulted signals from the PPG acquisition (arrow 1) and from the acquired SCG, along the axis visualized during the acquisition (arrow 2). A pop-up indicates the internal storage path of the .txt file with the sensor data (arrow 3).

On the “Graph3Activity”, the user can visualize the obtained signals: the upper graph shows the computed PPG (Figure 2.2.41, arrow 1), while the graph below (Figure 2.2.41, arrow 2) shows the acceleration captured along the axis visualized on the real-time graph in the previous activity (Figure 2.2.40, arrow 5). When the activity is launched, a message with the .txt file smartphone internal storage path is shown (Figure 2.2.41, arrow 3).

If the user has not set the PPG on board computation, only the SCG signal will be shown.

All these passages are synthesized in the Figure 2.2.42.

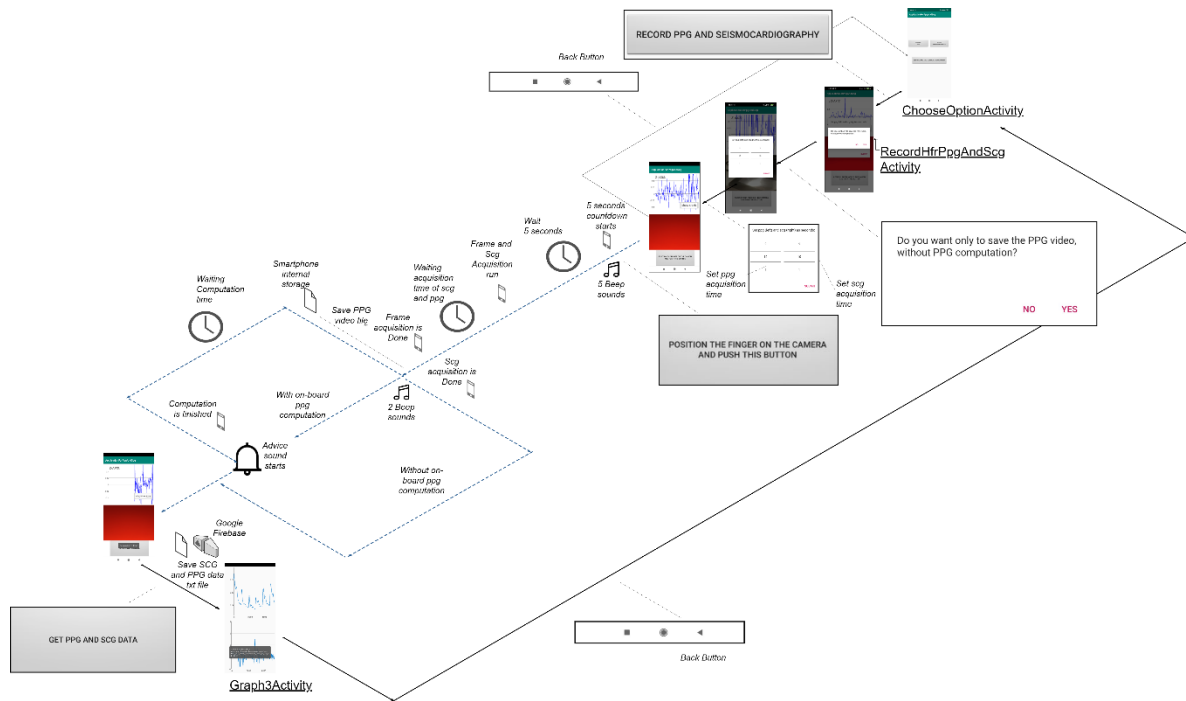


Figure 2.2.42 Flowchart of the possible operations that the user can act, from the choice of the “RecordHfrPpgAndScgActivity” to the graphs of the PPG and SCG signals on “Graph3Activity”.

2.2.1.6.1 Behind the SCG and PPG acquisition module design: the “CapturePpgAndScgMode” fragment and the main Android SDK classes

As the “RecordHfrPpgActivity” class, the “RecordHfrPpgAndScgActivity” has the function to instantiate the Android fragment called “CapturePpgAndScgMode” (represented as Java class on Android Studio in the Figure 2.2.2), which implemented the core of the code to acquire the SCG and PPG signal simultaneously. The “CapturePpgAndScgMode” use the same classes, methods, attributes and logic of “RecordHfrPpgActivity” and “RecordScgActivity”, which are described in the paragraphs 2.2.1.4.1, 2.2.1.4.2 and 2.2.1.5.1. One difference relies on the use of a different *Listener* class, called “Listener3”, and of the “Graph3Activity” class on Android Studio (Figure 2.2.2).

The choice of using another *Listener* class is due to the need of having different flags allowing the communication between the “Listener3” and the “CapturePpgAndScgMode” classes. These flags allow the synchronization of the beginning of the acquisition between the camera and the IMU sensors. Despite that the Android SDK doesn’t allow a perfect synchronization between two subsystems of the same smartphone device, there are different possibilities to assess this time delay between different sensor types, and compensate that problem (Wang *et al.*, 2018).

For what concerns the “Graph3Activity” (Figure 2.2.41), it shows two graphs in the same layout, differently from the “GraphActivity”, that allows the visualization of only one signal.

2.2.1.6.2 Behind the SCG and PPG acquisition module design: the camera and motion sensor sampling frequency

As explained in the paragraph 2.2.1.5.1, the *registerListener* method of the *SensorManager* class allows to set the desired sampling frequency of the motion sensors. To this aim, the `SENSOR_DELAY_FASTEST` parameter was set by software, leaving the sensor free to reach the maximum possible sampling rate. However, *registerListener* method can only suggest to the hardware to set the delay between two consecutive listen events: it is then important to verify this performance. Moreover, as in this modulus the SCG is recorded simultaneously to the camera, this could affect the sensor performance. For the same reason, the camera frame rate needs to be tested, according to the three different possible frame rates that the user can set (paragraph 2.2.1.2).

The results of 9 trials applying three durations of acquisitions (10, 20 and 30 seconds) are summarized in Table 2.2.3. The accelerometer and gyroscope sampling frequencies maintained the same values with the same jitters along all acquisitions, despite changes in the acquisition duration and camera frame rate settings. Similarly, the camera sampling frequency shows a high stability for 30 fps, with a narrow interval of fluctuation until 60 fps. When the camera works at 120 fps, the jitters augment due to the behavior explained in the paragraph 2.2.1.4.3.

Table 2.2.3 An overview of trial results to test the sensor sampling frequency stability during simultaneous acquisitions of the SCG and PPG data. The tests were conducted at three acquisition durations (10, 20, 30 seconds) at three different possible camera frame rates (30, 60 and 120 fps).

Sensor sampling frequency medians [25 th ; 75 th] (Hz)			
Acquisition duration	Camera frame rate set at 30 fps		
	Accelerometer samp. freq. [Hz]	Gyroscope samp. freq. [Hz]	Camera samp. freq. [Hz]
10 seconds	250.14 [249.34; 250.94]	250.14 [249.34; 250.94]	30.02 [30.00; 30.04]
20 seconds	250.14 [249.34; 250.94]	250.14 [249.34; 250.94]	30.02 [29.99; 30.05]
30 seconds	250.14 [249.34; 250.94]	250.14 [249.34; 250.94]	30.02 [29.99; 30.05]
Sensor sampling frequency medians [25 th ; 75 th] (Hz)			
Acquisition duration	Camera frame rate set at 60 fps		
	Accelerometer samp. freq. [Hz]	Gyroscope samp. freq. [Hz]	Camera samp. freq. [Hz]
10 seconds	250.14 [249.34; 250.94]	250.14 [249.34; 250.94]	59.74 [59.60; 59.87]
20 seconds	250.14 [249.34; 250.94]	250.14 [249.34; 250.94]	59.74 [59.64; 59.84]
30 seconds	250.14 [249.34; 250.94]	250.14 [249.34; 250.94]	59.74 [59.60; 59.87]
Sensor sampling frequency medians [25 th ; 75 th] (Hz)			
Acquisition duration	Camera frame rate set at 120 fps		
	Accelerometer samp. freq. [Hz]	Gyroscope samp. freq. [Hz]	Camera samp. freq. [Hz]
10 seconds	250.14 [249.34; 250.94]	250.14 [249.34; 250.94]	120.00 [117.07; 122.93]
20 seconds	250.14 [249.34; 250.94]	250.14 [249.34; 250.94]	120.00 [115.74; 124.25]
30 seconds	250.14 [249.34; 250.94]	250.14 [249.34; 250.94]	120.00 [114.36; 125.64]

Another way to test the stability of the sensors during a simultaneous acquisition of SCG and PPG data was to count how many samples of the accelerometer were present at every camera frame acquisition cycle. This evaluation was done calculating the ratio

$$\frac{\text{Number of accelerometer samples}}{1 \text{ camera cycle}}$$

compared to the reference value, that is equal to the ratio between the accelerometer sampling frequency and the set camera frame rate. The corresponding results are shown in the Table 2.2.4.

Table 2.2.4 Ratio of accelerometer samples over a camera cycle calculated at three different acquisition times (10, 20, 30 seconds) at every possible camera frame rate. The obtained ratio is compared to the reference value, which is equal to the ratio between the accelerometer sampling frequency and the set camera frame rate.

Ratio (number of acc. samples/1 camera cycle) evaluation		
Acquisition duration	30 fps	
	Mean ratio	Reference value (acc. sampling freq. / camera fps)
10 seconds	8,26±0,79	8,27
20 seconds	8,30±0,50	8,25
30 seconds	8,31±0,47	8,34
Ratio (number of acc. samples/1 camera cycle) evaluation		
Acquisition duration	60 fps	
	Mean ratio	Reference value (acc. sampling freq. / camera fps)
10 seconds	4,16±0,46	4,15
20 seconds	4,17±0,39	4,15
30 seconds	4,17±0,40	4,19
Ratio (number of acc. samples/1 camera cycle) evaluation		
Acquisition duration	120 fps	
	Mean ratio	Reference value (acc. sampling freq. / camera fps)
10 seconds	2,09±0,40	2,12
20 seconds	2,11±0,63	2,10
30 seconds	2,12±0,73	2,10

Results in Table 2.2.4 underline the ability of the SCG and PPG sensors in being stable along all acquisitions, reaching a value close to the ideal reference, with narrow intervals of variation. These small changes in the ratio values during the acquisitions are mainly due to jumps in the camera frame acquisition, which results in an increase in accelerometer samples over the camera cycle. This behavior was previously shown in the paragraph 2.2.1.4.3 and represented by the Figure 2.2.17. Here, this method allowed a comparison of the performance of the two embedded sensors working together, which maintained a certain coherence during the acquisitions.

3 THE EXPERIMENTAL PROTOCOLS AND OUTCOME ANALYSIS

To test the feasibility of the previously described app (paragraph 2.2.1) to derive the PPG and SCG biological signals, two different experimental protocols were designed. The first one aimed to retrieve the participant HRs by the frequency spectrum analysis of the separately acquired PPG and SCG signals (chapter 2, paragraphs 2.2.1.4 and 2.2.1.5, respectively), while the second one was focused to test the HR and PTT extraction by exploiting the app module (chapter 2, paragraph 2.2.1.6) for the simultaneous acquisition of the PPG and SCG signals.

In particular, the first protocol framework was structured with the purpose of extracting the user HR and, in the meanwhile, studying the capability of the app of being integrated in a home environment, leaving the volunteers as free as possible in the app usage after an initial informative training, whereas the second protocol used “gold standard” measurements for the HR validation and to test the feasibility of estimating the PTT, that were acquired by a Nexfin instrument in collaboration with the IRCCS Auxologico of San Luca (MI).

3.1 FIRST PROTOCOL: HR ESTIMATION AND APP USABILITY EVALUATION

For this aim, 7 subjects with a median age of 28 [27; 29] years old, a median weight of 62 [52; 72] kg and a median height of 170 [165; 180] cm were studied.

3.1.1 The experimental setup

During the signal acquisitions, the smartphone was kept by the subjects with the right hand using the configuration explained in the figure 2.2.8 of the paragraph 2.2.1.4 for the PPG signal, while it was positioned autonomously by the subjects on the chest (Figure 3.1.1), in order to capture the SCG signal. Before the beginning of the SCG acquisitions, every subject tried to find the best position for the SCG by looking at the real-time signal shown by the app (fig. 2.2.27, arrow 1, paragraph 2.2.1.5). Typically, the chosen smartphone location was the left-upper chest position (Figure 3.1.1).

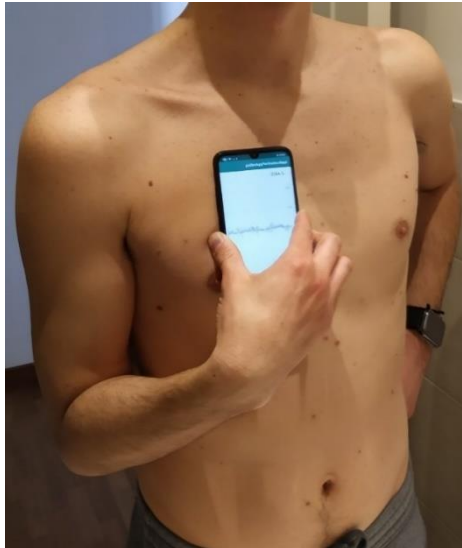


Figure 3.1.1 Before signal acquisition, the subjects chose autonomously the best smartphone position on the chest for capturing the SCG signal, by looking at the real time SCG graph offered by the app.

The experiments were done inside rooms artificially illuminated (Figure 3.1.2).



Figure 3.1.2 The picture shows a house living room artificially illuminated. The subject assumed a supine position lying down on a sofa during the PPG acquisition.

3.1.2 Protocol

As shown in detail in the Table 3.1.1 and in the flowchart of the Figure 3.1.3, the experiment was structured as follow. At the beginning, the subjects inserted through the app their personal info, the needed camera frame rate (30 fps) and the acquisition time (30 seconds),

saving these data both into the internal storage and on Google cloud. Successively, the SCG and PPG signals were acquired separately by the Redmi Note 7 one time for each possible position: standing (Figure 3.1.1) and supine (Figure 3.1.2). The acquisitions were done during a basal (relax) condition.

At the end of all experiments, 3 different types of questionnaires were administered to the subjects. The first represents an international standard survey to evaluate the system usability scale (SUS) (Bangor, Kortum and Miller, 2008), the second is an ad-hoc questionnaire to understand the app usability from the user point-of-view, and the third is called TWEETS, which concerns e-health engagement (Kelders and Kip, 2019).

The total number of obtained signals for each subject was 2 PPGs, one in standing position and one in the supine posture, and 2 SCGs, with the same differentiation of PPG signals.

The acquisition duration was set to 30 seconds for all the experiments, with 30 Hz camera frame rate and 250 Hz SCG sampling frequency, as summarized in the Table 3.1.1.

Table 3.1.1 First experimental protocol used sampling frequencies: the camera frame rate was set for every acquisition at 30 fps, while the accelerometer and gyroscope sampling frequency at 250 Hz, which is the maximum reachable by the inertial sensors.

FIRST EXPERIMENTAL PROTOCOL SENSOR SAMPLING FREQUENCIES		Position	
		Supine	Standing
PPG	Frame Rate (fps)	30	30
SCG	accelerometer sampling frequency (Hz)	250	250
	gyroscope sampling frequency (Hz)	250	250

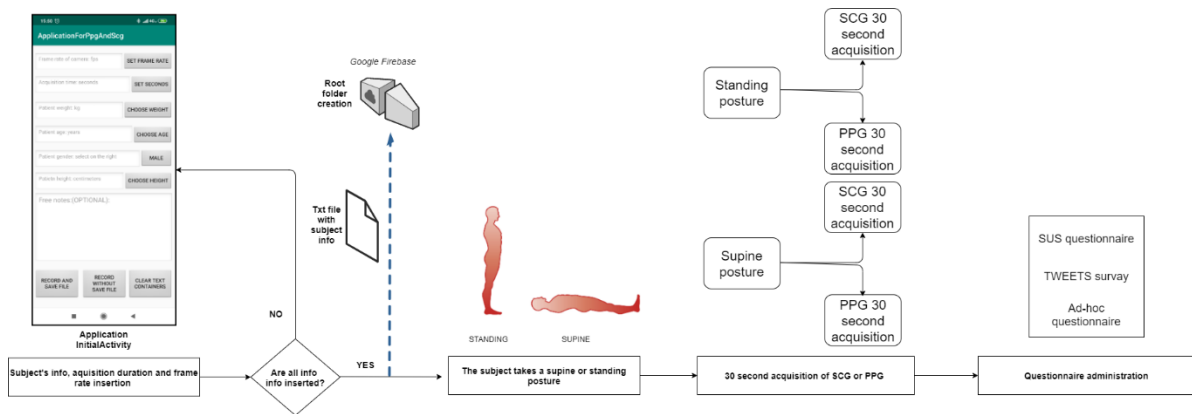


Figure 3.1.3 The flowchart of the first experimental protocol. The subject initially inserted his/her info on the app and the acquisition setting (camera fps and duration), recording them on a txt file on the cloud and in the smartphone internal storage. After, the subject assumed a supine or a standing position, during that the SCG and PPG signals were acquired in a basal condition. At the end, the subject filled in 3 types of questionnaire about app usability and e-health patient engagement.

Every acquisition session was defined by different steps, depending on which signal was acquired, the PPG (Figure 3.1.4) or SCG (Figure 3.1.5).

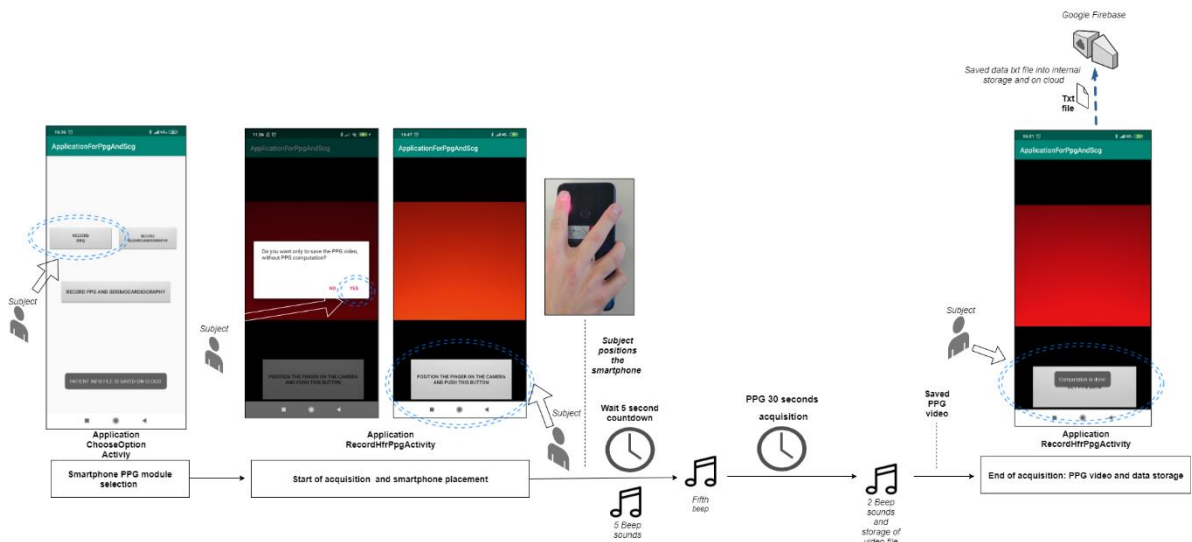


Figure 3.1.4 Flowchart of PPG acquisition session. The subject chose the PPG app module and set the option of saving the recorded video without on-board PPG computation. The subject run the acquisition with the button and positioned the fingertip on the camera. After the acquisition time (30 seconds), the subject saved the recorded data and video on the cloud by pressing the designated button.

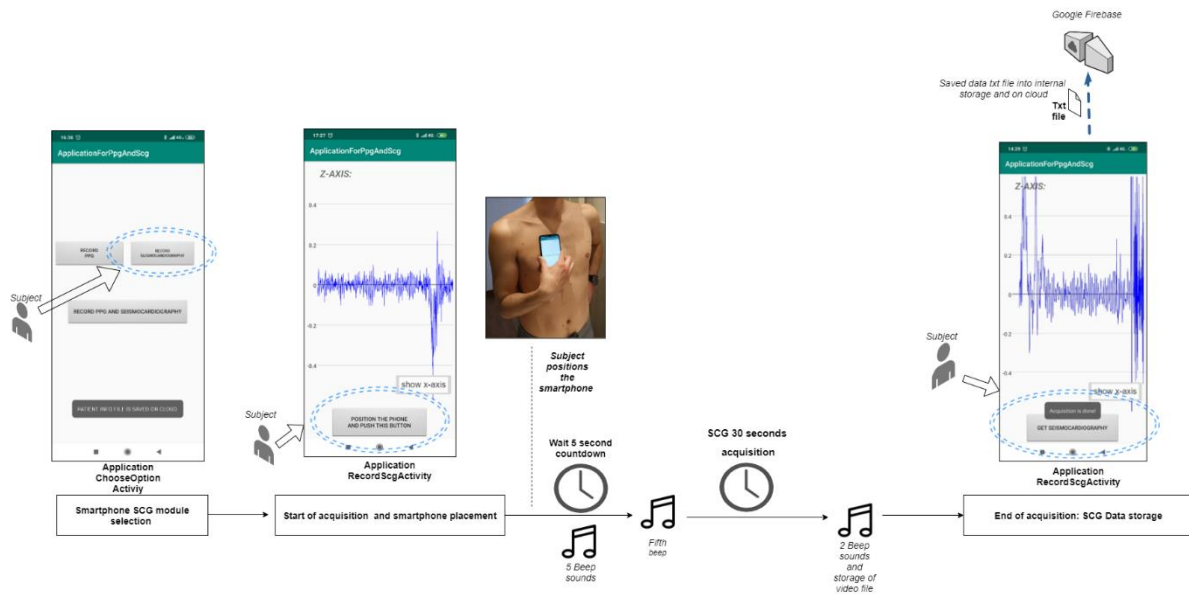


Figure 3.1.5 Flowchart of SCG acquisition session: the subject chose the SCG app module and run the acquisition with the button. The smartphone was placed at the position chosen by the subject looking at the real-time plot. At the end of acquisition time (30 seconds), the subject saved the recorded SCG data on the cloud by pressing the designated button.

For the PPG acquisition, the button “RECORD PPG” (paragraph 2.2.1.3) was pressed by the users. On the PPG module, the subjects were instructed to choose the option of not computing the PPG on-board, which allowed to save the recorded video file without waiting for the time of PPG evaluation. Successively, the subjects placed the index fingertip of the right hand on the camera, covering the flash and leaving free the depth sensor, as explained in the Figure 2.2.8. At this point, the subjects run the acquisition, which started after a 5 seconds countdown. After 30 seconds, the smartphone app warned the users about the acquisition end with two beeps, while the video was automatically saved in the smartphone internal storage. At this point, the subjects pressed the button to save the .txt file with the PPG data into the internal storage and on the Google cloud. In this way, the video was saved on cloud as well.

For the SCG recording selection, the button “RECORD SEISMOCARDIOGRAPHY” (paragraph 2.2.1.3) was pressed by the users. Before starting the acquisition, the subjects autonomously tried to find the best position to place the smartphone on their chest, looking at the real-time SCG graph offered by the app. When the position was found, the subjects run the 30 seconds acquisition, which started after a 5 seconds countdown. After 30 seconds, the smartphone app warned the users about the acquisition end with two beeps and the subjects could press the button to save the .txt file with the SCG data on the internal storage and on Google cloud.

The obtained smartphone data were analyzed offline using MATLAB.

3.2 SECOND PROTOCOL: HR MEASUREMENT VALIDATION AND PTT ESTIMATION

To validate the HR measurements extracted from the smartphone and to test the capability of the app for the simultaneous acquisition of the PPG and SCG signals (see paragraph 2.2.1.6) for the estimation of PTT interval, the smartphone results were compared to the mean HR and the PAT obtained by the synchronous acquisition of plethysmography (PLT) and ECG signals acquired by a Nexfin instrument, typically used to monitor fundamental physiological parameters, such as the HR and blood pressure (BP) (Figure 3.2.1).



Figure 3.2.1 Nexfin monitor of Istituto Auxologico San Luca.

The smartphone signal synchronization represents a fundamental prerogative to compute the correct PTT. As mentioned by Wang et al. in 2018, the Android programming tools didn't allow the synchronization between the different smartphone sensor subsystems (Wang *et al.*, 2018). Indeed, this affects the timestamps associated to the accelerometer and camera samples, introducing an initial error in the phase between the signals. Wang et al. computed this delay by inserting a noise contemporarily inside the video audio and in the accelerometer signal, with 3 beeps played by the smartphone speaker (Figure 3.2.2), with the smartphone lying down on a surface. After a first analysis, they computed a mean error of synchronization between the accelerometer and camera sensors of 170 ± 15 msec (Wang *et al.*, 2018). The standard deviation of this error suggests that this can vary for each acquisition as well.

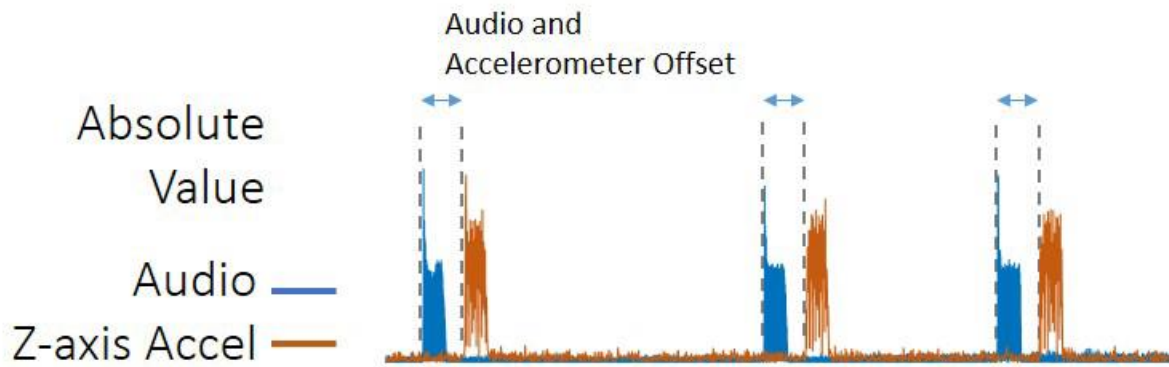


Figure 3.2.2 A series of three beeps is played through the phone's speaker to synchronize the camera and accelerometer subsystems (Wang et al., 2018).

To reproduce a similar strategy, an ad-hoc algorithm was developed, in order to extract the delay between the camera and the IMU sensors at the beginning of the simultaneous SCG and PPG acquisition, when this acquisition was selected. The Android programming tools allowed making the smartphone vibrate; this vibration is captured by the accelerometer signal. To exactly synchronize the camera with the accelerometer, the flashlight, which initially was on, was switched off when the vibration started. With the smartphone positioned by the flashlight side on a surface, this changing of light was captured by the PPG video. After, the flashlight was re-activated after few seconds. This additional phase lasted 5 seconds and it was added to the 5-seconds countdown belonging to the normal functions of this app module (paragraph 2.2.1.6). In addition, other 10 seconds of duration of the acquisition were added, to allow time to the user to place the smartphone on the chest, after this initialization phase. Thus, the effective PPG and SCG acquisition started after a time period of 20 seconds, marked by 20 synchronized beeps including: the time for the 5-seconds countdown, 5 seconds for the synchronization algorithm and 10 seconds to place the smartphone on the chest for the acquisition.

For this purpose, a healthy female volunteer with an age of 22 years old, a weight of 58 kg and a height of 165 cm was studied in standing position. The experiments were conducted at the IRCCS Istituto Auxologico of San Luca (MI).

3.2.1 The experimental setup

In order to acquire the gold standard measurements, the Nexfin cuff was positioned at the index finger of the left hand to extract the BP and PLT of the subject from the built-in photo-

plethysmograph sensor in the cuff, while the electrodes of the Nexfin 3 + 3 leads module were placed on the body, as shown in Figure 3.2.3.



Figure 3.2.3 Configuration of Nexfin ECG module electrodes and the Nexfin cuff on the index finger of the left hand of the subject. The smartphone was positioned on the upper-middle chest.

The smartphone was grabbed by the subject with the natural hand using the configuration explained in the Figure 2.2.8 of the paragraph 2.2.1.4 for the acquisition of the PPG signal, while the smartphone was positioned by the screen side on the subject chest, in order to capture the SCG signal. During the setup, the upper-middle chest position to place the smartphone for the SCG was chosen by the subject (Figure 3.2.3).

The experiments were done inside a room artificially illuminated.

3.2.2 Protocol

The experiment was subdivided in 3 different sessions (Table 3.2.1), each one (Figure 3.2.4) using the different possible camera frame rates offered by the app: 30, 60 and 120 fps. The Redmi note 7 motion sensors sampling frequencies for SCG were always set at 250 Hz, that represent the highest possible values. The acquisition durations were set to 30 seconds. The Nexfin ECG signal was sampled at 1000 Hz, while the PLT signal at 200 Hz, and after oversampled at 1000 Hz with a parabolic interpolation.

Table 3.2.1 The number of sessions is based on the used smartphone camera frame rate (30, 60 and 120), with the respective motion sensor sampling frequencies. The subject always assumed a standing posture.

Experimental sessions with acquisition duration of 30 seconds	Position: Standing		
	Session 1	Session 2	Session 3
Camera frame rate (fps)	30	60	120
Accelerometer sampling frequency (Hz)	250	250	250
Gyroscope sampling frequency (Hz)	250	250	250

At the end, 3 PPG signals were acquired, each one at a different camera frame rate (30, 60 and 120) together with their corresponding SCG acquired simultaneously at 250 Hz, for a total of 3 SCG signals.

Initially, the subject run the app on the Redmi Note 7 and inserted its parameters and the camera sampling rate (30, 60 or 120), as explained in the paragraph 2.2.1.2. When all the information were inserted, the .txt file was saved and the subject could choose among the app acquisition modules. For this purpose, the module for acquiring simultaneously the PPG and SCG was always used (paragraph 2.2.1.6), with 30 seconds acquisitions for both signals.

At this point, the calibration phase of the Nexfin begun, running the automatic Physiological calibration algorithm (Eeftinck Schattenkerk *et al.*, 2009; Garnier *et al.*, 2012). After this phase was completed, the subject run the app acquisition of SCG and PPG signals.

When the subject has started the acquisition, the 5-seconds countdown with 5 synchronized beeps run. During this time, the subject positioned the smartphone by the flashlight side on a surface, leaving the synchronization algorithm working for 5 seconds. Then, the user had other 10 seconds to place the smartphone on the chest and position the index fingertip on the camera, marked by 10 synchronized beeps played by the speaker. This function was used to synchronize the Nexfin acquisition with the smartphone by inserting a marker on the Nexfin signals at the 20th beep (5 beeps for the initial countdown + 5 beeps for the synchronization algorithm + 10 beeps for the smartphone positioning). After the 30 second acquisition was completed, the smartphone speaker played two beeps, which were used to insert the end marker on Nexfin. The video was saved in that moment into the smartphone internal storage.

By pressing the button on the screen, the subject stored the acquired data in a .txt file inside the smartphone internal storage and on the Google Cloud Service, together with the video.

The subject was in rest conditions, spontaneously breathing during all sessions, and the Nexfin was recalibrated automatically between every trial, waiting for the steady-state condition of the subject physiological parameters, avoiding as much as possible the activation of the autonomic nervous system which could affect the pre-ejection time (PEP).

To accelerate the process, the smartphone built-in PPG computation was disabled; the Nexfin and smartphone data were analyzed offline using MATLAB.

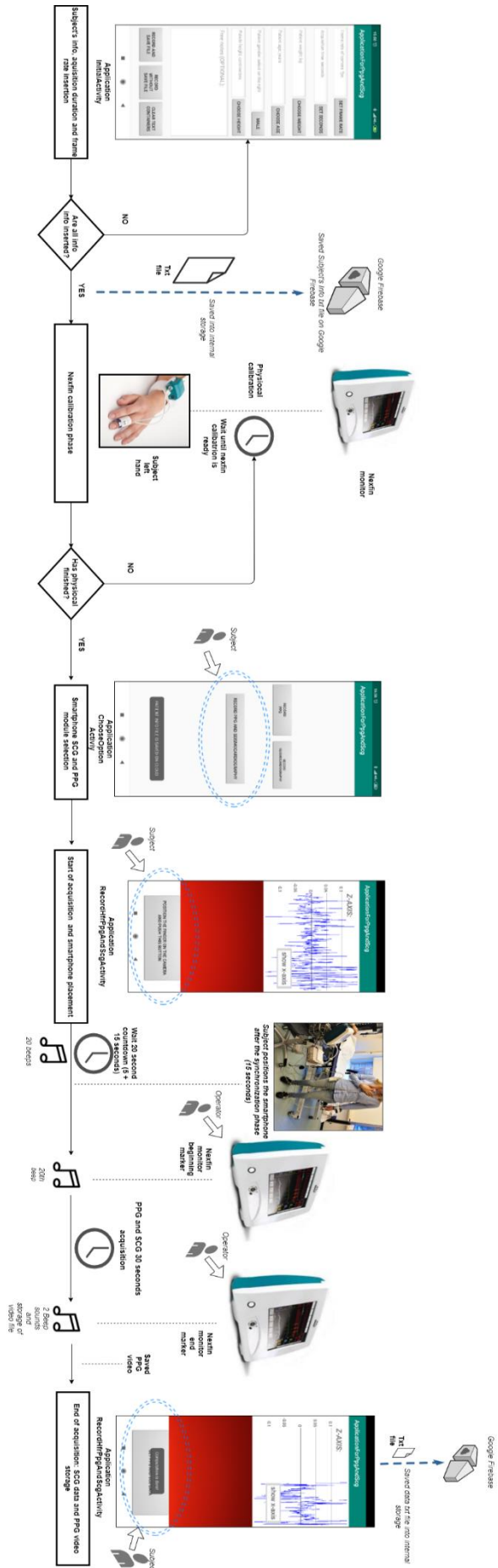


Figure 3.2.4 Flowchart of the steps during the simultaneous PPG and SCG acquisition session.

3.3 FIRST PROTOCOL: DATA ANALYSIS

3.3.1 Smartphone data processing and HR extraction

The accelerometer and camera data on the .txt files (Figure 2.2.31 and Figure 2.2.14, respectively) and the PPG video obtained during the first protocol were downloaded from the Google Firebase Cloud.

For the PPG analysis, the video frames were extracted (see paragraph 2.2.1.4.2), and a 50x50 region of interest (ROI) positioned in the center of the image, using the red channel (Figure 3.3.2 on the top, ROI number 2), was selected. These settings were established to be the best and used for all analysis after a comparison between three ROI positions and the 3 RGB channels (red, green and blue), as shown in an example in the Figure 3.3.1 and Figure 3.3.2. The red channel showed the best robustness and consistency, while the green and blue channels sometimes tended to saturate (Figure 3.3.1). The centered ROI, the nearest ROI to the flashlight and the ROI farthest from the flashlight (Figure 3.3.2 on the top, ROI 2, 3 and 1, respectively) showed practically the same behaviors. Differences were found on the mean values, that have no effect on the signal quality because they were far from saturation value (equal to 1 for the normalized PPG), while the standard deviations were practically the same (Figure 3.3.2, graph on the bottom). Anyway, the ROI in the center had a mean value that was farther from the lowest value (0) and from the saturation value (1) than the other two ROIs.

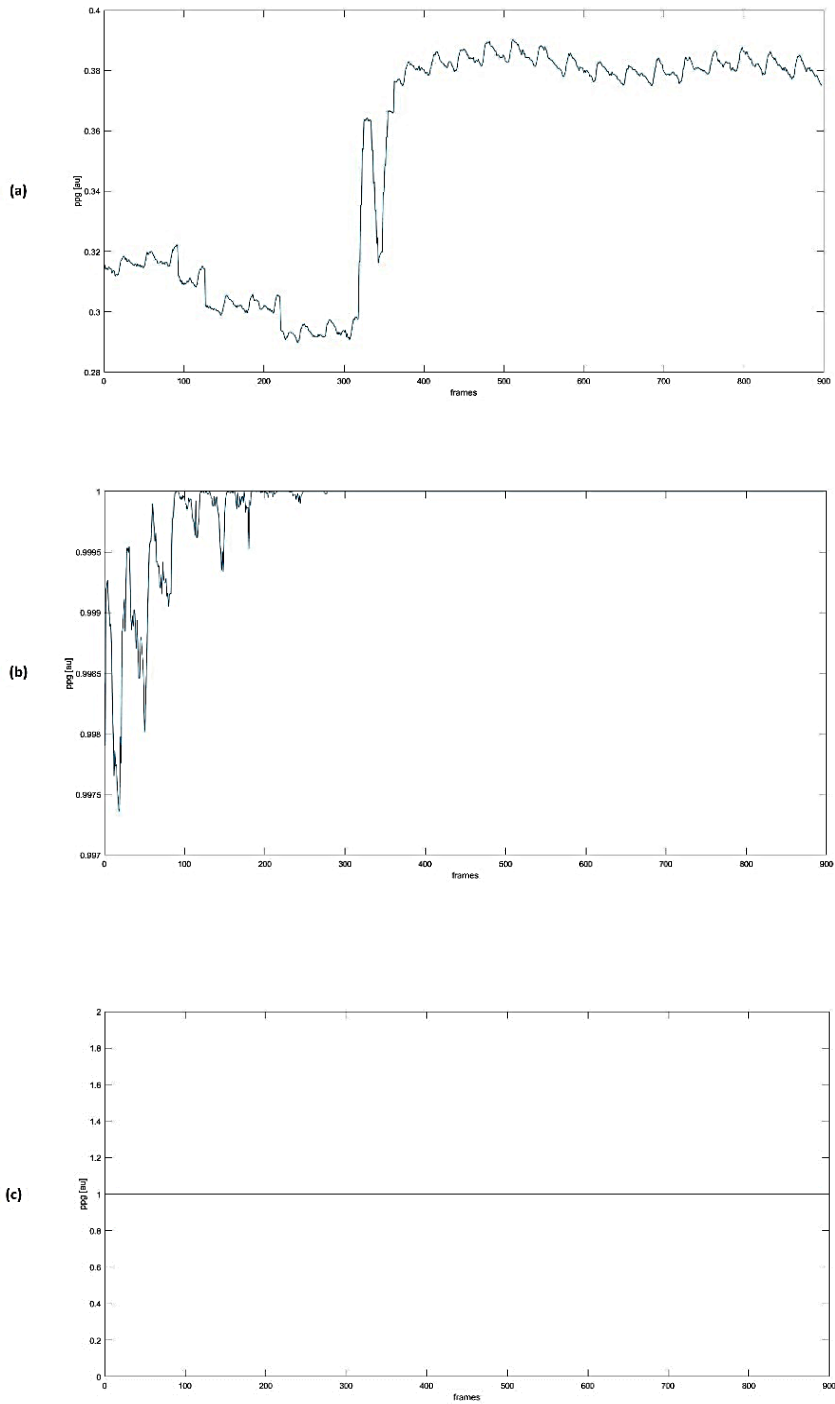


Figure 3.3.1 The figure shows the red (a), green (b) and blue (c) channel PPGs extracted with a central 50x50 ROI on the frame center. The red channel PPG is the only one that does not saturate. This acquisition was done at 60 Hz for a duration of 30 second.

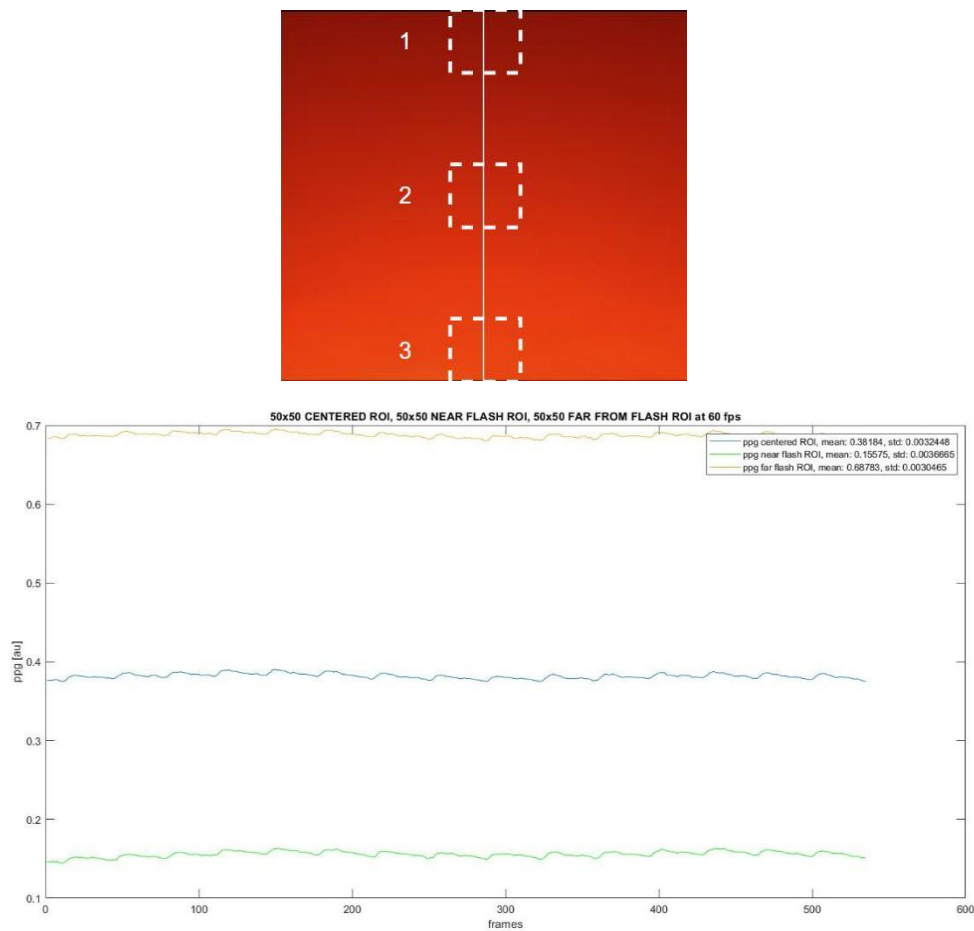


Figure 3.3.2 The figure on the bottom shows the red channel PPG signal behavior using 3 different 50x50 ROI positions: the blue line indicates the PPG extracted with a ROI centered in the frame (ROI 2 on the top figure); the green line represents the PPG with the nearest ROI to the flash (ROI 3, on the top figure) and the yellow line represents the ROI far from the flash (ROI 1, on the top figure). All the signals were extracted from a video captured at 60 fps as camera frame rate.

After the PPG signal extraction (Figure 3.3.3), the unfiltered raw data were used for the HR evaluation using a frequency domain analysis, based on fast Fourier's Transform (FFT). The peak on the spectrum after the DC component was chosen as representative of heart beats and its frequency multiplied by 60 seconds, to obtain the HR in beats per minute (bpm) (Figure 3.3.4).

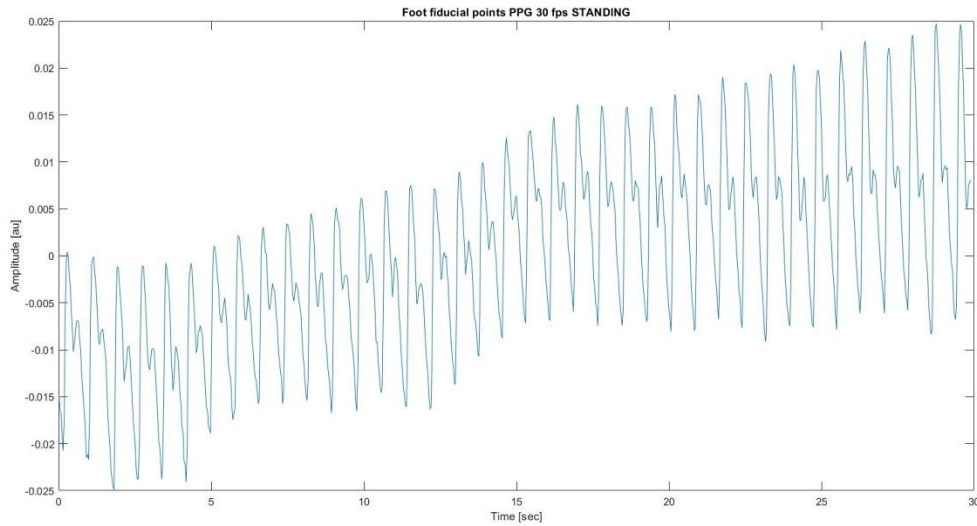


Figure 3.3.3 Example of raw PPG signal from subject 7 in standing posture.

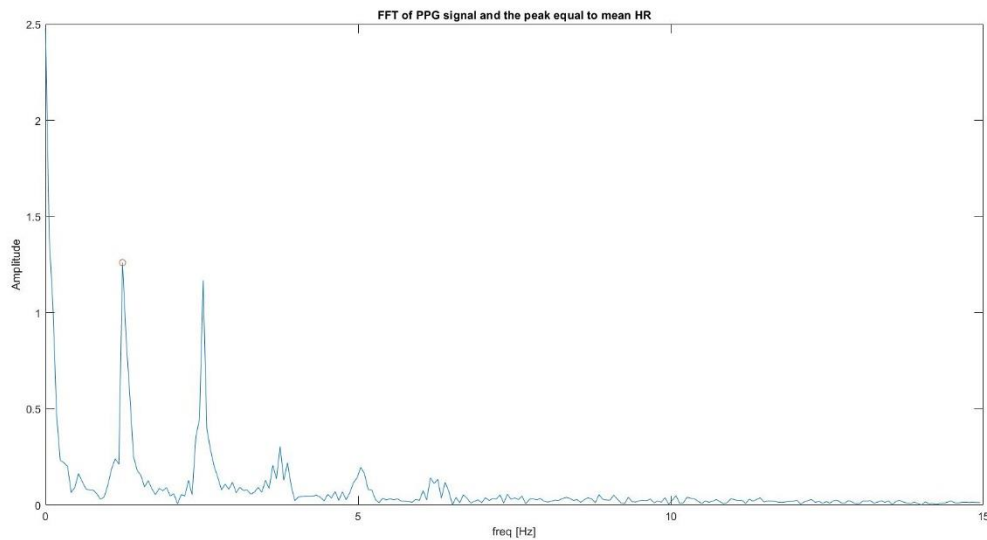


Figure 3.3.4 Example of the FFT of the raw PPG signal of the subject 7, acquired in standing position. The peak chosen as the heart frequency is underlined by the red circle.

For the SCG analysis, the raw accelerometer data along the z axis were chosen for further analysis and extracted from the .txt file (zSCG). The zSCG represents the heart movements with respect to the sagittal plane (or anteroposterior axis) of the subject, corresponding to the z axis of the smartphone accelerometer. The zSCG signals were filtered using an order 8th

Butterworth bandpass filter between 5 and 25 Hz. An example of zSCG after the filtering is shown in the Figure 3.3.5.

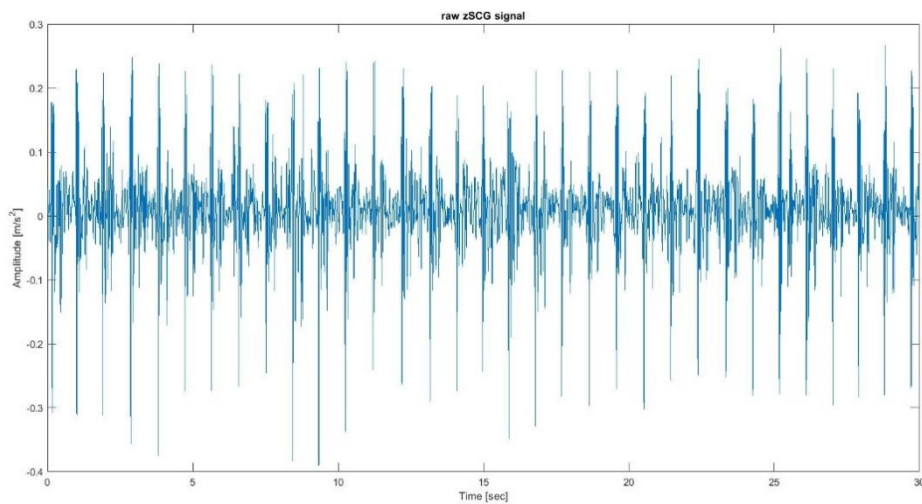


Figure 3.3.5 Example of filtered SCG along the z axis of the subject 4 in standing position.

For the HR extraction, a frequency domain-based method which exploited the FFT of the signal envelope was used (Figure 3.3.6). The squared values of the zSCG upper and lower envelopes were computed and successively summed up to find the heartbeat pattern (Figure 3.3.6, top figure). Then, the peak after the DC component was chosen as representative of the cardiac activity and multiplied by 60 seconds to extract the HR in bpm (Figure 3.3.6, bottom figure).

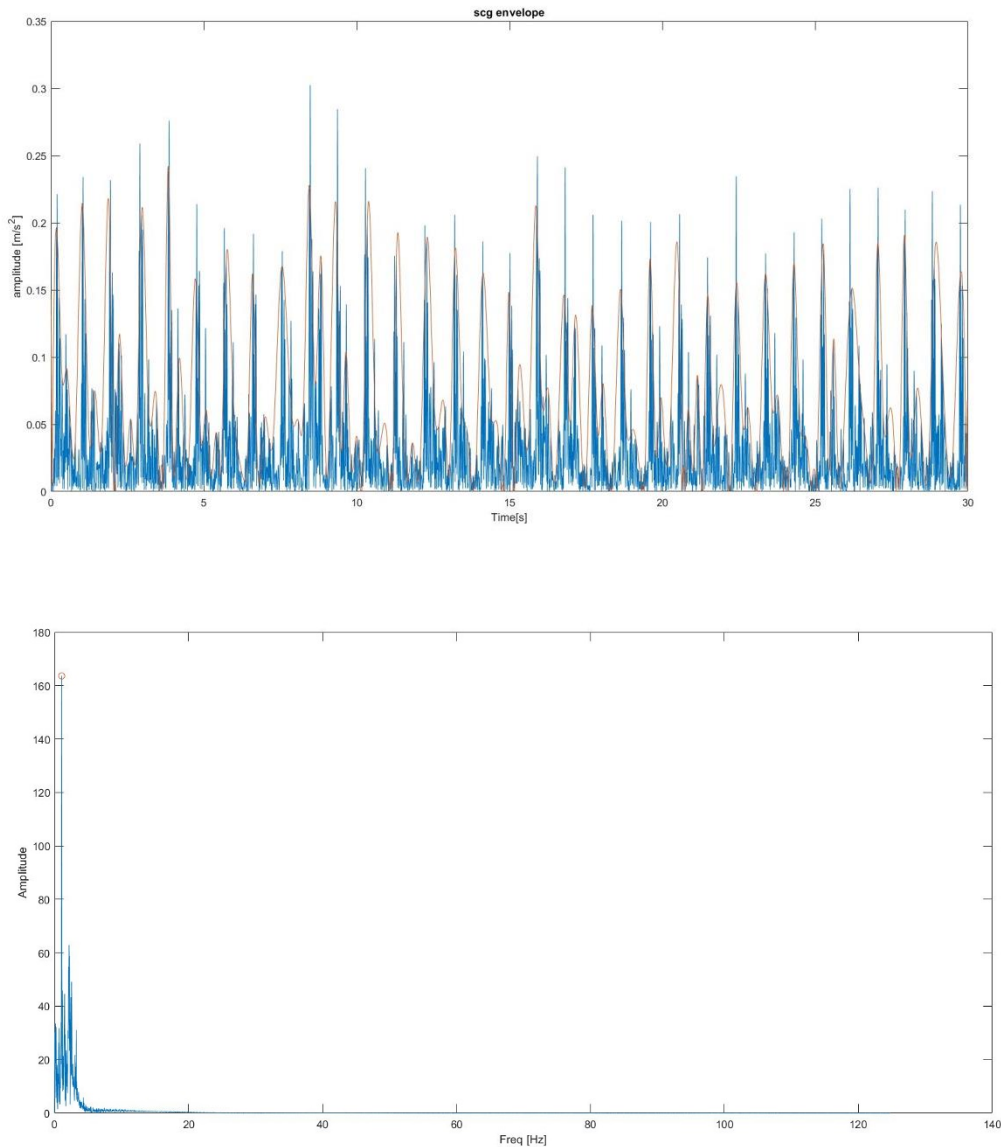


Figure 3.3.6 The plot on the top shows the envelope superimposed on the absolute value of the zSCG signal, which allowed to identify the pattern for the frequency domain analysis. The plot on the bottom represents the envelope FFT, with the red circle that identifies the mean heart frequency during entire 30 second acquisition.

The results of this experimental protocol were analyzed to verify if the expected change in HRs, passing from standing to supine position, were detected, separately for the PPG and SCG signals.

3.3.2 Questionnaire score analysis

As described in the paragraph 3.1.2, three questionnaires were administered to the subjects at the end of all acquisitions to evaluate the app usability and the subject engagement.

The first was the SUS (Bangor, Kortum and Miller, 2008), which was created by John Brooke in 1986 to measure the usability of electronic office systems, but it's now applied to a wide variety of web or technology-based applications to measure how easy or difficult they are to be used. It consists of 10 questions that can be answered on a five-point Likert scale from "Strongly Disagree" to "Strongly Agree." The questions are:

1. I think that I would like to use this system frequently.
2. I found the system unnecessarily complex.
3. I thought the system was easy to use.
4. I think that I would need the support of a technical person to be able to use this system.
5. I found the various functions in this system were well integrated.
6. I thought there was too much inconsistency in this system.
7. I would imagine that most people would learn to use this system very quickly.
8. I found the system very cumbersome to use.
9. I felt very confident using the system.
10. I needed to learn a lot of things before I could get going with this system.

The second questionnaire (the "ad-hoc" questionnaire) was specifically designed for this app in order to assess the smartphone maneuverability and app usability. The possible scores were defined as the SUS scale, with 10 items alternatively phrased positively or negatively:

1. It is possible to use the app without the need to modify my habits.
2. It was difficult to learn using the app.
3. I think the smartphone is easy to place and hold in that positions.
4. I think I would need someone to help me managing the app.
5. The positioning method of the device for the PPG acquisition makes simple the usage of the app.
6. I found the positioning method of the smartphone for the SCG acquisition uncomfortable for using the app.
7. I think I would be able to use the device autonomously (placement, activation, app management, etc...).
8. I think the button position to start the acquisition and get the data could be changed.
9. I think I could use the app for a long period.
10. I think that the use of the app would negatively affect my daily activities.

The last questionnaire is the “Twente engagement with eHealth technologies scale” (TWEETS) (Kelders and Kip, 2019). This has been proposed to measure the user engagement at different moments in time: after first (day of) use (expectations of engagement); during usage (current engagement) or after finishing usage/when intervention is finished (past engagement). For this purpose, the app was evaluated with respect to the expectations of engagement felt by the users after the first (day of) use.

The TWEETS is composed by 9 questions:

1. I think using this app can become part of my daily routine.
2. I think this app is easy to use.
3. I think I will be able to use this app as often as needed (to achieve my goals).
4. I think this app will make it easier for me to work on my health self-assessment.
5. I think this app will motivate me to measure PPG and SCG autonomously.
6. I think this app will help me to get more insight into my wellbeing.
7. I think I will enjoy using this app.
8. I think I will enjoy seeing the progress I make in this app.
9. I think this app will fit me as a person.

Every item of the TWEETS questionnaire is scored on a 5-point Likert-scale (from 0 to 4): strongly disagree, disagree, neutral agree, agree and strongly agree.

For the SUS and the “ad-hoc” questionnaires, to the obtained scores (from 1 to 5) of each odd item one was subtracted, while to each even item the scores (from 1 to 5) were replaced by the result of $5 - X$, with X equal to the score assigned by the participant. The recalculated item scores for each questionnaire were summed up, and the result multiplied by 2.5, thus resulting in survey rankings between 0 and 100. Finally, the medians of the obtained rankings were calculated, and compared with a threshold value to evaluate if the outcome could be considered either positive or negative. In particular, the SUS total score median should be greater than 68 (Sauro and Lewis, 2011) to state that the volunteers appreciated the device in terms of usability, while for the “ad-hoc” questionnaire an arbitrary threshold of 50 was chosen to prove a high maneuverability and usability of the app, if higher.

Regarding the single items of the SUS and “ad-hoc” surveys, the single subject item scores and the median item scores among the subjects were graphed on the radar plots, that presents along its rays (variables) the score of each item. The obtained graphs were compared with the ideal pattern that would be obtained with the best positive results (Figure 3.3.7).

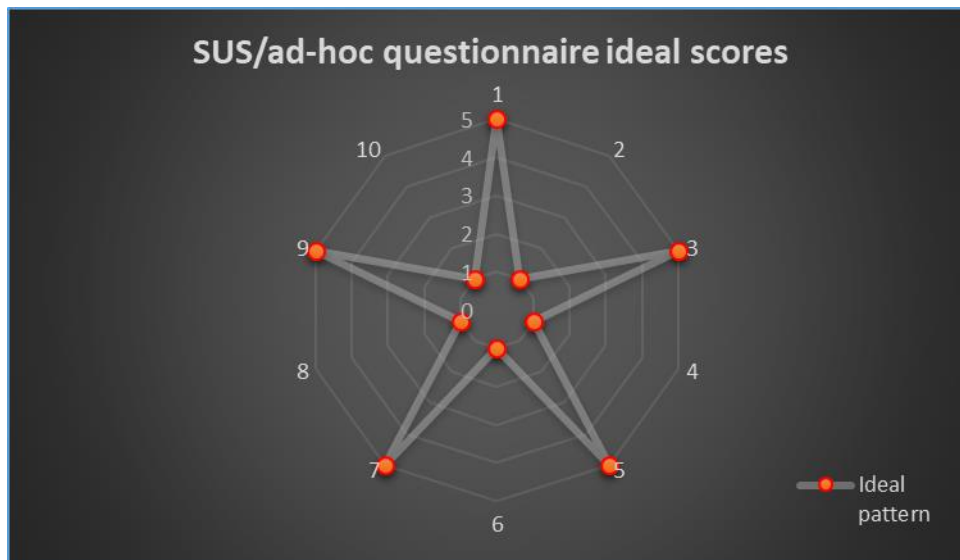


Figure 3.3.7 This radar plot represents the ideal pattern that the item scores (variables) of the SUS and ad-hoc questionnaire should follow to have the best result.

For the TWEETS questions, the scores were left unchanged. In addition, the items of this survey can be separated in three different components: items 1, 2, 3 cover behavioral engagement; items 4, 5, 6 cover cognitive engagement, while items 7, 8, 9 cover affective engagement. The scores were summed for each of these three components (range 0 – 12), as well as for the overall survey (range 0 – 36). The median of the summations of the item scores for each questionnaire was calculated. Moreover, the median of the resulted rankings for every compartment (items 1-3, items 4-6 and items 7-9) were computed as well and analyzed to evaluate the user expectation of an eventual future usage.

The TWEETS item scores for each subject and their median were graphed on the radar plots as the other questionnaire types. The Figure 3.3.8 shows the ideal pattern that the score trend should follow in the best case.

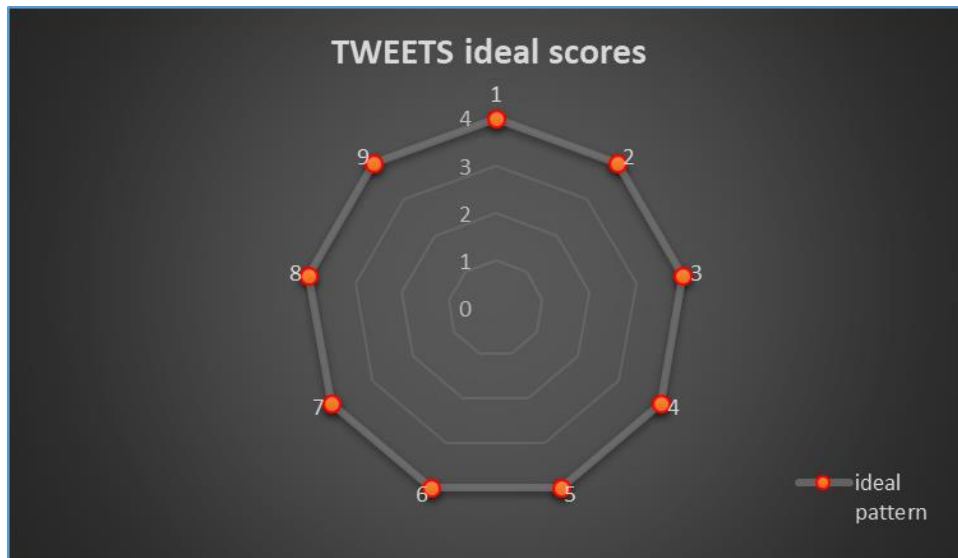


Figure 3.3.8 This radar plot represents the ideal pattern that the item scores (variables) of the TWEETS questionnaire should follow to have the best result.

3.4 SECOND PROTOCOL: DATA ANALYSIS

3.4.1 HR extraction from smartphone and Nexfin signals

A first aim was to validate the mean HR estimations obtained from the app (see 3.3.1 paragraph) with the mean HR obtained from the ECG and PLT “gold standard” measurements acquired by the Nexfin device.

To this aim, a beat-to-beat analysis was performed applying a simple peak detection algorithm to extract the R-peaks from the ECG and the foot points from the PLT signal (Figure 3.4.1 and Figure 3.4.2, respectively). These points were used to compute the beat-to-beat duration in seconds. Their median values were then transformed into beat per minutes by taking the inverse of the median and multiplying it by 60, obtaining the reference mean HR in bpm.

These median values were compared with the HR obtained from the SCG and the PPG using this protocol, as described in paragraph 3.3.1.

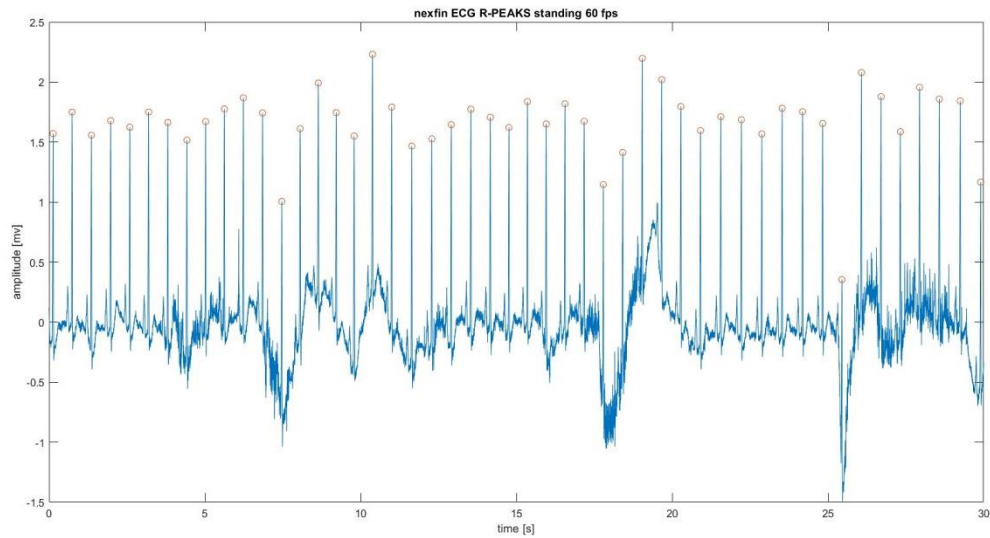


Figure 3.4.1 Example of the ECG captured by the Nexfin ECG module during the second session of the experiment (camera frame rate at 60 fps). The red circles superimposed to the signal represent the detected R-peaks.

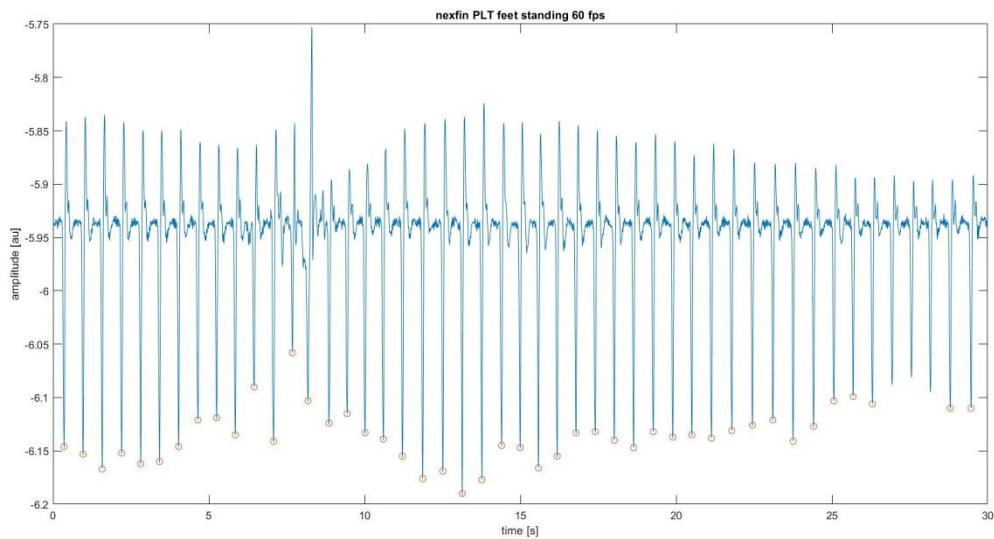


Figure 3.4.2 Example of the PLT signal captured by the Nexfin cuff at the index finger during the second session of the experiment (camera frame rate at 60 fps). The red circles superimposed to the signal represent the foot PLT fiducial points.

3.4.2 PTT and PAT estimation from smartphone and Nexfin signals

To evaluate the feasibility of the developed app to acquire simultaneously and synchronously the PPG and SCG signals, from which potentially extract the PTT, a first validation was done by comparing it to the pulse arrival time (PAT) obtained using the Nexfin signals. It is known

that the PAT differs from PTT due to the inclusion of PEP time (Figure 1.3.8); however, this difference was supposed constant having acquired the signals in a basal condition, thus making the PAT and PTT potentially comparable except a possible bias.

To compute the PTT from the SCG and PPG signals, a point as proximal reference and a point as distal reference need to be identified. The AO points of the zSCG were selected as proximal reference, while the PPG foot points were identified as distal references.

The zSCG was first filtered with an 8th order Butterworth bandpass with cut-off frequencies at 5 and 25 Hz, then the beat-by-beat AO points were detected by using a customized peak detection algorithm (Figure 3.4.3). When an AO point was skipped by the algorithm, the correct point was inserted manually.

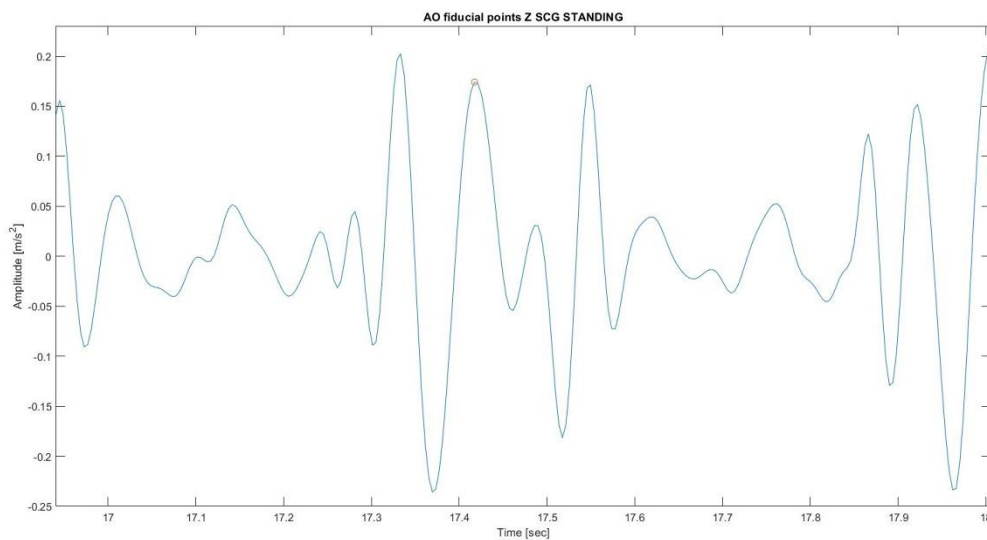


Figure 3.4.3 The plot shows a correct identified AO point detected by the customized peak detection algorithm. The zSCG was acquired during the second session, when the camera frame rate was set at 60 fps.

The PPG signals did not need any filtering method and the foot points were detected using the built-in MATLAB peak detection algorithm (Figure 3.4.4).

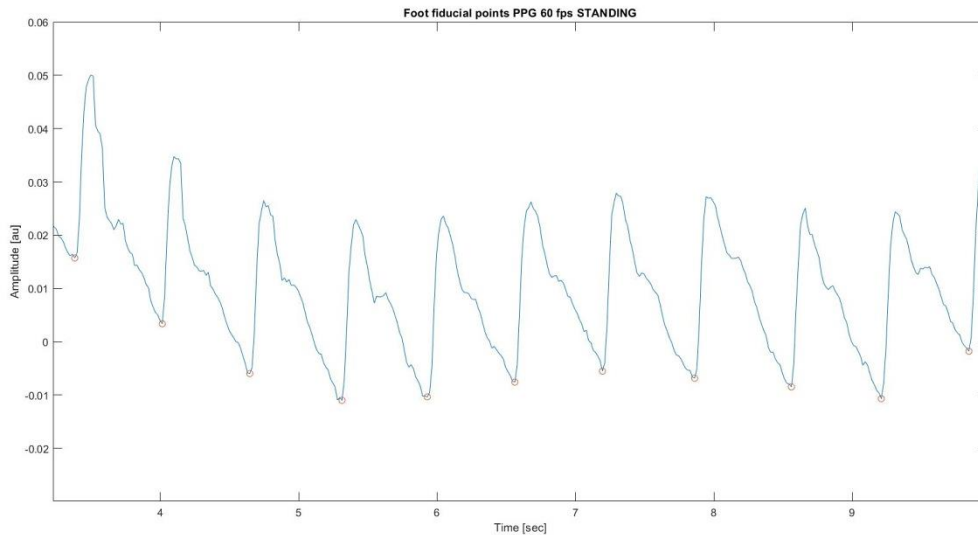


Figure 3.4.4 The plot shows a series of correct identified foot points detected by the MATLAB built-in peak detection algorithm. The PPG was acquired during the second session, when the camera frame rate was set at 60 fps.

The differences between the occurrence in time of the AO points and the presentation time of the foot points for the corresponding heartbeats were computed, obtaining the PTT estimations (Figure 3.4.5).

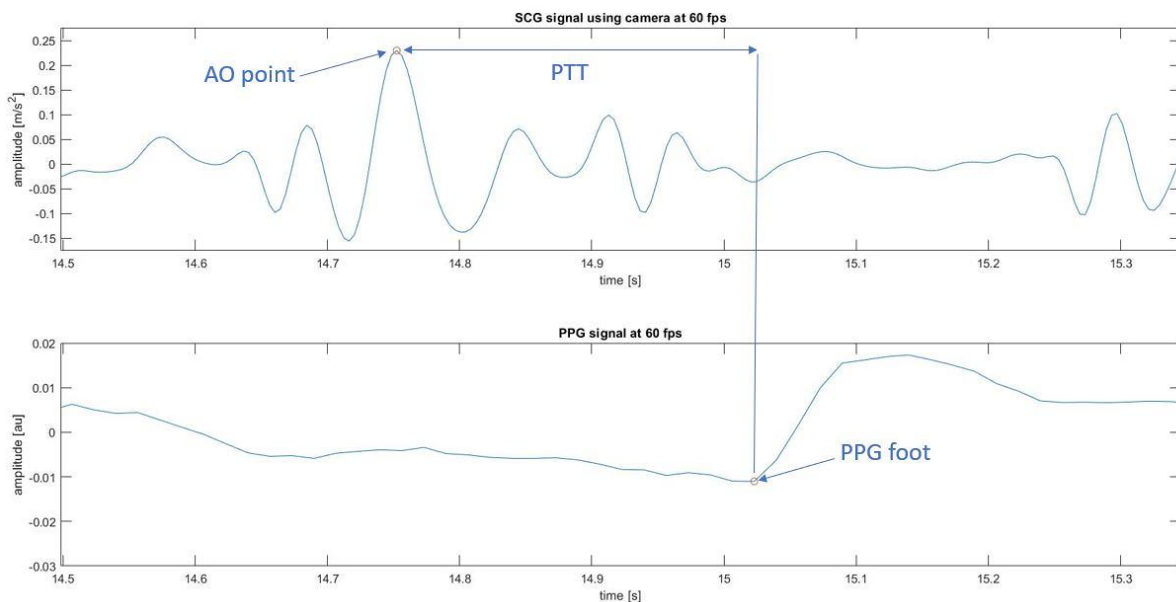


Figure 3.4.5 The graph on the top represents the AO point extracted from the SCG signal, that is used as proximal reference for the PTT calculus, while the bottom plot represents the PPG foot point used as the distal reference. The time difference between them identifies the PTT estimation.

As explained in the paragraph 3.2, the developed app synchronization algorithm allowed evaluating the delay between the camera and accelerometer of the Android system. By plotting the first 5 seconds of the two-signal acquisition (after the initial 5 seconds-countdown), the initial delay could be extracted (Figure 3.4.6), resulting in a value of 167 msec. This value was then subtracted from the accelerometer timestamps to properly temporally align the PPG and SCG signals.

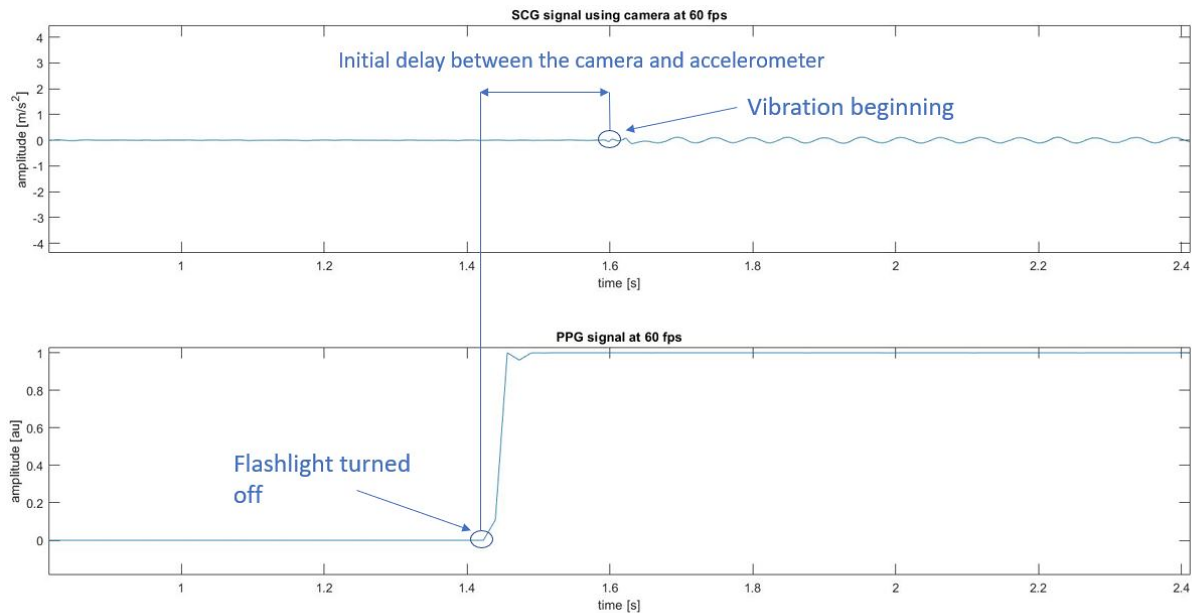


Figure 3.4.6 The PPG and SCG signals during the first 5 seconds: the time difference between the time instant in which the flashlight was turned off and the vibration started represented the internal time delay between the camera and IMU sensors.

For the Nexfin, the same beat-to-beat analysis described in the previous paragraph 3.4.1 was applied, thus obtaining the beat-to-beat R-peaks and PLT local minima (foot points) (Figure 3.4.1 and Figure 3.4.2). These points were used to estimate the pulse-arrival-time (PAT). The beat-to-beat differences between the occurrences in time of the R-peak and the PLT foot point times were calculated, finding the PAT (Figure 3.4.7).

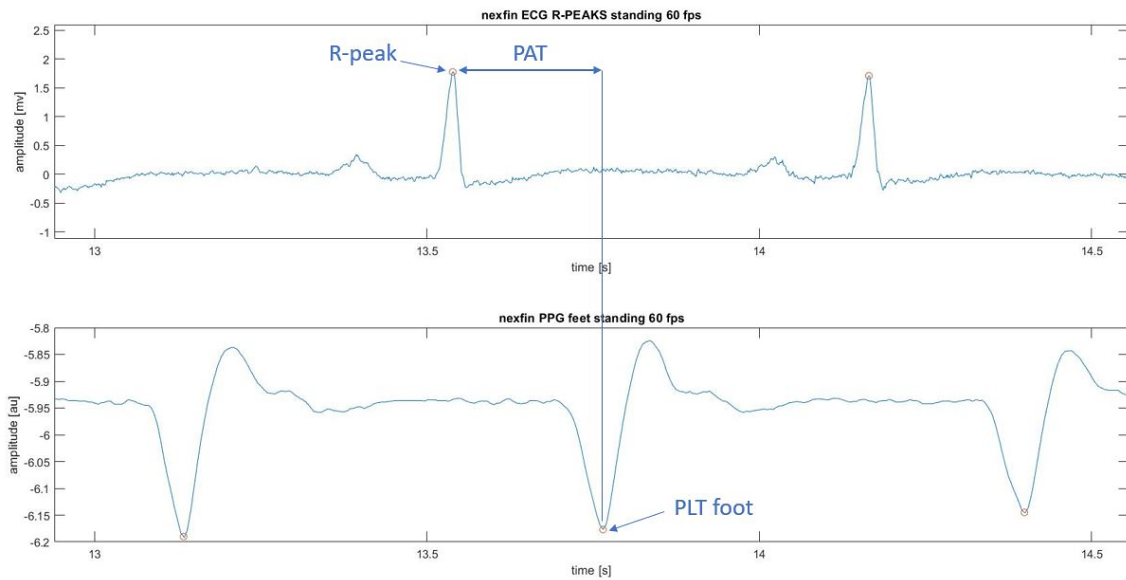


Figure 3.4.7 The graph on the top represents the R-peak extracted from the subject ECG signal, that is used as proximal reference for the PAT calculus, while the bottom plot represents the PLT foot point used as the distal reference. The time difference between them identifies the PAT estimation.

The Figure 3.4.8 summarizes the analysis steps for the first and second protocols.

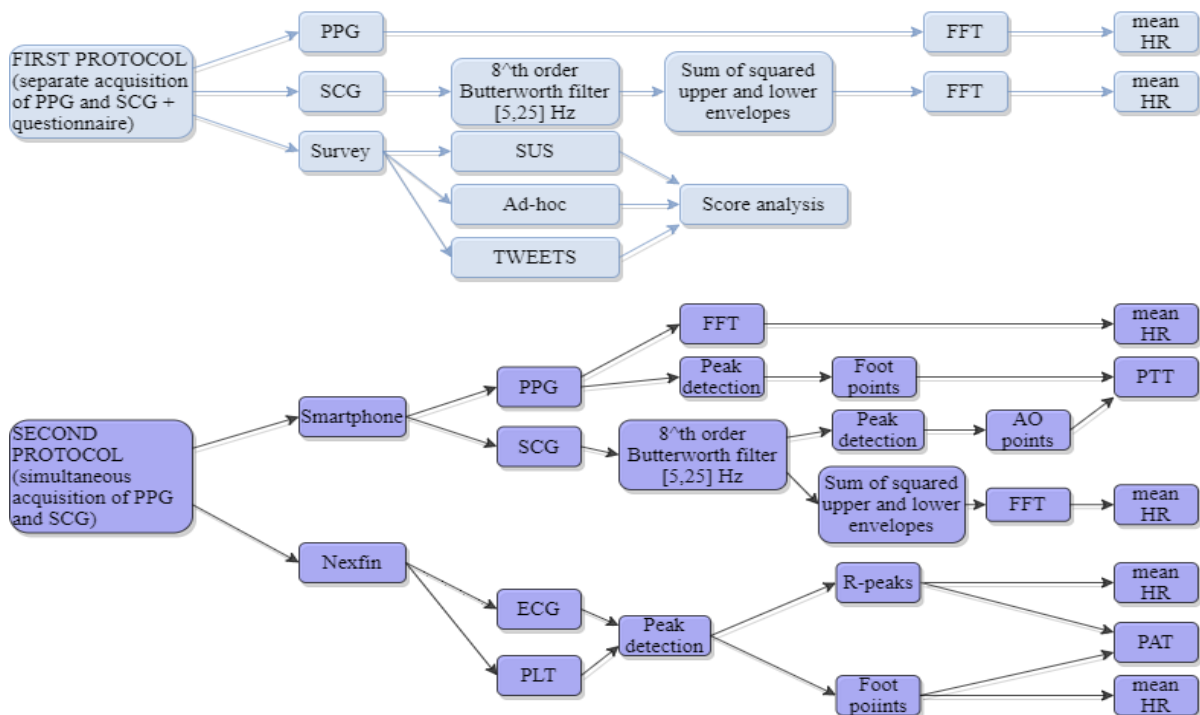


Figure 3.4.8 Overview of the analysis steps executed separately for the first and second protocols.

4 RESULTS

In this chapter, the results will be presented, relevant to the two performed protocols.

4.1 FIRST PROTOCOL

4.1.1 HR results from smartphone PPG and SCG signals

The results of the analysis of the PPG and SCG signals in terms of HR, extracted by the two separate app modules (paragraphs 2.2.1.4 and 2.2.1.5), in supine and standing posture for each of the seven studied subjects, are presented in Table 4.1.1. Furthermore, the Figure 4.1.1 and Figure 4.1.2 underline how the PPG and SCG HR values, respectively, differ passing from the standing to the supine position, which is reflected by a decrease in HR values.

Table 4.1.1 Comparison of HR values extracted from the PPG and SCG signals of the subjects, passing from a standing (left column) to a supine posture (right column).

Subject	Signal	Position	
		Standing HR [bpm]	Supine HR [bpm]
Subject 1	PPG	66	49
	SCG	52	46
Subject 2	PPG	84	70
	SCG	72	62
Subject 3	PPG	84	60
	SCG	90	58
Subject 4	PPG	63	56
	SCG	64	52
Subject 5	PPG	77	67
	SCG	74	64
Subject 6	PPG	88	74
	SCG	-	-
Subject 7	PPG	75	72
	SCG	82	71

Unfortunately, for subject 6, the HR values from the SCG signal were not available due to the failure in the SCG signal storage (the subject forgot to save the data with the specific app button).

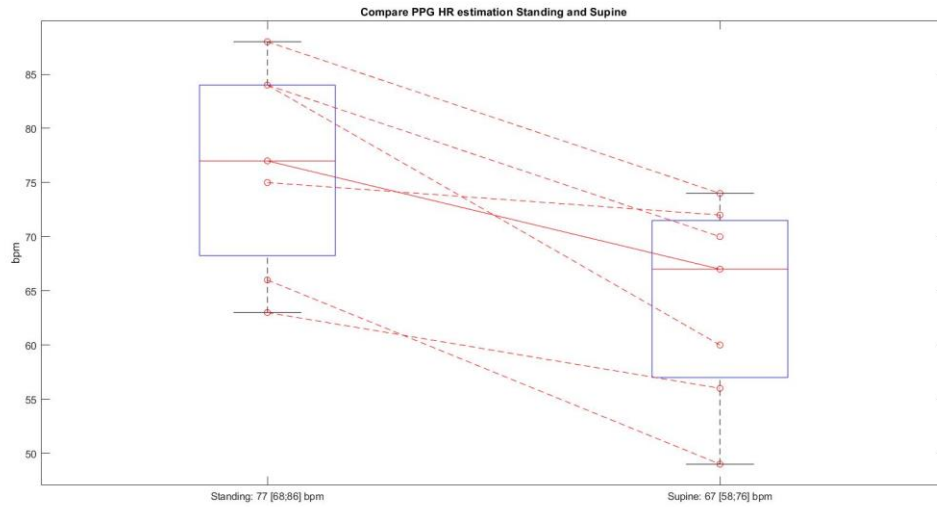


Figure 4.1.1 Results of the comparison of HR obtained from PPG in standing and supine, presented as boxplot with median and 25th and 75th percentiles. Dashed lines represent the individual values.

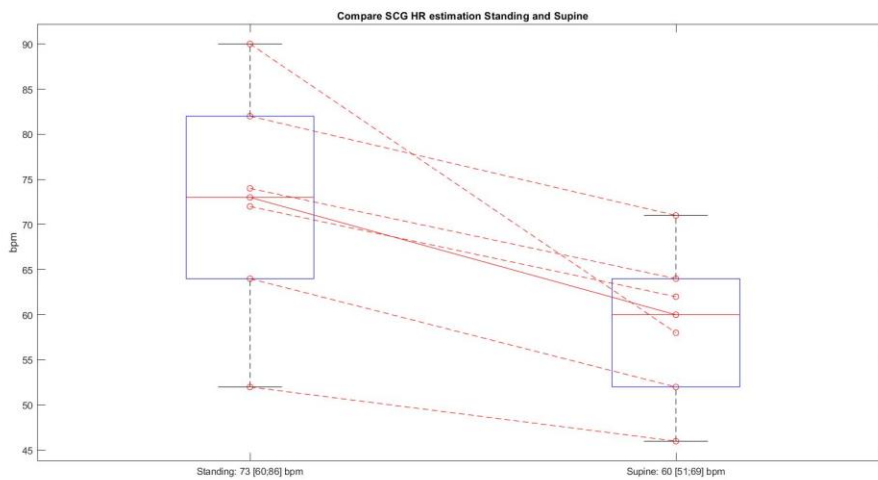


Figure 4.1.2 Results of the comparison of HR obtained from SCG in standing and supine, presented as boxplot with median and 25th and 75th percentiles. Dashed lines represent the individual values.

A statistical paired t-test was conducted separately for the PPG and SCG signals, comparing standing and supine values. For the HRs estimated from both the PPG and the SCG signals, a statistically significant difference ($p < 0.003$ and $p < 0.02$, respectively) between the standing and supine values was found, thus supporting the hypothesis that the signals obtained by the smartphone are able to properly obtain a HR value accurate enough to identify the expected postural changes.

4.1.2 Questionnaires results

4.1.2.1 The SUS scores

In appendix A, the radar plots resulting from each SUS questionnaire are reported, while the radar plot of Figure 4.1.3 shows the median item scores computed among the seven volunteers (in yellow), superimposed to the ideal score (in red). Moreover, the Table 4.1.2 shows an overview of the questionnaire results, describing the scores item-by-item and the total scores calculated following the steps explained in the paragraph 3.3.2 (Table 4.1.2, last column). The last row of the table contains the medians of the scores for each item and the median of the recalculated total scores, resulting in a final score within a 0 to 100.

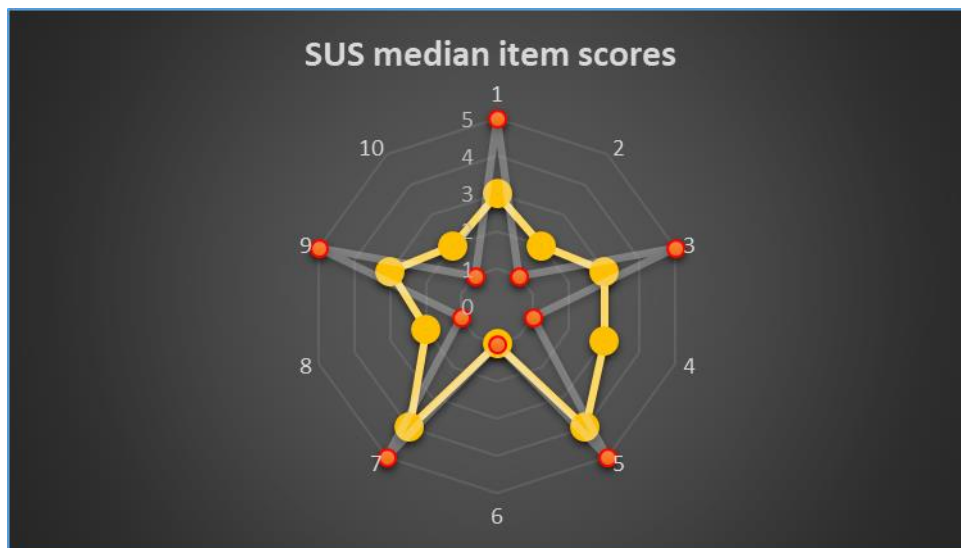


Figure 4.1.3 Item score medians from SUS among all subjects (yellow) over the ideal series (red).

The radar plot (Figure 4.1.3) intuitively shows a good agreement for the positively phrased items 5 (“I found the various functions in this system were well integrated”) and 7 (“I would imagine that most people would learn to use this system very quickly”). These suggest that

the development choices to integrate the three different modules inside the app and to keep the usage simple were appreciated by the end-users. Moreover, the strong disagreement with respect to the negatively phrased items 2 (“I found the system unnecessarily complex”), 6 (“I thought there was too much inconsistency in this system”), 8 (“I found the system very cumbersome to use”) and 10 (“I needed to learn a lot of things before I could get going with this system”) demonstrates the app low complexity, a perceived coherence across the different modules, and again the recognition of the simple interaction between the app and the users. The user replies were more neutral with respect to items 1 (“I think that I would like to use this system frequently”), 3 (“I thought the system was easy to use”), 4 (“I think that I would need the support of a technical person to be able to use this system”) and 9 (“I felt very confident using the system”), which concerned in particular a frequent use and the need of a support to understand the system.

Table 4.1.2 The SUS answer scores exposed subject-by-subject for each item (item 1 to 10, where + and – highlight the positive or negative meaning) and the summation of recalculated scores (last column) between 0 and 100. The last row represents the medians along the rows for each column.

SUS results											
Subjects	Item 1 (+)	Item 2 (-)	Item 3 (+)	Item 4 (-)	Item 5 (+)	Item 6 (-)	Item 7 (+)	Item 8 (-)	Item 9 (+)	Item 10 (-)	Recalculated Score summation [0-100]
Subject 1	4	4	3	3	3	4	4	2	2	4	82,5
Subject 2	3	2	3	3	3	2	3	3	3	1	65
Subject 3	3	2	3	4	4	2	3	3	3	2	72,5
Subject 4	5	2	3	4	3	1	3	1	3	3	70
Subject 5	2	1	3	3	4	1	4	1	4	3	67,5
Subject 6	3	2	3	2	4	1	5	2	3	1	65
Subject 7	2	1	5	2	5	1	5	1	5	2	72,5
Median scores	3	2	3	3	4	1	4	2	3	2	70

The median value of the total scores, equal to 70, overcomes the set threshold of 68, thus stating that the volunteers appreciated the device in terms of usability.

4.1.2.2 The “ad-hoc” scores

In appendix B, the radar plots resulting from each “ad hoc” questionnaire are reported, while the radar plot of figure 4.1.4 shows the median item scores computed among the seven volunteers (in yellow), accompanied by the Table 4.1.3 structured as the Table 4.1.2.

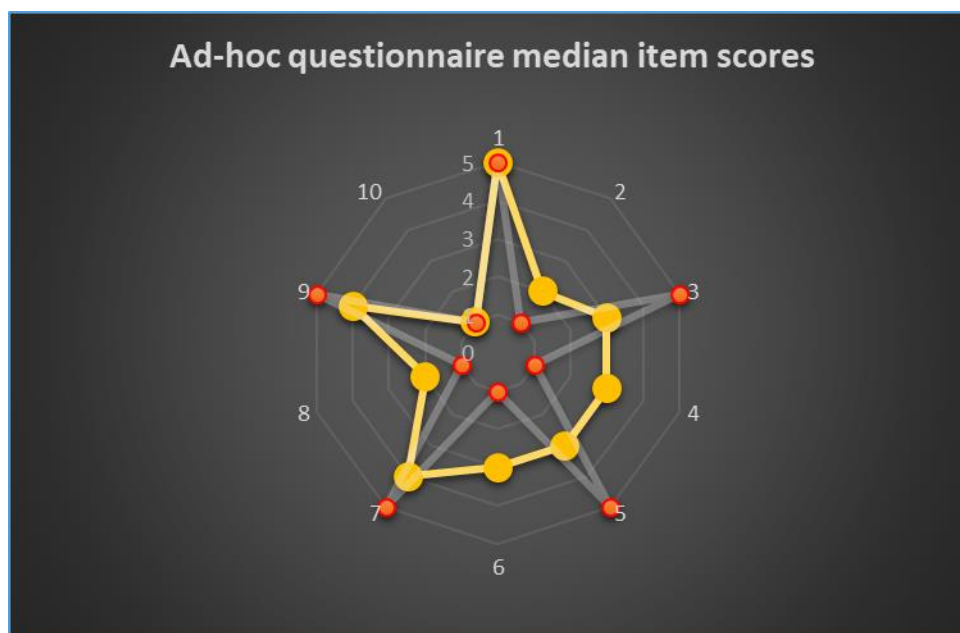


Figure 4.1.4 Item score means from ad-hoc questionnaire among all subjects (yellow) over the ideal series (red).

The radar plot of Figure 4.1.4 shows a strong agreement for the positively phrased items 1 (“It is possible to use the app without the need to modify my habits”), 7 (“I think I would be able to use the device autonomously (placement, activation, app management, etc...)”) and 9 (“I think I could use the app for a long period”). These suggest that the users felt generally comfortable with the app, being sufficiently stimulated in engaging with it. Furthermore, the high score for item 7, combined with the neutral score for item 4 of SUS, suggest that the user after the initial training could be able and willing to use the app autonomously.

Moreover, the strong disagreement with respect to the negatively phrased items 2 (“It was difficult to learn using the app”), 8 (“I think the button position to start the acquisition and get the data could be changed”) and 10 (“I think that the use of the app would negatively affect

my daily activities”) demonstrates the success in the app design to make it simple and not cumbersome to be used.

For the items 3 (“I think the smartphone is easy to place and hold in that positions”), 4 (“I think this app will make it easier for me to work on my health monitoring”), 5 (“The positioning method of the device for the PPG acquisition makes simple the usage of the app”), and 6 (“I found the positioning method of the smartphone for the SCG acquisition uncomfortable for using the app”), the user scores were neutral, thus suggesting some concerns about managing the correct position of the smartphone to acquire the signals; these aspects are strongly dependent to the selected smartphone and to the user handling ability.

Table 4.1.3 The ad-hoc questionnaire answer scores exposed subject-by-subject for each item (item 1 to 10, where + and - highlight the positive or negative meaning) and the summation of recalculated scores (last column) with a ranking between 0 and 100. The last row represents the median along the rows for each column.

Ad-hoc questionnaire results											
Subjects	Item 1 (+)	Item 2 (-)	Item 3 (+)	Item 4 (-)	Item 5 (+)	Item 6 (-)	Item 7 (+)	Item 8 (-)	Item 9 (+)	Item 10 (-)	Recalculated Scores [0-100]
Subject 1	5	2	3	3	4	2	4	2	4	1	75
Subject 2	4	1	3	2	3	3	4	2	4	1	72,5
Subject 3	5	2	1	4	3	3	3	2	3	1	57,5
Subject 4	5	2	3	4	4	3	3	2	4	1	67,5
Subject 5	4	1	3	4	2	4	4	4	4	1	57,5
Subject 6	5	2	3	2	3	3	3	3	4	1	67,5
Subject 7	5	1	5	1	5	3	5	2	5	1	92,5
Median scores	5	2	3	3	3	3	4	2	4	1	68

The last column of Table 4.1.3 shows the median of the total scores was greater than the predefined threshold of 50, thus showing a general appreciation of the user while managing the app.

4.1.2.3 The TWEETS scores

In appendix C, the radar plots resulting from each TWEETS questionnaire are reported, while the radar plot of Figure 4.1.5 shows the median item scores computed among the seven volunteers (in yellow), where Table 4.1.4 shows the scores given by each subject subdivided into the three compartments previously defined (see paragraph 3.3.2), with the last row representing the medians of them along all subjects.

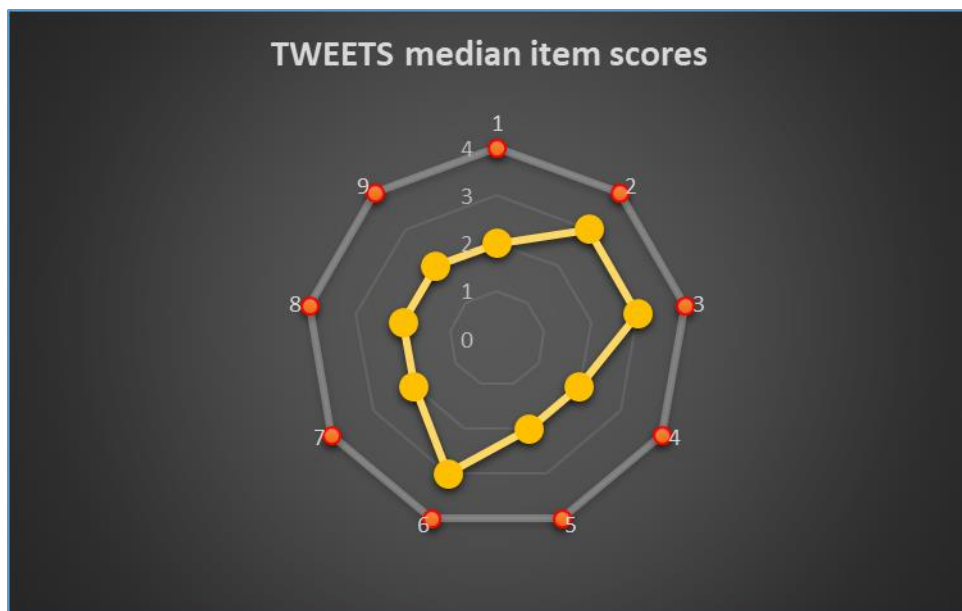


Figure 4.1.5 Item score median values from TWEETS among all subjects (yellow) over the ideal series (red).

The radar plot of Figure 4.1.5 shows high scores for the items 2 (“I think this app is easy to use”), 3 (“I think I will be able to use this app as often as needed (to achieve my goals)”) and 6 (“I think this app will help me to get more insight into my wellbeing”). In particular, scores of the items 2 and 3 are coherent with the scores on usability in the previous questionnaires, and show potentially high behavioral engagement, confirmed by the high median score obtained for the first three questions (Table 4.1.4, first column).

As regards cognitive engagement (items 4-6), while for the high score of item 6 suggests the potentiality of the app to stimulate in the user a good reason to use it, items 4 (“I think this app will make it easier for me to work on my health self-assessment”) and 5 (“I think this app will motivate me to measure PPG and SCG autonomously”), results were more neutral. For

the items 7 (“I think I will enjoy using this app”), 8 (“I think I will enjoy seeing the progress I make in this app”) and 9 (“I think this app will fit me as a person”), covering affective engagement, the users expressed a neutral agreement, that could be explained by the fact that the app was not able to create emotional connection with the participants, probably due to its minimalistic design. This resulted in a lower median score of 6 for this compartment, compared to the other two where a value of 8 was reached.

In Table 4.1.5 an overview of all items scores is shown, together with the total scores ranged between 0 and 36. The median of the item score summations equal to 23 demonstrates a general good expectation of engagement felt by the users.

Table 4.1.4 The scores are subdivided in three compartments: the “Compartment 1” that represents the behavioral engagement, identified by the sum of the first three items (item 1-3); the “Compartment 2” that represents the cognitive engagement, identified by the sum of the items from 4 to 6, and the “Compartment 3” that represents the affective engagement equal to the sum of the last three items (items 7-9). The last row contains the median scores for each compartment among all subjects.

TWEETS compartment results			
Subjects	Compartment 1 (items 1-3)	Compartment 2 (items 4-6)	Compartment 3 (items 7-9)
Subject 1	9	10	6
Subject 2	7	7	9
Subject 3	8	11	8
Subject 4	8	9	7
Subject 5	7	5	5
Subject 6	7	7	5
Subject 7	9	8	4
Median scores	8	8	6

Table 4.1.5 The TWEETS answer scores exposed subject-by-subject for each item (item 1 to 9) and the summation of overall scores (last column) with a ranking between 0 and 36. The last row represents the median along the rows for each column.

TWEETS results										
Subjects	Item 1	Item 2	Item 3	Item 4	Item 5	Item 6	Item 7	Item 8	Item 9	Item score summation [0-36]
Subject 1	3	3	3	2	4	4	2	2	2	25
Subject 2	3	2	2	2	2	3	3	3	3	23
Subject 3	2	3	3	3	4	4	3	4	1	27
Subject 4	3	2	3	3	2	4	2	2	3	24
Subject 5	2	3	2	2	1	2	1	2	2	17
Subject 6	2	2	3	2	2	3	1	2	1	18
Subject 7	1	4	4	3	2	3	0	1	4	22
Median scores	2	3	3	2	2	3	2	2	2	23

4.2 SECOND PROTOCOL

After a first qualitative analysis, for the HR estimation by spectral method, of all the PPG and SCG signals analyzed in the three acquisitions, only the PPG signal acquired during the first session at 30 fps was not reliable to be considered. Conversely, only the SCG and PPT signals from the second session (60 fps) were suitable for beat-to-beat analysis and PTT estimation, resulting in a feasibility of 83% and 33%, respectively, of this preliminary analysis in one subject only.

Indeed, the PPG signal waveform extracted from the first session (30 fps) was highly corrupted by noise, thus the extraction of the HR was not achievable (Figure 4.2.1). Moreover, the PTT estimation from the session at 120 fps was not reliable due to the noise superimposed to the PPG valleys where the foot fiducial points should lie (Figure 4.2.2).

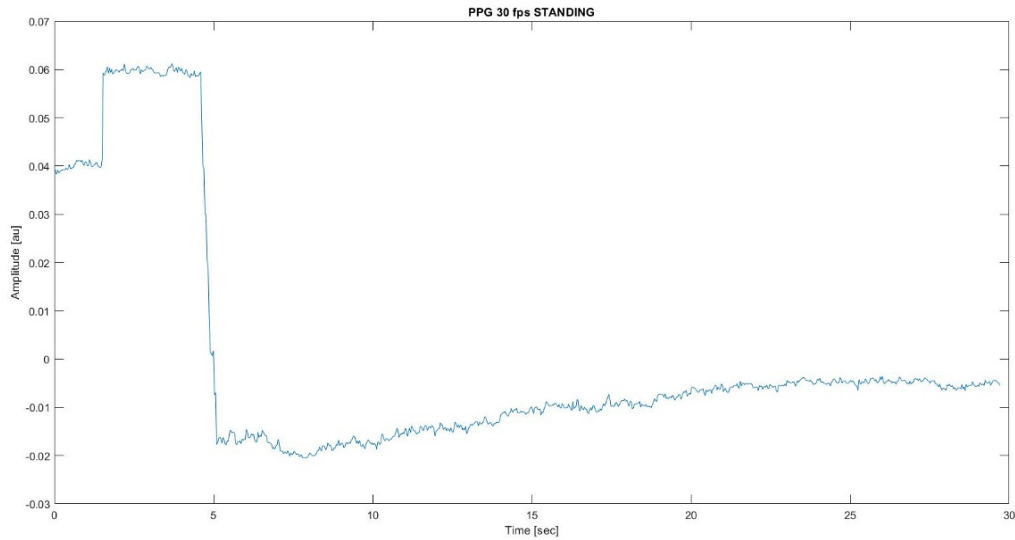


Figure 4.2.1 PPG signal extracted from the first session at 30 fps, where the high corruption by noise is visible, preventing beats identification.

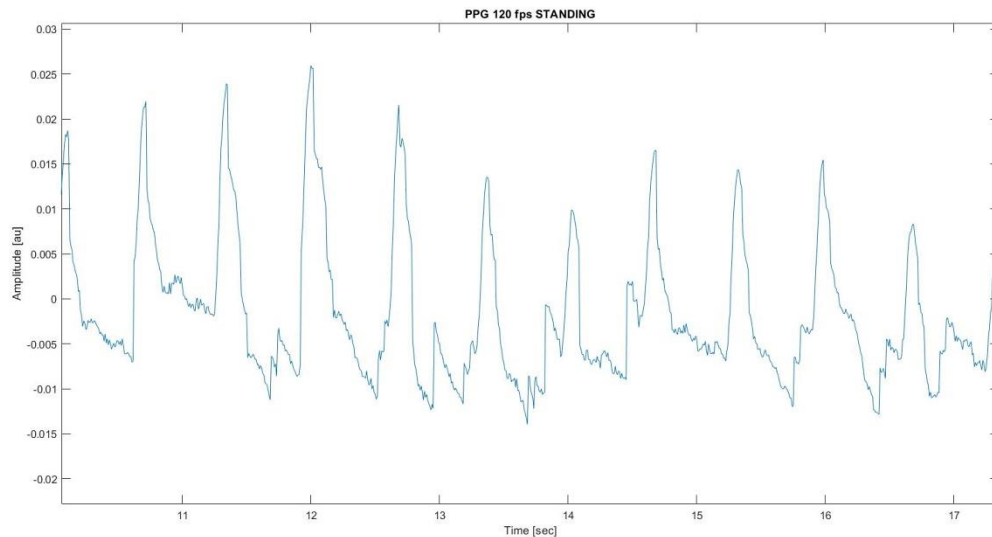


Figure 4.2.2 Segment of the PPG signal extracted from the third session at 120 fps, where the noise in correspondence to the PPG valleys made impossible the accurate detection of the foot fiducial points.

As regards the HR estimation, the comparison between the mean HRs extracted from the smartphone signals by frequency domain analysis and the HRs calculated from the ECG and PLT gold standards is visualized in the following Table 4.2.1.

Table 4.2.1 The HR values extracted from the smartphone SCG and PPG FFT analysis are compared to the HRs calculated from the PLT and ECG gold standards \pm their standard deviations.

Signal	Standing position		
	HR [bpm] at 30 fps	HR [bpm] at 60 fps	HR [bpm] at 120 fps
Reference PLT	95 \pm 9	97 \pm 12	96 \pm 7
Smartphone PPG	-	98	98
Absolute error for PPG	-	1	2
Relative error for PPG	-	0,01 (1%)	0,02 (2%)
Reference ECG	95 \pm 5	97 \pm 4	95 \pm 6
Smartphone SCG	98	93	94
Absolute error for SCG	3	4	1
Relative error for SCG	0,03 (3%)	0,04 (4%)	0,01 (1%)

From these results, the ability in measuring the mean HR with an error $<5\%$ in respect of the gold standards from both synchronously acquired SCG and PPG, when the signal is not corrupted by noise, using a simple frequency analysis method, was verified.

Also, as the SCG was always acquired at 250 Hz, the accuracy of the HR obtained from the PPG seemed independent from the frame rate settings of the acquisition.

The beat-to-beat PTT values, estimated from the beat-to-beat analysis of the PPG at 60 fps and SCG signals, were compared to the respective PAT values extracted from the difference between the PLT and ECG fiducial points, representing the gold standard measurements. Table 4.2.2 shows the mean \pm SD of the PTT and PAT values along the entire acquisition, while Figure 4.2.3 and Figure 4.2.4 show the linear correlation and Bland-Altman (B-A) plots among corresponding beat-to-beat measurements, respectively.

Table 4.2.2 The mean PTT extracted by the difference of the smartphone PPG and SCG fiducial points compared to the mean PAT calculated from the difference of the Nexfin ECG and PLT fiducial points.

Mean PTT [ms]	Mean PAT [ms]
130 \pm 16	214 \pm 6

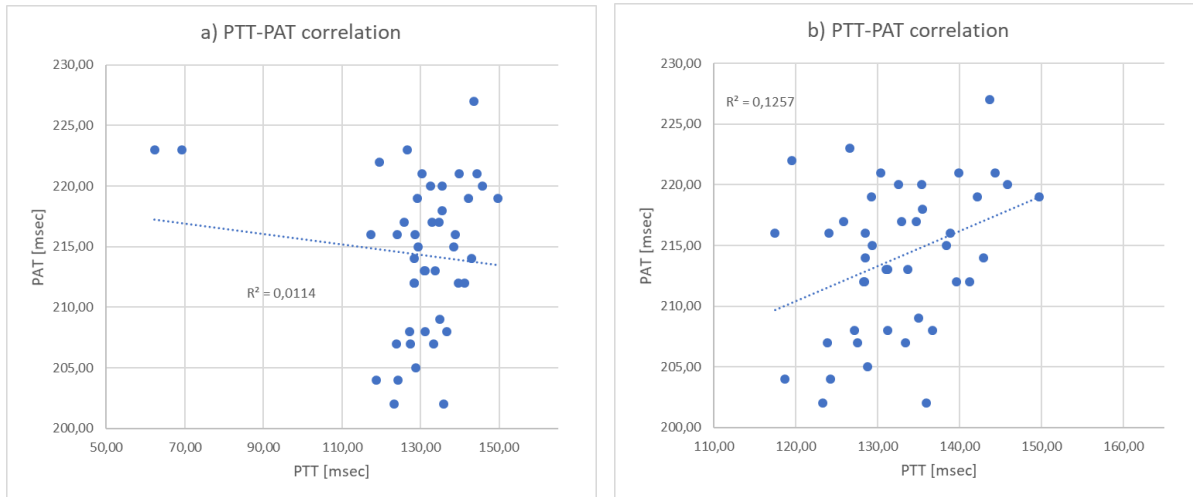


Figure 4.2.3 On the left, the linear correlation obtained considering all the corresponding beat-to-beat PAT and PTT measurements, with a $r^2 = 0,01$. On the right, the same plot where the two outliers were removed ($r^2 = 0,13$).

The Table 4.2.2 shows an underestimation of 83 msec of PTT compared to PAT values, resulting from $PAT - PTT$. This bias could be considered physiologically reasonable, due to the intrinsic PEP (Figure 1.3.8) time ranging in an interval of 30 and 40 msec for healthy subjects (Lewis *et al.*, 1977) included in the PAT interval, which represents the time between the heart action potential arrival to the ventricles (ECG R-peak) and the aortic valve opening (AO peak). The additional component of the measured bias (around 40-50 msec) could be partially due to uncertainty relevant to the lower SCG (250 Hz) and PPG sampling rate (60 fps) compared to the Nexfin gold standard (1000 Hz), as well as other unknown causes.

A very low level of correlation between the corresponding beat-to-beat PAT and PTT measurements was obtained, probably due to the narrow range of values measured in this single acquisition, while B-A (with two outliers removed) confirmed the existence of the underestimation bias of 83 msec, with narrow limits of agreement ($SD=8msec$) resulting in a coefficient of variation $CV(\%)=100*SD/bias$ of about 10%, thus representing the level of uncertainty of the measure around the measured value.

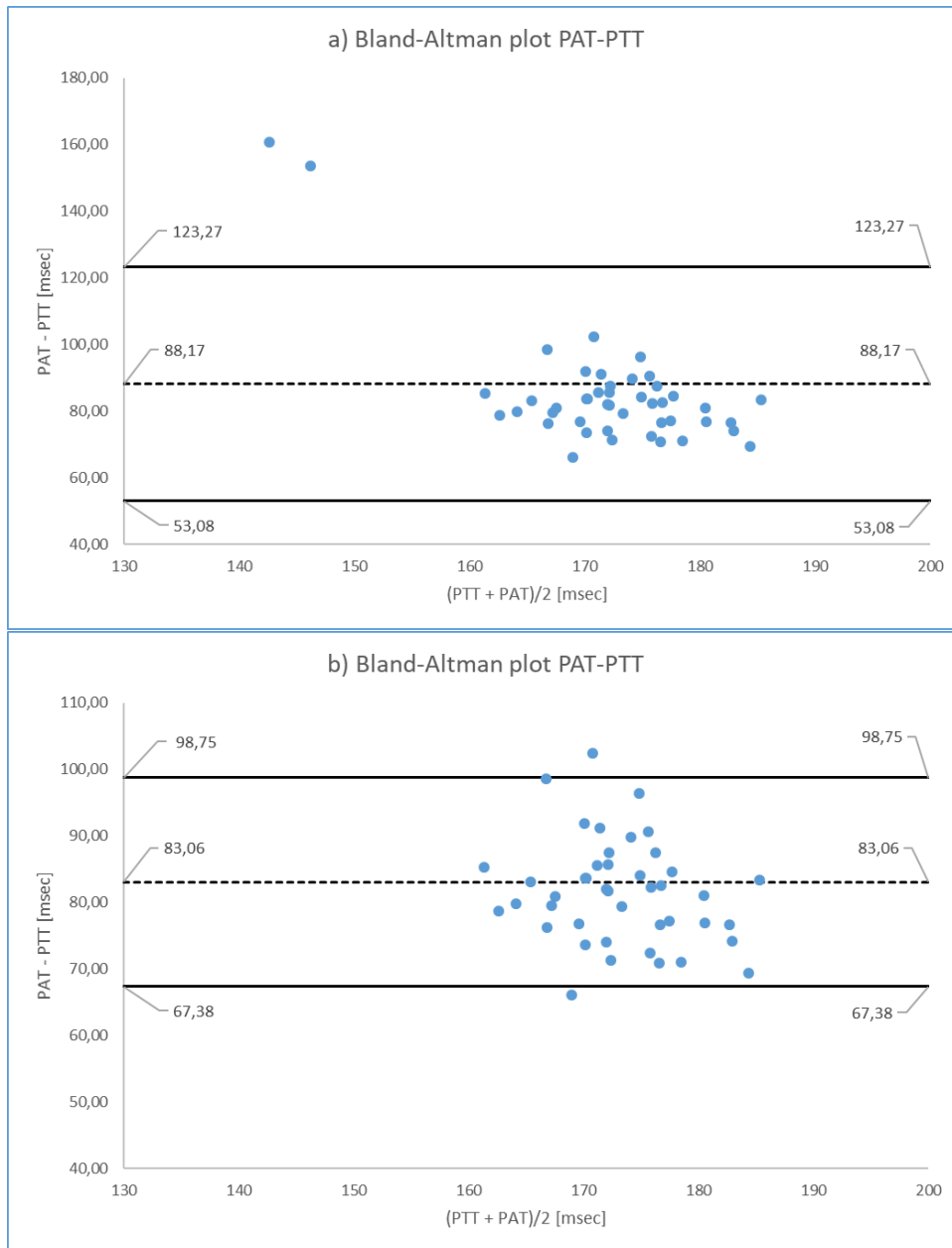


Figure 4.2.4 a) Bland-Altman plot comparing beat-to-beat values of smartphone PTT with gold standard PAT. The dotted line represents the mean of the differences as a measure of the bias among the two measurements, whereas the horizontal continuous lines represent the 95% confidence interval [bias - 2*SD; bias + 2*SD]. In b) the same plot is shown, where the two outliers were removed.

5 DISCUSSIONS AND CONCLUSIONS

In this study, an Android app composed by 3 modules was developed in order to acquire separately or simultaneously the PPG and SCG signals using a Xiaomi smartphone Redmi Note 7, and to store the acquisition on both the smartphone internal memory and in a remote cloud integrated service.

The design concept was structured to create a simple, fluent and versatile app usage, with the goal of creating an instrument that could be used for research purposes and, perhaps, as core for direct user utilization in a daily context. The project exploited the ability of the Xiaomi smartphone sensors of acquiring the PPG at three different frame rates (30, 60 and 120 fps), with an implemented on-board PPG computation, and the SCG with a high and stable sampling frequency at 250 Hz. Initial tests aimed at the evaluation of the stability of the sampling frequency of the accelerometer and camera sensors and its variations along the acquisition. For SCG, accelerometer and gyroscope sampling frequencies demonstrated a very good stability and a very narrow range of jitter. For PPG, a high stability independent from acquisition durations (from 10 to 30 sec) for 30 fps and 60 fps was found, with some fluctuations when 120 fps was selected. Moreover, the high consistency and robustness of the PPG signal while using indifferently left or right hands, while covering the flashlight and leaving uncovered the depth sensor, were verified, and these settings included as the optimal procedure in the final protocols. The camera and inertial sensor stabilities were also proved to be maintained during the simultaneous acquisition of the PPG and SCG signals (see paragraph 2.2.1.6.2), thus opening the opportunity to study physiological biomarkers related to combined analysis of these signals, which in literature represents a relevant challenge (Wang *et al.*, 2018 , Carek *et al.*, 2017).

As regards the feasibility and accuracy of measurements to be extracted from PPG and SCG signals (acquired separately and simultaneously), they were tested by two different experimental protocols.

5.1 APP MODULES FOR THE SEPARATE SCG AND PPG ACQUISITIONS

The first protocol aimed at capturing separately the PPG (30 fps) and SCG signals (250 Hz) by the use of the two dedicated modules in the app (see paragraphs 2.2.1.4 and 2.2.1.5, respectively) by subjects in a home-like setting with session durations of 30 seconds, considered enough for this purpose (Landreani and Caiani, 2017). The absence of gold

standard measurements is justified by the already proved ability of detecting HR from PPG (Jonathan and Leahy, 2011, Kurylyak, Lamonaca and Grimaldi, 2012, Abinaya, Prabhakaran and Jaisankar, 2014) and SCG signals (Lee, Lee and Whang, 2018) acquired by a smartphone. Moreover, this decision was also guided by the goal to avoid a lab setting, with relevant additional constraint to the subjects, thus allowing them to evaluate the app usability and perceived engagement. In order to have an indirect validation of the accuracy of the obtained HR measures, the acquisition was repeated in standing and supine posture, to evidence expected higher values in standing than in the supine position (Patel *et al.*, 2016).

At the end of the experiments, three different questionnaires were administered, two of which (SUS and TWEETS) already proposed and used in literature for studying the usability of mobile applications (Kortum and Sorber, 2015) and e-health engagement derived from apps for physical activities (Kelders and Kip, 2019). The third one, an ad-hoc survey developed for the specific evaluation of the characteristics of this app, was also used.

The performance of these 2 app modules was evaluated by computing the mean HR in the acquired 30 seconds.

In particular, an offline simple FFT-based method was conducted to extract the HR from the signals. For the PPG signal obtained from the video analysis, the FFT was applied to the unfiltered raw data, computing the spectrum and taking the peak after the DC component as the HR fundamental frequency. For the SCG, pre-processing by an 8th order Butterworth bandpass filter was applied to reduce noise, and only the z-component of the accelerometer was considered for analysis. Then, the envelope of the signal was computed to further reduce the noise still present in the signal, and the FFT applied to it, thus facilitating the identification of the heart beat frequency (Choudhary, Sharma and Bhuyan, 2018, Siecinski and Kostka, 2018). As with the PPG, the peak frequency after the DC component in the SCG spectrum was considered as the mean HR value.

The choice of extracting a mean HR was guided by three factors having in mind the potential usage settings for self-tracking: 1) the possibility to implement in the future the algorithm on-board, thus providing the user with the measured HR immediately after the acquisition; 2) the need to obtain a stable measurement despite the self-acquisition, which could result in possible artifacts and outliers; 3) the need to give as feedback a simple and clear clinical parameter that can be easily interpreted by every user.

The obtained results demonstrated that both PPG and SCG signals were able to significantly differentiate between supine and standing posture considering subjects' HR. Table 5.1.1, reports the median HR values obtained from the seven subjects HRs, captured separately by the smartphone PPG and SCG signals, when standing and supine.

Table 5.1.1 Summary of the obtained median HR values subdivided by the acquired signal and the assumed posture.

Signal	Median standing HR [bpm]	Median supine HR [bpm]	Paired t-test
PPG	77 [68; 86]	67 [58; 76]	< 0.003
SCG	73 [60; 86]	60 [51; 69]	< 0.02

As regards the app design evaluation through the questionnaires, the SUS and ad-hoc scores needed to be processed in order to obtain a ranking between 0 and 100.

For the TWEETS, the item scores were evaluated both separately and grouping them in 3 different compartments, to evaluate three types of engagement: behavioral, cognitive, and affective, together with their sum.

In Table 5.1.2, the text of the questions of the three questionnaires are summarized, color-coded in green to indicate a positive appreciation (median result > 3 for SUS and ad-hoc, and > 2 for TWEETS), and in orange to indicate a neutral judgement (=3 for SUS and ad-hoc, and = 2 for TWEETS). To be noted, no question received a median score under the neutral one.

Table 5.1.2 Summary of the administered questionnaire question texts. The orange indicates the questions which were answered by the users with a median neutral agreement (3 for the SUS and the ad-hoc questionnaire, while 2 for the TWEETS), while the green represents the answers that obtained a median score over the neutral value (4 or 5 for the SUS and ad-hoc questionnaire, while 3 or 4 for TWEETS). The (+) indicated the question phrased positively, while (-) symbolized the questions phrased negatively.

Item number	Item texts		
	SUS	Ad-hoc questionnaire	TWEETS
1	I think that I would like to use this system frequently (+)	I think it will be possible to use the app without the need to modify my habits (+)	I think using this app can become part of my daily routine
2	I found the system unnecessarily complex (-)	It was difficult to learn using the app (-)	I think this app is easy to use
3	I thought the system was easy to use (+)	I think the smartphone is easy to place and hold in that positions (+)	I think I will be able to use this app as often as needed (to achieve my goals)
4	I think that I would need the support of a technical person to be able to use this system (-)	I think I would need someone to help me managing the app (-)	I think this app will make it easier for me to work on my health self-assessment
5	I found the various functions in this system were well integrated (+)	The positioning method of the device for the PPG acquisition makes simple the usage of the app (+)	I think this app will motivate me to measure PPG and SCG autonomously
6	I thought there was too much inconsistency in this system (-)	I think I would be able to use the device autonomously (placement, activation, app management, etc...) (-)	I think this app will help me to get more insight into my wellbeing
7	I would imagine that most people would learn to use this system very quickly (+)	I think I would be able to use the device autonomously (placement, activation, app management, etc...) (+)	I think I will enjoy using this app
8	I found the system very cumbersome to use (-)	I think could be changed the button position to start the acquisition and get the data (-)	I think I will enjoy seeing the progress I make in this app
9	I felt very confident using the system (+)	I think I could use the app for a long period (+)	I think this app will fit me as a person
10	I needed to learn a lot of things before I could get going with this system (-)	I think that the use of the app would negatively affect my daily activities (-)	-

The results of the SUS and ad-hoc surveys, summarized in Table 5.1.3, showed a general user appreciation about the app usability intrinsically related to the chosen hardware, as well as about the biomedical purpose of the app, with both total scores resulting higher than the threshold values considered for indicating a positive result.

Table 5.1.3 Overview of the median scores among the subjects obtained for the SUS and ad-hoc questionnaire, after the rearrangement of the ranking between 0 and 100, that were compared with the respective thresholds.

Questionnaires	Median of total scores among subjects	Threshold
SUS	70 [64;76]	68
Ad-hoc questionnaire	68 [56;79]	50

Anyway, for the SUS the 1st quartile of the score distribution below the threshold suggest that some users did not completely appreciate some system features.

For the ad-hoc questionnaire, the threshold of 50 was chosen arbitrarily as the minimum positive score. Obtained results were in support of the specific design choice to use a minimalistic user interface to interact with the app for signal acquisition, but also evidencing a not strong agreement with the maneuverability of the smartphone during the signal acquisition. This was strictly related to the smartphone shape and design (i.e, size, camera position, etc.), which imposed certain configuration choices on to acquire the signals and how to hold the smartphone.

Regarding the TWEETS, the results in Table 5.1.4 showed the ability of the app in reaching an e-health engagement of the users, particularly relevant to the behavioral and cognitive components.

Table 5.1.4 Overview of the median scores for each TWEETS compartment among the users, accompanied by the median of the overall rankings.

TWEETS score summary	Compartment 1: item 1,2,3 [0-12] (behavioral engagement)	Compartment 2: items 4,5,6 [0-12] (cognitive engagement)	Compartment 3: items 7,8,9 [0-12] (affective engagement)	Overall ranking [0-36]
Median scores among subjects	8	8	6	23

While the not invasive capability to measure HR, in a perspective of a daily use, was well received, the app didn't seem to be able to build an affective link with the user, probably due to the limited usage scenario (subjects were not asked to repeat daily the acquisitions) and absence of pathology (that could increase the interest in using it), as well as the current absence of feedback or previous historical values.

5.2 APP MODULE FOR SIMULTANEOUS PPG AND SCG ACQUISITION

A second protocol was aimed at validating HR extraction while the PPG and SCG signals were acquired simultaneously, also testing the potential capability in deriving PTT measurements from proximal (from SCG) and distal (from PPG) beat-to-beat reference points.

Accordingly, acquisitions were performed in a laboratory setting at IRCCS Istituto Auxologico San Luca (MI), simultaneously with gold standard measurements captured by a Nexfin monitor. Due to circumstances, it was possible to recruit only one healthy female (22 years old) subject. Acquisitions were repeated in standing position, with 30 seconds duration, changing the frame rate of the PPG (30, 60, 120 fps), while SCG sampling rate was kept constant at 250 Hz, resulting in 3 sessions.

After a preliminary analysis, the PPG signal extracted from the sessions at 30 fps resulted not reliable for both PTT and HR evaluation, due to the high level of noise that corrupted the signal (Figure 4.2.1), probably related to the specifications of smartphone handling required for the simultaneous acquisition, and relevant finger movement on the camera. For the same reasons, the PPG signal acquired at 120 fps (Figure 4.2.2) was not usable for the beat-to-beat analysis in order to detect the fiducial points for the PTT estimation, but maintaining the periodicity useful for the HR extraction through the FFT application. On the contrary, the SCG and PPG signals acquired during the 60-fps session were usable also for the PTT estimation (33% feasibility). These preliminary results highlight the poor feasibility of this combined acquisition; besides it needs to be tested in further experiments.

Table 5.2.1 Results for the mean HR comparison between the smartphone and gold standard measurements. The PPG was compared with the Nexfin PLT, while the SCG with the ECG.

Comparison of smartphone HR with the corresponding Nexfin mean HR	PPG-PLT		SCG-ECG		
	60 fps	120 fps	30 fps	60 fps	120 fps
Absolute error [bmp]	1	2	3	4	1
Relative error	0,01 (1%)	0,02 (2%)	0,03 (3%)	0,04 (4%)	0,01 (1%)

As shown in Table 5.2.1, the smartphone mean HR deviated from the Nexfin mean HR with a maximum relative error <5%, which can be considered acceptable for a HR measurement system (Gregoski *et al.*, 2012).

The robustness and the coherence of the sampling frequencies of the different sensors during the simultaneous acquisition was proven during the design phase (paragraph 2.2.1.6.2). However, the comparison of PTT with a similar “gold standard”, represented by PAT extracted by Nexfin, needed further adjustment. In fact, this is highly dependent on two signal synchronizations: 1) the SCG and PPG timestamps need to be aligned in order to extract the PTT from their combination; 2) the ECG and PLT timestamps need to be synchronized with the smartphone acquisition. The first synchronization problem were overcome by computing the delay between the smartphone camera and inertial sensors using an ad-hoc implemented algorithm (paragraph 3.2), exploiting the capability of the smartphone to produce light and sound triggers, while the second synchronization problem was solved by inserting two markers on the Nexfin data acquisition at the beginning and at the end of the smartphone acquisitions, identified by beep-sounds emitted by smartphone speaker, thus being able to synchronize the first (and last) heart-beat.

The assessment of the PTT required in this case a beat-to-beat approach to be applied to both SCG and PPG signals: this was achieved by focusing on the detection of the AO peak of the SCG and the foot of the PPG waveforms, according to literature ((Wang *et al.*, 2018), (Carek *et al.*, 2017)).

For the PAT, the R-peaks and PLT foot points were also detected and the interval between them computed, to be compared with the corresponding smartphone PTT values.

The performed comparison resulted in poor correlation, probably due to the narrow range of values recorded in one single subject during 30 seconds, together with a bias showing an underestimation of 83 msec of the smartphone measured PTT versus the gold standard PAT, that included also the PEP time. However, the relatively narrow confidence interval for the PTT measurements around the measured value ($CV \approx 10\%$) proved a potential coherence in time of the two sensors during the 30 seconds of acquisition, without any drift along duration of the acquisition.

5.3 LIMITATIONS

Despite all the attempts to minimize them, the developed study suffers from some limitations:

- 1) the strict dependence between the quality of the signals and the achievement of the correct position of the smartphone for the acquisition, in particular when a combined acquisition was performed. For the PPG, the incorrect position of the index finger on the camera, the obstruction of the depth sensor, or the missed complete covering of the flashlight would cause the corruption of the signal. For the SCG, the artifacts introduced by the inexact positioning of the smartphone on the chest could yield to the impossibility of detecting the AO points by simple detection algorithms, which could be easily embedded into on-board algorithms in the app.
- 2) The choice of an Android operating system to develop the simultaneous acquisition of the PPG and SCG signal limited the synchronization between the two different sensor sub-systems, not allowing the control of such feature. To overcome this problem, an ad-hoc procedure to start vibration with the simultaneous shutdown of the flashlight and related algorithm to find the time delay between the two sensors timestamps was implemented and integrated into the app module for the simultaneous acquisition. However, this does not ensure the correctness of the computed real delay (which remains unknown), potentially introducing a systematic error in the measurements.
- 3) Composition and the number of the participants. For the first protocol, the investigation included only seven healthy volunteers, with an age between 27 and 29 years old, thus narrowing the sample variability for the app evaluation about its usability and the perceived eHealth engagement. For the second protocol, acquiring only 1 female participant, also due to hospital access restrictions due to COVID-19 pandemics, resulted in a low number of reliable PTT measurements for a rigorous validation of this biometric parameter.

- 4) Related to the design choices regarding the app appearance, a limitation was the low affective engagement gained by this tool. Representing a first prototype, this new app lacked persuasive design features, such as feedback, historical values, motivational clues, that could have overcome this limit, in particular in a scenario of daily self-measurement by a patient with chronic disease.

5.4 CONCLUSIONS

In this study, the design and development of an Android app to acquire with different settings the PPG and SCG signals using embedded sensors in the smartphone, and its first validation to evaluate its feasibility and accuracy in measuring mean heart rate and pulse transit time through two experimental protocols, was performed.

Three different types of acquisition were implemented: 1) the PPG signal; 2) the SCG signal, and 3) the simultaneous acquisition of both PPG and SCG signals, organized in 3 dedicated app modules, with data storage both inside the smartphone memory, and on the Google Cloud Service, thus providing the bases for remote monitoring and interpretation of the user parameters.

This choice allows for high flexibility (duration of acquisition, camera frame rate) in different research and usage scenarios, also offering future possibilities of development, such as integrating in each module new features, based on persuasive design, that could encourage its use.

Experimental validation showed good feasibility and accuracy in deriving mean HR, together with good user involvement and acceptance of this new technology that could be the basis to encourage the user self-assessment in a possible future app dissemination. Further research is needed to evaluate feasibility and accuracy for PTT measurement obtained from synchronous acquisition of SCG and PPG.

Bibliography:

Abinaya, M., Prabhakaran, S. and Jaisankar, N. (2014) 'Photoplethysmography On Smart Phone Using Savitzky-Golay Filter', *Ijser.Org*, 5(6), pp. 45–49. Available at: <http://www.ijser.org/researchpaper%5CPhotoplethysmography-On-Smart-Phone-Using-Savitzky-Golay-Filter.pdf>.

Acharya, U. R. *et al.* (2006) 'Heart rate variability: A review', *Medical and Biological Engineering and Computing*, 44(12), pp. 1031–1051. doi: 10.1007/s11517-006-0119-0.

Amerini, I. *et al.* (2016) 'Robust smartphone fingerprint by mixing device sensors features for mobile strong authentication', *IS and T International Symposium on Electronic Imaging Science and Technology*, (Micc), pp. 1–8. doi: 10.2352/ISSN.2470-1173.2016.8.MWSF-088.

Bangor, A., Kortum, P. T. and Miller, J. T. (2008) 'An empirical evaluation of the system usability scale', *International Journal of Human-Computer Interaction*, 24(6), pp. 574–594. doi: 10.1080/10447310802205776.

Caetano, J. and Delgado Alves, J. (2015) 'Heart rate and cardiovascular protection', *European Journal of Internal Medicine*. European Federation of Internal Medicine., 26(4), pp. 217–222. doi: 10.1016/j.ejim.2015.02.009.

Carek, A. *et al.* (2017) 'SeismoWatch: Wearable Cuffless Blood Pressure Monitoring Using Pulse Transit Time', *Proceedings of the ACM on Interactive, Mobile, Wearable and Ubiquitous Technologies*, 1(3), pp. 1–16. doi: 10.1145/3130905.

Choudhary, T., Sharma, L. N. and Bhuyan, M. K. (2018) 'Standalone Heartbeat Extraction in SCG Signal Using Variational Mode Decomposition', *2018 International Conference on Wireless Communications, Signal Processing and Networking, WiSPNET 2018*, (August), pp. 2–5. doi: 10.1109/WiSPNET.2018.8538723.

Dongfeng Zhang MD, Weijing Wang MD, F. L. M. (2012) 'Association between resting heart rate and coronary artery disease, stroke, sudden death and noncardiovascular diseases: a meta-analysis', 184(2), pp. 169–177. doi: 10.1503/cmaj.

Eeftinck Schattenkerk, D. W. *et al.* (2009) 'Nexfin noninvasive continuous blood pressure validated against Riva-Rocci/Korotkoff', *American Journal of Hypertension*, 22(4), pp. 378–383. doi: 10.1038/ajh.2008.368.

Garnier, R. P. *et al.* (2012) 'Level of agreement between Nexfin non-invasive arterial pressure

with invasive arterial pressure measurements in children’, *British Journal of Anaesthesia*. British Journal of Anaesthesia. Published by Elsevier Ltd., 109(4), pp. 609–615. doi: 10.1093/bja/aes295.

Glowicz (2017) ‘A Wearable Vital Signs Monitor at the Ear for Continuous Heart Rate and Pulse Transit Time Measurements’, *Physiology & behavior*, 176(5), pp. 139–148. doi: 10.1016/j.physbeh.2017.03.040.

Gregoski, M. J. *et al.* (2012) ‘Development and validation of a smartphone heart rate acquisition application for health promotion and wellness telehealth applications’, *International Journal of Telemedicine and Applications*, 2012. doi: 10.1155/2012/696324.

Holz, C. and Wang, E. (2017) ‘Glabella: Continuously Sensing Blood Pressure Behavior using an Unobtrusive Wearable Device’, *Proceedings of the ACM on Interactive, Mobile, Wearable and Ubiquitous Technologies*, 1(3), pp. 1–23. doi: 10.1145/3132024.

Jafari Tadi, M. *et al.* (2014) ‘Accelerometer-based method for extracting respiratory and cardiac gating information for dual gating during nuclear medicine imaging’, *International Journal of Biomedical Imaging*. Hindawi Publishing Corporation, 2014. doi: 10.1155/2014/690124.

Jonathan, E. and Leahy, M. J. (2011) ‘Cellular phone-based photoplethysmographic imaging’, *Journal of Biophotonics*, 4(5), pp. 293–296. doi: 10.1002/jbio.201000050.

Kelders, S. M. and Kip, H. (2019) ‘Development and initial validation of a scale to measure engagement with eHealth technologies’, *Conference on Human Factors in Computing Systems - Proceedings*, pp. 1–6. doi: 10.1145/3290607.3312917.

Kortum, P. and Sorber, M. (2015) ‘Measuring the Usability of Mobile Applications for Phones and Tablets’, *International Journal of Human-Computer Interaction*, 31(8), pp. 518–529. doi: 10.1080/10447318.2015.1064658.

Kurylyak, Y., Lamonaca, F. and Grimaldi, D. (2012) ‘Smartphone-Based Photoplethysmogram Measurement’, (May 2014).

Kwon, S. *et al.* (2011) ‘Validation of heart rate extraction through an iPhone accelerometer’, *Proceedings of the Annual International Conference of the IEEE Engineering in Medicine and Biology Society, EMBS*. IEEE, pp. 5260–5263. doi: 10.1109/IEMBS.2011.6091301.

Landreani *et al.* (2019) ‘Assessment of Ultra-Short Heart Variability Indices Derived by

Smartphone Accelerometers for Stress Detection’, *Sensors*, 19(17), p. 3729. doi: 10.3390/s19173729.

Landreani, F. and Caiani, E. G. (2017) ‘Smartphone accelerometers for the detection of heart rate’, *Expert Review of Medical Devices*. Taylor & Francis, 14(12), pp. 935–948. doi: 10.1080/17434440.2017.1407647.

Laurin, A., Blaber, A. and Tavakolian, K. (2013) ‘Seismocardiograms return valid heart rate variability indices’, *Computing in Cardiology*, 40, pp. 413–416.

Lázaro, J. *et al.* (2015) ‘Respiratory rate derived from smartphone-camera-acquired pulse photoplethysmographic signals’, *Physiological Measurement*. IOP Publishing, 36(11), pp. 2317–2333. doi: 10.1088/0967-3334/36/11/2317.

Lee, Hyunwoo, Lee, Hana and Whang, M. (2018) ‘An enhanced method to estimate heart rate from seismocardiography via ensemble averaging of body movements at six degrees of freedom’, *Sensors (Switzerland)*, 18(1), pp. 1–12. doi: 10.3390/s18010238.

Lewis, R. P. *et al.* (1977) ‘REVIEWS OF CONTEMPORARY LABORATORY METHODS Arnold M . Weissler , M . D ., Editor A Critical Review of the Systolic Time Intervals’, *Circulation*, 56(5), pp. 146–158.

Matsumura, K. *et al.* (2014) ‘iPhone 4s photoplethysmography: Which light color yields the most accurate heart rate and normalized pulse volume using the iPhysioMeter application in the presence of motion artifact?’, *PLoS ONE*, 9(3), pp. 1–12. doi: 10.1371/journal.pone.0091205.

Passaro, V. M. N. *et al.* (2017) ‘Gyroscope technology and applications: A review in the industrial perspective’, *Sensors (Switzerland)*, 17(10), pp. 1–18. doi: 10.3390/s17102284.

Patel, K. *et al.* (2016) ‘Effect of postural changes on cardiovascular parameters across gender’, *Medicine (United States)*, 95(28), pp. 1–7. doi: 10.1097/MD.0000000000004149.

Pelegris, P. *et al.* (2010) ‘A novel method to detect heart beat rate using a mobile phone’, *2010 Annual International Conference of the IEEE Engineering in Medicine and Biology Society, EMBC’10*, (February 2014), pp. 5488–5491. doi: 10.1109/IEMBS.2010.5626580.

Peng, R. C. *et al.* (2015) ‘Extraction of heart rate variability from smartphone photoplethysmograms’, *Computational and Mathematical Methods in Medicine*, 2015(1). doi: 10.1155/2015/516826.

Sauro, J. and Lewis, J. R. (2011) ‘When designing usability questionnaires, does it hurt to be positive?’, *Conference on Human Factors in Computing Systems - Proceedings*, pp. 2215–2223. doi: 10.1145/1978942.1979266.

Scully, C. G. *et al.* (2012) ‘Using time-frequency analysis of the photoplethysmographic waveform to detect the withdrawal of 900 mL of uylod’, *Anesthesia and Analgesia*, 115(1), pp. 74–81. doi: 10.1213/ANE.0b013e318256486c.

Shaffer, F. and Ginsberg, J. P. (2017) ‘An Overview of Heart Rate Variability Metrics and Norms’, *Frontiers in Public Health*, 5(September), pp. 1–17. doi: 10.3389/fpubh.2017.00258.

Shin, H. S., Lee, C. and Lee, M. (2009) ‘Adaptive threshold method for the peak detection of photoplethysmographic waveform’, *Computers in Biology and Medicine*. Elsevier, 39(12), pp. 1145–1152. doi: 10.1016/j.compbiomed.2009.10.006.

Siecinski, S. and Kostka, P. (2018) ‘Heart beat detection from smartphone SCG signals: comparison with previ- ous study on HR estimation Szymon’. doi: 10.1038/srep37524.

Wang, E. J. *et al.* (2018) ‘Seismo: Blood pressure monitoring using built-in smartphone accelerometer and camera’, *Conference on Human Factors in Computing Systems - Proceedings*, 2018-April, pp. 1–9. doi: 10.1145/3173574.3173999.

Yardley, L. *et al.* (2015) ‘The person-based approach to intervention development: Application to digital health-related behavior change interventions’, *Journal of Medical Internet Research*, 17(1), pp. 1–11. doi: 10.2196/jmir.4055.

Zhang, X. Y. and Zhang, Y. T. (2005) ‘The effect of local cold exposure on pulse transit time’, *Annual International Conference of the IEEE Engineering in Medicine and Biology - Proceedings*, 7 VOLS, pp. 3522–3525. doi: 10.1088/0967-3334/27/7/008.

Bibliography [internet]:

Minhang Bao (2005) *Analysis and Design Principles of MEMS Devices book* | [internet]
Available from:
https://books.google.it/books?id=No7NNfc1pfYC&printsec=frontcover&hl=it&source=gsb_a tb#v=onepage&q&f=false

Statistics for analysis of the potential use of smartphone technology among world population and mHealth application interest.

1. Statista. Global smartphone sales to end users 2007-2020 | Statistic [internet]. Available from: <https://www.statista.com/statistics/263437/global-smartphone-sales-to-end-users-since-2007/>
2. Statista. Global smartphone shipments forecast 2010-2023 | Statistic [internet]. Available from: <https://www.statista.com/statistics/263441/global-smartphone-shipments-forecast/>
3. Statista. Global smartphone sales to end users 2007-2020 | Statistic [internet]. Available from: <https://www.statista.com/statistics/263437/global-smartphone-sales-to-end-users-since-2007/>
4. Statista. Global smartphone shipments forecast 2010-2022 | Statistic [internet]. Available from: <https://www.statista.com/statistics/263441/global-smartphone-shipments-forecast/>
5. Statista. Italian population projections for 2020-2050 | Statistic [internet]. Available from: <https://www.statista.com/statistics/263441/global-smartphone-shipments-forecast/>
6. Statista. Top funded health IT technologies worldwide between 2010 and 2017 | Statistic [internet]. Available from: <https://www.statista.com/statistics/736136/top-funded-health-it-technologies-worldwide/>
7. Statista. Top funded global digital health categories h1 2019 | Statistic [internet]. Available from: <https://www.statista.com/statistics/736136/top-funded-health-it-technologies-worldwide/>
8. Statista. Most attractive healthcare sectors for mHealth app companies-2017 | Statistic [internet]. Available from: <https://www.statista.com/statistics/795584/top-healthcare-sectors-for-mhealth-app-companies-2017/>

9. Statista. Smartphone vendors market share worldwide 2016-2019 [internet]. Available from: <https://www.statista.com/statistics/266220/global-smartphone-market-share-by-vendor-in-2007-and-2008/>

APPENDIX A- SUS QUESTIONNAIRE DATA

The Figure A1 shows the overview of the SUS scores obtained by the subjects which has participated to the first protocol. The yellow points indicate the score assigned by the subject to the single items, while the red points represent the ideal values.

The Table A1 shows the item texts as reference to read the data.

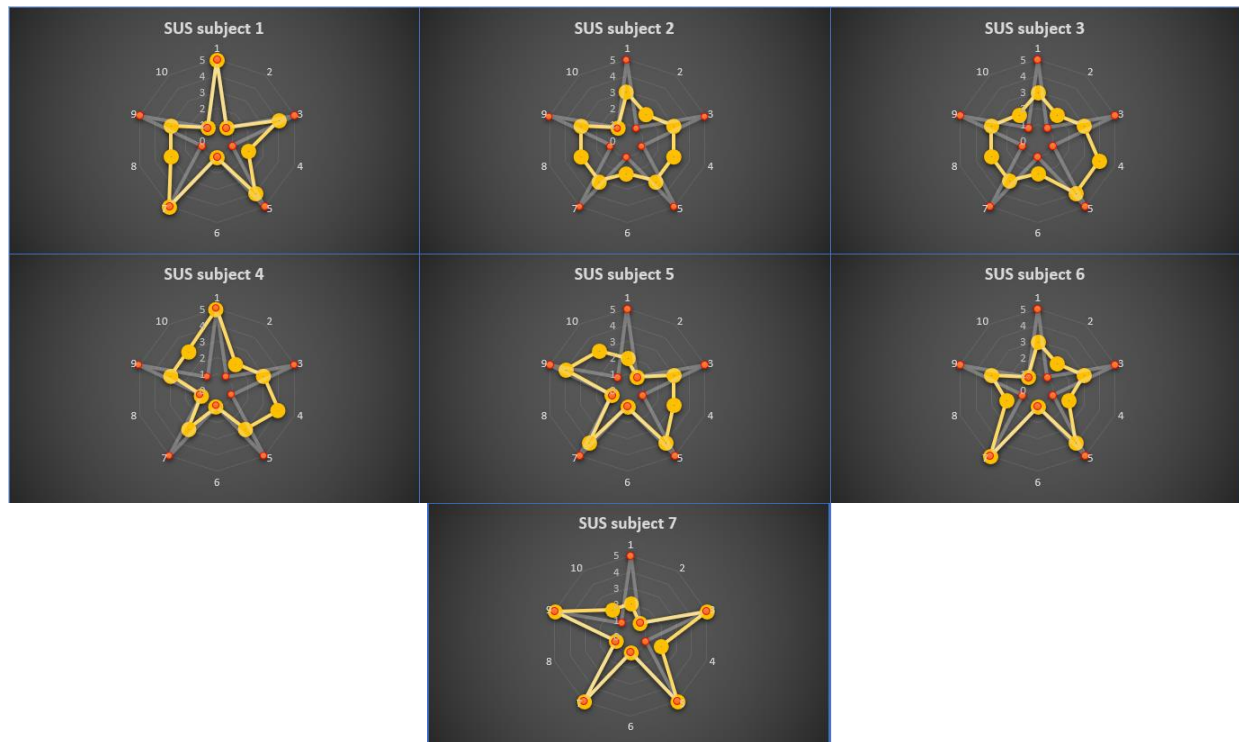


Figure A1 Item scores obtained by subject 1 to 7 (yellow) from the administered SUS over the ideal series (red)

Table A1 Sentences associated to the SUS items. The (+) sign flanked to the item number indicates that the sentences have a positive meaning, while (-) indicates the opposite.

Item number	Text
1 (+)	I think that I would like to use this system frequently
2 (-)	I found the system unnecessarily complex
3 (+)	I thought the system was easy to use
4 (-)	I think that I would need the support of a technical person to be able to use this system
5 (+)	I found the various functions in this system were well integrated
6 (-)	I thought there was too much inconsistency in this system
7 (+)	I would imagine that most people would learn to use this system very quickly
8 (-)	I found the system very cumbersome to use
9 (+)	I felt very confident using the system
10 (-)	I needed to learn a lot of things before I could get going with this system

APPENDIX B- AD-HOC QUESTIONNAIRE DATA

The Figure B1 shows the overview of the ad-hoc questionnaire scores obtained by the subjects which has participated to the first protocol. The yellow points indicate the score assigned by the subject to the single items, while the red points represent the ideal values.

The Table B1 shows the item texts as reference to read the data.

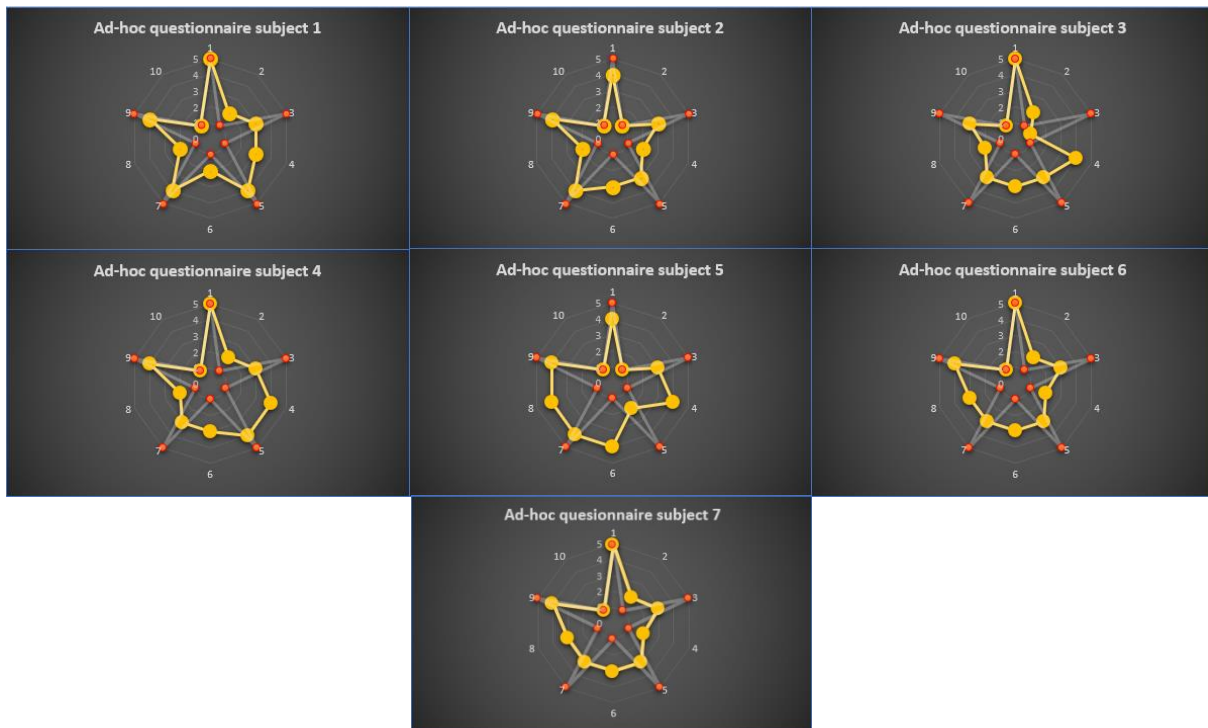


Figure B1 Item scores obtained by subject 1 to 7 (yellow) from the administered ad-hoc questionnaire over the ideal series (red)

Table B1 Sentences associated to the ad-hoc questionnaire items. The (+) sign flanked to the item number indicates that the sentences have a positive meaning, while the (-) indicates the opposite.

Item number	Text
1 (+)	I think that I would like to use this system frequently
2 (-)	I found the system unnecessarily complex
3 (+)	I thought the system was easy to use
4 (-)	I think that I would need the support of a technical person to be able to use this system
5 (+)	I found the various functions in this system were well integrated
6 (-)	I thought there was too much inconsistency in this system
7 (+)	I would imagine that most people would learn to use this system very quickly
8 (-)	I found the system very cumbersome to use
9 (+)	I felt very confident using the system
10 (-)	I needed to learn a lot of things before I could get going with this system

APPENDIX C- TWEETS QUESTIONNAIRE DATA

The Figure C1 shows the overview of the TWEETS questionnaire scores obtained by the subjects which has participated to the first protocol. The yellow points indicate the score assigned by the subject to the single items, while the red points represent the ideal values.

The Table C1 shows the item texts as reference to read the data.

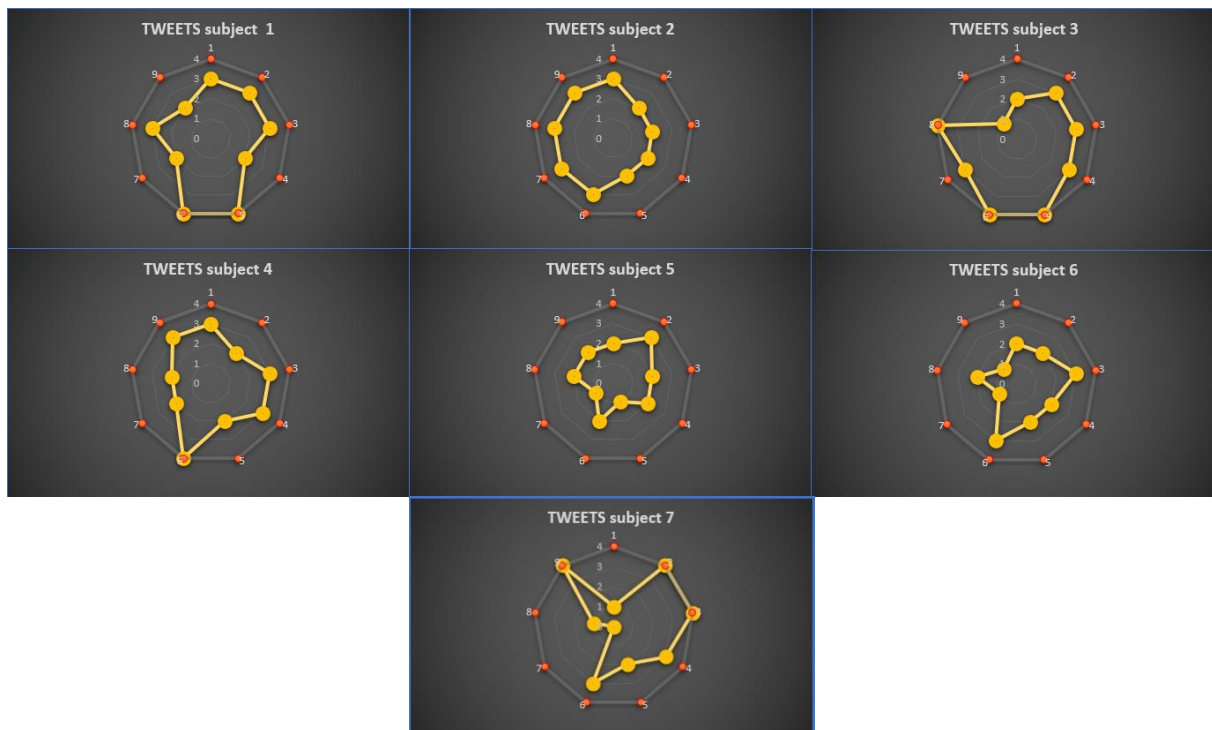


Figure C1 Item scores obtained by subject 1 to 7 (yellow) from the administered TWEETS over the ideal series (red)

Table C1 Sentences associated to the TWEETS items. The (+) sign flanked to the item number indicates that the sentences have a positive meaning, while the (-) indicates the opposite.

Item number	Text
1	I think that I would like to use this system frequently
2	I found the system unnecessarily complex
3	I thought the system was easy to use
4	I think that I would need the support of a technical person to be able to use this system
5	I found the various functions in this system were well integrated
6	I thought there was too much inconsistency in this system
7	I would imagine that most people would learn to use this system very quickly
8	I found the system very cumbersome to use
9	I felt very confident using the system